

## End Permian to Middle Triassic plant species richness and abundance patterns in South China

Xu, Zhen; Hilton, Jason; Yu, Jianxin; Wignall, Paul; Yin, Hongfu; Xue, Qing; Ran, Weiju; Li, Hui; Shen, Jun; Meng, Fansong

DOI:

[10.1016/j.earscirev.2022.104136](https://doi.org/10.1016/j.earscirev.2022.104136)

License:

Creative Commons: Attribution-NonCommercial-NoDerivs (CC BY-NC-ND)

*Document Version*

Peer reviewed version

*Citation for published version (Harvard):*

Xu, Z, Hilton, J, Yu, J, Wignall, P, Yin, H, Xue, Q, Ran, W, Li, H, Shen, J & Meng, F 2022, 'End Permian to Middle Triassic plant species richness and abundance patterns in South China: coevolution of plants and the environment through the Permian–Triassic transition', *Earth Science Reviews*, vol. 232, 104136.

<https://doi.org/10.1016/j.earscirev.2022.104136>

[Link to publication on Research at Birmingham portal](#)

### General rights

Unless a licence is specified above, all rights (including copyright and moral rights) in this document are retained by the authors and/or the copyright holders. The express permission of the copyright holder must be obtained for any use of this material other than for purposes permitted by law.

- Users may freely distribute the URL that is used to identify this publication.
- Users may download and/or print one copy of the publication from the University of Birmingham research portal for the purpose of private study or non-commercial research.
- User may use extracts from the document in line with the concept of 'fair dealing' under the Copyright, Designs and Patents Act 1988 (?)
- Users may not further distribute the material nor use it for the purposes of commercial gain.

Where a licence is displayed above, please note the terms and conditions of the licence govern your use of this document.

When citing, please reference the published version.

### Take down policy

While the University of Birmingham exercises care and attention in making items available there are rare occasions when an item has been uploaded in error or has been deemed to be commercially or otherwise sensitive.

If you believe that this is the case for this document, please contact [UBIRA@lists.bham.ac.uk](mailto:UBIRA@lists.bham.ac.uk) providing details and we will remove access to the work immediately and investigate.

1 End Permian to Middle Triassic plant species richness and  
2 abundance patterns in South China: coevolution of plants and  
3 the environment through the Permian–Triassic transition

4  
5 Zhen Xu<sup>a</sup>, Jason Hilton<sup>b</sup>, Jianxin Yu<sup>a,\*</sup>, Paul B. Wignall<sup>c</sup>, Hongfu Yin<sup>a</sup>, Qing Xue<sup>a</sup>,  
6 Weiju Ran<sup>a</sup>, Hui Li<sup>d</sup>, Jun Shen<sup>e</sup>, Fansong Meng<sup>f</sup>

7  
8 <sup>a</sup> *School of Earth Sciences, State Key Laboratory of Biogeology and Environmental Geology, China*  
9 *University of Geosciences, Wuhan, Hubei 430074, PR China*

10 <sup>b</sup> *School of Geography, Earth and Environmental Sciences and Birmingham Institute of Forest*  
11 *Research, University of Birmingham, Edgbaston, Birmingham B15 2TT, UK*

12 <sup>c</sup> *School of Earth and Environment, University of Leeds, Leeds, LS2 9JT, UK*

13 <sup>d</sup> *Jiangxi Key Laboratory of Mass Spectrometry and Instrumentation, East China University of*  
14 *Technology, Nanchang, Jiangxi 330105, PR China*

15 <sup>e</sup> *State Key Laboratory of Geological Processes and Mineral Resources, China University of*  
16 *Geosciences, Wuhan, Hubei 430074, PR China*

17 <sup>f</sup> *Wuhan Geological Survey Center (Yichang Base), China Geological Survey, Yichang, Hubei 443005,*  
18 *PR China*

19  
20 \* Corresponding author. Tel: +86 18986112835; fax: +86 27 67882345.

21 E-mail address: yujianxin@cug.edu.cn (J. Yu)

22  
23

ABSTRACT This study reviews plant species richness and abundance change from the End Permian to Middle Triassic in South China and examines the co-evolutionary relationship between the flora and the environment through this critical interval in the history of terrestrial biotas. A normalized macro-fossil plant record, that considers only one taxon per whole plant, is produced. This identifies four broad phases of plant evolution. Phase 1 is marked by pre-extinction floras that demonstrate a long-term decline of species richness beginning in the Late Permian (lower Changhsingian) that culminates in the distinct End Permian Plant Crisis (EPPC) at the end of the Changhsingian. Other evidence for the health of the flora, including palynology, biomarkers, wildfire proxies, soil erosion and weathering proxies show a drastic loss of plant abundance (biomass) and increase of wildfire frequency (suggestive of increasing seasonal aridity) during the EPPC. A Phase 2 survival interval, during the Changhsingian–Griesbachian transition, has a severely impoverished plant assemblage consisting of opportunistic lycopods and a short-lived holdover flora. Phase 3 (Late Griesbachian–Smithian) saw the modest recovery of species richness as several groups began to radiate, notably conifers and ferns. Diversity increases substantially and persistently during the succeeding Phase 4 and sees the dominant lycopods/herbaceous bryophytes of Phase 3 replaced by conifer-dominated floras. Plant abundance recovery began earlier than the resumption of coal formation which only initiated in the Anisian following its disappearance during the EPPC. Only in the Late Triassic did the flora recover to a level comparable to that seen in the Permian. The flora of South China thus took ~15 million years to completely recover from the profound environmental and climatic effects of the Permo-Triassic mass extinction.

*Keywords:* plant–environment coevolution, mass extinction, coal gap, Permo-Triassic and end-Permian, gigantopterids, lycopod

## 1. Introduction

The 60 million years from the Middle Permian to the end-Triassic was one of the most stressful in life's history. It witnessed the Permo-Triassic Mass Extinction

(PTME), the most severe crisis of the Phanerozoic, together with the end-Triassic mass extinction and several lesser crises (e.g., Wignall, 2015). The result was a fundamental change of incumbents in both marine and terrestrial realms. Terrestrial tetrapod dynasties changed several times. The dinocephalians of the Middle Permian were a distant memory by the time dinosaurs rose to dominance in the Jurassic. The composition of plant communities also underwent fundamental overhaul during the Permian and Triassic but the nature of this transition and its relationship with other biosphere changes has long remained enigmatic (e.g., Knoll, 1984; Rees, 2002). In particular, it is unclear if plant communities underwent a series of abrupt mass extinctions, such as seen amongst the marine biota and tetrapods, or instead showed more gradual long-term changes (McElwain & Punyasena, 2007).

In an influential study, Knoll (1984) suggested that there was a protracted changeover from a Paleophytic to a Mesophytic flora separated by a transitional or mixed flora, but with no abrupt extinction event at the Permo-Triassic boundary. Subsequent work suggests that this distinction is between floras from different biomes and has no chronostratigraphic significance (DiMichele et al., 2008). Nonetheless, the idea that plants did not suffer mass extinction, even during the Permo-Triassic transition survives. Many studies based on literature compilations favour a non-catastrophic floral history at the end of the Permian (e.g., Rees, 2002; Ouyang and Zhu, 2007; Nowak et al., 2019), and some field studies also support the notion that there were relatively few losses at this time (e.g., Krassilov & Karasev, 2009; Hochuli et al., 2010; Xiong & Wang, 2011; Yang et al., 2021). In contrast, there is clear evidence for a major upheaval in plant communities at the end of the Permian, including the short-term proliferation of fungal spores (*Reduviasporonites*) at the expense of plant palynomorphs (Visscher et al., 1996), the abrupt loss of palynomorphs from woody species suggesting forest die-off (Looy et al., 1999) and the abrupt and prolonged disappearance of coals from the geological record: a 20 myr “coal gap” (Retallack, 1995, 1996). Clearly, something happened to plants at the end of the Permian (Yu et al., 2015).

Prior to the PTME, plants are divided into four main paleogeographic regions

(e.g., Hilton and Cleal, 2007) whilst low diversity survivors were similar after the crisis (Grauvogel-Stamm and Ash., 2005; Yu et al., 2015; Feng et al., 2020). Compositionally, the survivors consist of holdover elements of the late Permian floras, notably in South China, together with a few, new Triassic forms (Yao et al., 1980; Chen et al., 2011; Yu et al., 2015). Some have argued, based on the palynological record from South China, Xinjiang and Greenland, that the main plant crisis occurred at the end of the Griesbachian, the first substage of the Triassic (Qu et al., 1986; Zhang et al., 2004; Yu et al., 2008; Peng et al., 2009; Hochuli et al., 2016). If this proved to be a global phenomenon then the fortunes of plants would be fundamentally out of kilter with that of terrestrial tetrapods and the marine biosphere (cf. Stanley, 2009; Sun et al., 2012; Song H.J. et al., 2018; Allen et al., 2020; Romano et al., 2020). It is notable that the onset of the “coal gap”, marking the loss of wetland peat-forming communities, coincided with the PTME and not the end of the Griesbachian.

Following the PTME, floras were of low diversity in the Early Triassic (e.g., Yu et al., 2015; Feng et al., 2020). Unlike the prosperous Late Triassic floras such as the Baoding, Jiuliang, Xujiache, Shazhenxi floras in South China, the Early to Middle floras are poorly understood (Li, 1964; Xu et al., 1979; Huang and Lu, 1992; Meng et al., 1994; Li et al., 1995). Recent discoveries of Early to Middle Triassic floras have helped fill in the blanks at this time (Meng et al., 1995; Broutin et al., 2020). Clearly, we have yet to achieve a full understanding of the dynamics of terrestrial recovery following the PTME, and questions still remain: were plants marching to a different beat compared to the marine biota or are the major differences caused by a poor understanding of the floral record, and why is there a “coal gap” during the Early and much of the Middle Triassic?

To address these questions, we here present a comprehensive review of the Permian to Triassic fossil plant assemblages of South China supplemented with extensive additional data from our own field collecting. This region comprises the Kangdian Oldland to the west and the Cathaysia Oldland to the East that were separated by the upper Yangtze Platform. Intensive studies during the past few decades have provided a major increase in our understanding of the flora which have

substantially increased our knowledge of changes in low paleolatitudes. We also incorporate information from other proxies for the health of the terrestrial biosphere. These include levels of total organic carbon (TOC), weathering proxies, carbon isotopic variations and black carbon and charcoal concentrations (as wildfire indicators). Our synthesis of fossil plant occurrences is placed in a detailed stratigraphic framework and, where available, zircon-derived radiometric dating (Shen S.Z. et al., 1995, 2011; Burgess et al., 2014; He et al., 2017). Our synthesis of the floral species richness and abundance differs from previous analyses (e.g., Yu et al., 2015; Chu et al., 2016; Feng et al., 2020) by normalizing the plant fossil occurrences to remove duplications that are an artefact of paleobotanical systematics, preservational types, and taxon recording (see Hilton and Cleal, 2007; Cleal et al., 2021). This provides a more realistic measure of plant species richness in the fossil record and unsurprisingly produces a substantially lower estimate of floral species richness than previous accounts.

## 2. Materials and methods

We use a combination of approaches to evaluate plant species turnover from the Middle Permian to the early Late Triassic in South China. The successive floras are documented in stratigraphic order (Fig. 1) and for each we review their stratigraphical relationships and depositional sedimentary facies to provide a taphonomic context for the palaeobotanical occurrences.

### *2.1. Sampling strategy*

Due to an absence of marine fauna and diachronism of plant-bearing units, we use the concept of an end-Permian plant crisis (EPPC) to represent the point of disappearance of plant macrofossils in the terrestrial South China successions. The EPPC is composed of two phenomena. One is the gradual alternation of plant assemblages during the Changhsingian associated with a gradual decline of species richness. The second phenomenon was a much more rapid extinction interval, at the

end of the Changhsingian, when many long-ranging elements disappeared, and plant abundance declined markedly.

For fossil plants we have adopted two different levels of stratigraphic resolution. For formations recording the EPPC of the Dalong, Xuanwei and Kayitou formations (Fig. 1), and its Lower to Middle Triassic aftermath in the Feixianguan, Lingwen and Badong formations (Fig. 1), we selected representative localities in terms of their fossil plant composition. For the Xuanwei Formation, we systematically collected plants from the Chahe and Chinahe sections in Guizhou and Yunnan provinces, for the Dalong Formation the Xinmin and Duanshan A, B sections in Guizhou Province, for the Feixianguan Formation the Chinahe, Tucheng and Mide sections in Yunnan and Guizhou provinces and the Pojiao and Lubei sections in Yunnan Province, for the Lingwen Formation the Lingwen Section in Hainan Province, and for the Badong Formation the Hongjiaguan and Furongqiao sections in Hunan Province. For each formation we have undertaken extensive fieldwork to identify and collect fossil plants *in situ* on a bed-by-bed basis to investigate them in stratigraphically high-resolution, with the floras of the Feixianguan being reported here in detail for the first time. For these formations all the fossils have been identified by the same individuals using reference materials such that the identifications are internally consistent and accurate, rather than being based solely on literature compilation. To reduce the influence of “Signor-Lipps” effect, all the published plant fossil records from each studied flora in South China are collected and used in calculating species richness and stratigraphical distributions. We have not applied statistical methods to correct for the Signor-Lipps effect (e.g. Marshall and Ward, 1996; Wang et al., 2014) due to the non-uniform rates of deposition, diachroneity, depositional hiatuses and taphonomic controls in terrestrial strata that affect fossil plant distribution and preservation. The location of all the included sections are marked on the paleogeographic map (Fig. 3, 8, 13).

For the floras of the Liangshan, Maokou and Longtan formations that predate the EPPC, and for the Upper Triassic floras of the Jiuligang, Daqiaodi and Dajing formations (Fig. 1), we have conducted lower-resolution investigations and have

summarized the sedimentology and floral compositions, but do not provide detailed stratigraphic ranges for individual species as that information is not presently available. Data collected from these sections can only be evaluated at stage level rather than to show origination and extinction rates within the respective formations.

## 2.2. *Evaluating fossil plant species richness and normalizing data occurrences*

While ideally our study would seek to identify species diversity, it is rarely possible to determine species evenness from the fossil plant record (Cleal et al., 2012, 2021). Here we focus on species richness that denotes the number of species present in a particular bed, locality, formation or flora and is measurable from the plant fossil record (see supplementary dataset). To assess plant species richness, it is necessary to evaluate patterns of species change over time (e.g., Li et al., 1995; Peng et al., 2009; Yu et al., 2015; Chu et al., 2016; Feng et al., 2020). This is achieved by constructing stratigraphic range diagrams for each species showing their first appearance datum (= origination) and last appearance datum (= extinction) in each geological section, and then correlating using litho-, bio- or chemostratigraphic methods to compile stratigraphic range charts. From this information the total number of species can be determined at particular time intervals, and origination and extinction rates calculated noting these are when species originate and go extinct in South China within the dataset. We do not extend the range of plant fossils by calculating confidence intervals or interpolation due to the complexity of terrestrial stratal deposition and taphonomy, utilizing the stratigraphic range of the raw, plant fossil occurrences as recorded in the field. In order to provide values for the Middle Permian Maokou Flora, we have also included data from the latest early Permian Qixia Flora to provide range-through data (e.g., Cleal et al., 2012, 2021). Likewise, to provide the same for the early Late Triassic Shazhenxi Flora, we have included data from latest Triassic (Rhaetian) Yangbaichong Flora (see supplementary data for additional details).

To meaningfully extract plant species richness patterns from the fossil data, it is important to eliminate duplicates that are an artefact of paleobotanical nomenclature (e.g., Hilton and Cleal, 2007; Cleal et al., 2012, 2021). A single reconstructed whole-



plant species in the fossil record includes numerous distinct organs (e.g., leaves, stems, roots, cones, seeds), each with their own generic and species name (see Chaloner, 1986; Bateman and Hilton, 2009). The solution we have adopted is to normalize the data (see Cleal et al., 2012, 2021) and evaluate only those organs whose fossil taxonomy is most likely to reflect the original whole organism taxonomy. This represents the first time this approach has been applied to plant species richness through the Permo-Triassic interval including the EPPC and its Triassic recovery. All previous studies have artificially inflated species richness by including names of organs from the same plant species. Species richness estimates for normalized taxa uses only one organ for each viable whole plant. The organ selected for normalization varies depending on the composition of individual fossil plant assemblages and requires critical evaluation. The process identifies from each systematic group the organ that and can be reliably identified and is the most diverse, selecting it as the most representative rather than other organs.

Our approach includes omitting accounts of genera that lack species-level identifications (e.g., *Tomiostrobus* (= *Annalepis*) sp.) from assemblages in which one or more identified species of the same genus occurs (e.g., *Tomiostrobus* (= *Annalepis*) *augusta*, *T. (A.) brevicystis*). This assumes that the specimens identified as “sp.” are likely poorly preserved or incomplete examples of named species. We have also omitted from species richness estimates fertile organs including gymnosperm seeds when other organs of the same plants are present in the same assemblage; in all cases where seeds are present, they co-occur with one or more species of gymnosperm leaf from which it is assumed that the seeds belonged to one or more of these plants. Lycopsid rootstock (*Stigmaria*), sporophylls (*Lepidostrobohyllum*) and cones (*Lepidostrobus*) are also omitted because, in all instances, these co-occur with stems (*Lepidodendron*) that are more distinctive and are typically identified to the species level (see Table 1). However, Mesozoic lycopods lack the leafy stems and branches of Paleozoic arborescent species, while their sporophylls tend to be well-preserved, systematically distinctive and diverse and so represent the best organ to measure richness. For Paleozoic sphenophytes we use their leaves (including species of

*Annularia*) as they are systematically distinctive and the most diverse organ. However, leaves of Mesozoic sphenophytes are typically simpler, lack features to reliably distinguish species, and are of limited diversity so we use their stems and branches to measure richness as they are more readily distinguished from one another and more diverse. For “ferns” including members of the Marattiales, as well as gymnosperms including conifers, cycads and ginkgophytes, vegetative leaves have been used for normalization as they are reliably identified to species and genus level and in each case have the highest diversity. The only exceptions are rare instances where whole plants have been reconstructed in which, irrespective of whatever organ is selected for normalization, the name of the whole plant is used for that particular occurrence rather than the name of the isolated organ, following paleobotanical convention (see Bateman and Hilton, 2009). We accept that normalizing fossil plant data is, to some extent, subjective and cannot readily be tested for their robustness, but we consider these data to provide more realistic estimates of paleobotanical species richness than simple, raw-data based accounts. All data are presented in the supplementary dataset including information on normalization.

### 2.3. *Fossil plant abundance*

There is no robust method to quantitatively assess plant abundance in terrestrial settings (Cleal et al., 2021) unless fossil floras are preserved in-situ by obrution events such as volcanic ash-falls (e.g., Wang et al., 2012). In a broad sense, plant abundance may be indicated by a number of indirect measures including the number of locations that contain fossil plants as well as the paleobotanical richness in terms of numbers of specimens at each location, but these are subject to a variety of controls including collection intensity, spatial heterogeneity of plant distributions in contemporaneous settings, and a variety of physical (biostratigraphic, sedimentary) and chemical taphonomic processes (Bateman, 1991; Allison and Bottjer, 2010). Here we focus on relative measure of abundance as well as using specific environmental proxies that provide crude insights into plant abundance in the environment in which they lived.

Firstly, having undertaken extensive fieldwork and collections-based

investigations on Permian–Triassic plant bearing sedimentary successions from South China, it is obvious that plant abundance varies considerably. In order not to overlook evidence for plants, we have considered all plant material, from fragmented plant debris to intact fossil plant organs because we are interested in assessing the presence of plants in the sedimentary system. As a crude measure of plant abundance, we use the relative descriptors absent, very rare, rare, common, abundant and very abundant to describe the amount of plant fragments encountered in each section in terms of (a) plant fossils on individual beds, and (b) the number of beds containing fossil plants.

Secondly, as coals represent accumulated peat, we consider coals to indicate high plant abundance for an extended time period. In contrast, the studied interval includes the Triassic “coal gap” (Retallack et al., 1996). While it is possible that the coal gap could represent widespread adverse preservation conditions for fossil plants (e.g., Vajda et al., 2020), in South China abundant waterlogged, fine grained paralic sedimentary facies occur in the early Triassic (Yu et al., 2008, 2010, 2015; Bercovici et al., 2015) that would have been suitable for preserving fossil plants if they were present in these settings. We therefore interpret the Triassic coal gap to indicate low plant abundance in paralic depositional sedimentary environments.

Thirdly, we consider environmental proxies related to soils on the basis that abundant vegetation cover is likely to bind soils together and diffuse water infiltration into the ground, thus having the net result of reducing surface water run-off (Zuazo and Pleguezuelo, 2009; Davies and Gibling, 2010). In contrast, bare, un-vegetated ground would be more susceptible to surface water run-off, physical weathering and erosion (Retallack, 2005; Algeo et al., 2011; Kaiho et al., 2016; Shen et al., 2015, 2022). We therefore use the presence of physical weathering in terrestrial settings as a rough proxy for plant abundance in terms of ground cover, highlighting the co-evolution of plants and the environment. Finally, we consider Total Organic Carbon (TOC) levels in sediments as a crude proxy for terrestrial biomass and plant abundance with the caveat that it requires careful interpretation because of diagenetic controls on the value.

## 2.4. Evaluating plant ecology

The geological and paleoecological contexts in which fossil plants occur is important to their interpretation to provide links between fossil plants and the environment(s) in which they grew. It also allows greater understanding of the conditions in which extinction survivors lived, identifying features that may have contributed to their resilience as well as identifying the locations and environments of refugia.

Paleoecological assessments for plant taxa here come primarily from the available literature and is based on plant fossil anatomy and morphology and the sedimentary depositional environments in which they occur (Yao, 1978; Meyen, 1987; Bateman, 1991; Yang, 1993; Yang, 1994; Taylor et al., 2009). Fossil plant specimens were evaluated for their shape, size and completeness to elucidate their taphonomy in terms of being transported long, medium or short distances from their growth environment. For example, entire or almost entire organs lacking signs of taphonomic fragmentation, abrasion or size-sorting were interpreted as having undergone minimal transportation. This included in-situ plants and fossil plants found in paleosols, e.g., whole plants of *Lepacyclotes* (= *Annalepis*) in the Badong Formation (Meng, 1995). Greater levels of transport result in higher levels of fragmentation and size sorting and culminate in fine grained, well sorted plant debris beds such as layers of dispersed branches of *Neocalamites* in the Badong Formation (Meng, 1995). Depositional environments of the plant fossil were determined by sedimentary analysis and from the literature, as well as their paleogeographic location.

## 3. Fossil plant occurrences

### 3.1. Qixia Flora (Artinskian, Cisuralian)

This flora comes from the Liangshan Formation and other strata of the Qixia regional Stage in South China (Fig. 1), the age of which is roughly Artinskian (late Cisuralian, Shen S.Z. et al., 2019). Neither the Liangshan Formation nor its plant assemblage has received much study. This flora consists of a *Emplectopteris triangularis* - *Taeniopteris multinervis* assemblage but lacks gigantopterids,

representing the early stage of the Cathayian flora (Li et al., 1995).

### 3.2. Maokou Flora (Wordian–Capitanian)

The Maokou Flora (Fig. 1) comes from the Maokou regional Stage in China, the age of which is roughly Wordian to Capitanian in age (Li et al., 1995 and references therein). It mainly occurs in southeastern part of South China including Fujian, Guangxi, Guangdong and Jiangsu provinces and seldomly occurs in eastern parts of the Yangtze Platform. In the Maokouan (Capitanian Stage), the Cathaysian (*Gigantopteris*) flora started to develop across South China. The dominant species are *Gigantonoclea*, *Gigantopteris* and *Gigantopteridium*, while *Tingia*, *Asterophyllites* and *Cordaitea* are common.

### 3.3. Longtan Flora (Wuchiapingian)

The Longtan flora (Fig. 1) from the Longtan Formation and lower Xuanwei Formation is of Wuchiapingian age (Li et al., 1995). It belongs to the Cathaysian (*Gigantopteris*) flora which steadily become more diverse and widespread during Wuchiapingian Stage (Li, 1997; Luo et al., 2021). In addition to southeastern parts of South China, the Cathaysian (*Gigantopteris*) flora spread to the west of the Yangtze massif including the Xizang (Tibet) and Qinghai areas in the Wuchiapingian.

### 3.4. Xuanwei Flora (Changhsingian, latest Permian)

The Xuanwei flora occurs in the upper part of the Xuanwei Formation that crops out in western Guizhou and Eastern Yunnan provinces (Figs 1–3). It occurs in siliclastic sediments and coals deposited in paralic settings (Li and Yao, 1980; Yu et al., 2015; Chu et al., 2016; Shen J. et al., 2019a). It rests stratigraphically on the Emeishan Basalt (Fig. 2) and is dated to the late Changhsingian (He et al., 2017). In the Chinahe section, in the Zhehai area (Fig. 2) ash bed zircons have yielded ages  $252.4 \pm 4.1$  Ma and  $252.30 \pm 0.07$  Ma (He et al., 2017; Shen S.Z. et al., 2011; Chu et al., 2016). The Xuanwei Formation contains abundant fossil plants that represent the last occurrence of the Cathaysian tropical wetland flora (e.g., Shen G.L., 1995; Hilton

and Cleal, 2007; Feng et al., 2020). Of the 35 locations known to preserve fossil plant assemblages in the Xuanwei Formation (Yu et al., 2015), the sections at Chahe (Bercovici et al., 2015; Yu et al., 2015) and Chinahe (Fig. 3) are selected for study as they are amongst the most continuous successions and have been studied in detail. Fossil plant data from these sections provide statistical information on plant distribution and evolutionary patterns through the Changhsingian, but information on evolutionary rates also use data on all fossils from South China reported from this time interval (see supplementary dataset).

#### 3.4.1. Chahe Section (Changhsingian, late Permian)

The Chahe section in Weining County, western Guizhou Province (Figs. 3, 4) has been well studied (e.g., Yu et al., 2015; Chu et al., 2016). The section exposes the Xuanwei Formation (Beds 1–70) and overlying Kaiyitou Formation (Beds 71–89) (Fig. 4) and is conformably overlain by the Dongchuan Formation. A zircon U-Pb date of  $252.30 \pm 0.07$  Ma from volcanic ash near the top of the Xuanwei Formation indicates a latest Permian age (Shen S.Z. et al., 2011), suggesting the Permian–Triassic boundary (PTB) is in the basal Kayitou Formation. Two layers of volcanic ash, with an intervening layer of black mudstone, provide a common lithostratigraphic marker for a level immediately below the Permo-Triassic Boundary in non-marine sections (Chu et al., 2016).

The Xuanwei Formation at the Chahe section contains numerous plant fossils including the Cathaysian wetland genera *Gigantopteris*, *Lepidodendron*, *Pecopteris*, and *Fascipteris*. Plant fossils are abundant in the 31 plant-bearing layers (Fig. 4) before disappearing at Bed 69 in the latest Permian, with only *Peltaspermum* sp. persisting in Bed 70 above the EPPC level. Fossil plants are absent in the overlying Kayitou Formation in the Chahe section (Fig. 4).

#### 3.4.2. Chinahe Section (Changhsingian, late Permian)

The Chinahe section of eastern Yunnan Province (Fig. 3) starts with the Emeishan Basalt (Bed 0) and is unconformably overlain by terrestrial facies of the Xuanwei

Formation (Beds 1–25). Paralic gray–blue–green mudstone facies of the Kayitou Formation (Bed 26) conformably overly the Xuanwei Formation (Fig. 5) which in turn is overlain by the purple red Dongchuan Formation (Wignall et al., 2020).

The Xuanwei Formation in the Chinahe section commences with a thick layer of gray–black mudstone (Bed 1), that contains large amounts of well-preserved plant fossils (Fig. 5, 6). In Bed 1, *Lobatannularia*, *Pecopteris* and *Gigantopteris* are common, but the flora in this bed is diverse and also contains a range of sphenopsids (*Lobatannularia cathaysiana*, *L. heianensis*, *Paracalamites stenocostatus* and *Schizoneura amnchuriensis*), marattialean ferns (*Pecopteris (Asterotheca) guizhouensis*, *P. (A.) orientalis*, *P. (A.) hemotelioides*, *P. sahnii*, *Fascipteris sinensis* and *F. hallei*), gigantopterids (*Gigantonoclea guizhouensis*, *G. rosulata*, *Gigantopteris dictyophylloides* and *Gigantopteris nicotianaefolia*), ferns (*Cladophlebis permica*, *C. ozakii*) and occasional gymnosperm leaves (*Neuropteridium* sp., *Peltaspermum* sp., *Taeniopteris multinervis*, *Rhipidopsis panii*). Above Bed 1, the lithology changes into gray yellow or gray green, thin-bedded muddy siltstone and thin coals, pale gray or gray blue, thin-bedded mudstone and yellow gray fine-grained sandstone (Bed 2–25). Thin-bedded mudstones developed above coals (in Beds 3, 12, 16, 25) contain some plants fragments that are not identifiable to species level, but include fragments of *Lepidostrobophyllum*, gigantopterids, *Compsopteris*, *Pecopteris* and *Taeniopteris*. Until Bed 25 there are more gray–black, medium bedded, siltstones mixed with shaly coals as well as gray yellow or green silty-mudstone. Above Bed 25, there are two gray, thin-bedded mudstones together with a black mudstone layer, which may be correlative with the sandwich-like lithologies seen in the Chahe section at the boundary of the Xuanwei and Kaiyitou formations. Above this “sandwich-like” mudstone layer, a gray–yellow, thin-bedded sandstone and a layer of black siltstone contains numerous of fragmentary specimens of *Peltaspermum*, *Lepidopteris*, *Pecopteris* and *Giantopteridium*. In the boundary of the Xuanwei and Kayitou formations (Bed 26), there is a monotypic layer of dispersed *Tomioostrobus* (= *Annalepis*) in the dark gray, thin-bedded siltstone (in the bottom of bed 26). After the layer of *Tomioostrobus* (= *Annalepis*) comes the blue to greenish blue, thick-bedded

siltstones of the Kayitou Formation, which contain no plants but abundant conchostraca and a few horizons of marine bivalves (Fig. 6).

### 3.5. *Dalong Flora (Changhsingian, late Permian)*

The Dalong Formation formed in the western part of the Yangtze shallow sea and is laterally equivalent to the Heshan Formation in eastern areas (Figs. 2). Fossil plants from the Dalong Formation were documented by Liu et al. (2007), Song et al. (2013, 2015) and Li et al. (2019). The marine formation consists of thin-bedded cherts, siltstones, and clays (Shen J. et al., 2012a, 2013; Fig. 7). The chert beds contain both plant fossils and a marine biota including radiolarian, brachiopods, bivalves, conodonts, and foraminifera (Fig. 7) that enables correlation with the PTB GSSP at Meishan (Yin et al., 2007; Shen J. et al., 2012a; Li et al., 2019). Based on conodont occurrences, the Dalong Formation has been dated to the Changhsingian (Li et al., 2019). Although the Dalong and Heshan formations are of subtly different age (Figs. 1, 2), they share similar plant fossils and so are discussed together here. From them, five locations contain plant fossils.

From the Dalong Formation we studied the plant fossils from three published sections: Xinmin, Duanshan A and Duanshan B sections (Fig. 7). In general, the gymnosperms are well-preserved while the typical Cathaysian floral elements are more fragmentary and abraded suggesting considerable transport into the depositional setting. Xinmin is the longest section and, based on the presence of the conodont *Hindeodus parvus*, is the only section where the Permian–Triassic boundary (PTB) is well defined (Zhang et al., 2014). In the following account, the Xinmin section is illustrated as the main section, with the Duanshan A and B sections providing additional data.

#### 3.5.1. *Xinmin Section*

The Xinmin section in Jiaozishan town, Anshun City, southern Guizhou Province is 105 km away from the Duanshan A and B sections of the Dalong Formation (Fig. 3). Lithologies in the Xinmin section (Fig. 7) comprise thin-bedded



chert and carbonates including micritic limestones, with siltstone interlayers and occasional thin, gray–green, volcanic tuff beds (Beds 1–6, Shen J. et al., 2012b; 2021). Plant fossils mainly come from the black, thin-bedded mudstone interlayers in the middle of Bed 2 and the top of Bed 4. These comprise large conifer branches including secondary or tertiary branches that can reach up to 50 cm long and *Taeniopteris* leaves with good cuticle, amongst smaller, fragmentary fossils of *Lepidostrobohyllum*, *Paracalamites*, *Pecopteris*, *Gigantopteris*, *Cordaite*s and *Sphenobaiera* (Li et al., 2019). The conifers with well-preserved cuticles have been identified as *Anshuncladus xinminensis*, *A. contiguous*, *A. aduncatus*, *Pseudoullmania frumentarioides* and *Szecladia multinervis*. Li et al. (2019) interpreted the conifers to be preserved very close to where they grew, inhabiting coastal habitats, due to their completeness. These conifers are only preserved in the terrestrial-marine interbedded facies of the Dalong and Heshan formations and are absent in terrestrial facies rich in fossil plants (Liu et al., 2007, 2013; Li et al., 2019). In contrast, the fragmentary *Gigantopteris* and *Pecopteris* leaves in the Dalong Flora were likely transported greater distances.

Based on the presence of the conodont *Hindeodus parvus* in the Dalong Formation, the PTB is placed in the middle of the limestone at the bottom of Bed 5. Beds 1 to 6 contain a Permian–Triassic fauna (Fig. 7) including bivalves (*Hunanopecten exilis* - *H. qujiangensis* in the Permian and *Claraia liuqiaoensis* in the Triassic), ammonites (*Pseudotirolites* - *Sinoceltites* of the Permian and Triassic *Xenaspis*), and conodonts (*Clarkina changxingensis*, *C. yini* Permian and *C. meishanensis*, *Hindeodus changxingensis*, *H. parvus* Triassic assemblages) (Zhang et al., 2014; Yang, 2015; Li et al., 2019). The biostratigraphic evidence shows that this section is complete (Li et al., 2019).

### 3.5.2. Duanshan A Section

The Duanshan A section is in the same town as the Xinmin section in Huishui County, Guizhou province (Fig. 3), and the two sections share similar plant as well as marine faunal records. The section is lithologically divided into eight Beds (Fig. 7)

that comprise gray, siliceous mudstone, gray blue, thin-bedded micritic limestone, with gray black or gray–yellow mudstone interlayers. This is quite similar to the succession in the Xinmin section, except that Bed 3 is composed of gray yellow mudstone and white volcanic ash. Beds 1–2 and 4–6 contain the *Hunanopecten exilis* - *H. qujiangensis* bivalve assemblage, the *Pseudotirolites* - *Sinoceltites* ammonite assemblage, and the *Albaillella triangularis* - *A. yaoi* radiolarida assemblages (Fig. 7) and allow us to correlate Beds 3–8 in this section with the middle of Bed 3 to the top of Bed 4 in the Xinmin section (Fig. 7).

### 3.5.3. Duanshan B Section

The Duanshan B section is on the opposite side of the road to the Duanshan A section (Fig. 3) and is much shorter. It contains more grayish yellow mudstone and pelitic siltstone than Duanshan A and shares a similar plant fossil record (Fig. 7). According to the lithological successions and the location of the Duanshan A and B sections, Beds 1–6 of Duanshan B corresponds to Bed 3 in Duanshan A (Fig. 7).

### 3.6. Kayitou Flora (Griesbachian interval, Permian–Triassic transition)

The Kayitou Formation conformably overlies the Xuanwei Formation and represents paralic facies (Fig. 1). According to the plant fossils and conchostracan biostratigraphy and other criteria, the PTB occurs near the base of the Kayitou Formation (Yu et al., 2010; Chu et al., 2016; Wignall et al., 2020). The Kayitou Flora occurs in the bottom of the Kayitou Formation, but its exact age is contentious (Chen et al., 2011). The widespread appearance in south China of the lycopod *Tomioostrobus* (= *Annalepis*) has been suggested to coincide with the end of the EPPC and the beginning of Triassic (Yu et al., 2010, 2015). Six sections contain the Kayitou Flora in South China and have similar plant fossil compositions (Fig. 8). To eliminate the influence of diachroneity, representative sections containing datable marine biota and typical plant fossils are selected in this study: the Chinahe, Tucheng and Mide sections. In general, these sections contain limited occurrences of plant fossils, typically within single beds and abundance is low. This is noticeably different from

plant fossil occurrences prior to the EPPC.

### 3.6.1. Chinahe Section

The Chinahe section in Xuanwei City, eastern Yunnan Province (Figs. 8, 9) contains terrestrial facies of the Xuanwei Formation (Beds 1–25) and marine facies of the Kayitou Formation (Bed 26–29). At Chinahe, the EPPC is defined at the level of disappearance of the Xuanwei Flora together with the last coal line in Bed 25 and the appearance of *Tomioostrobus* (= *Annalepis*) (Fig. 9) between Beds 25 and 26 at the lithologic boundary between the Xuanwei and Kayitou formations. The last coal in the Xuanwei Formation marks the top of the Xuanwei Formation at Chinahe. Bed 26 at the base of the Kayitou Formation contains *Tomioostrobus* (= *Annalepis*) *augusta*, *T. (A.) brevicystis*, *T. (A.) latiloba*, *T. (A.) zeilleri*, *T. (A.)* spp., *Sphenopteris tenuis*, *Fasciapteris stena*, *Peltaspermum martinisii*, and fragmentary remains of *Gigantopteris* spp. and *Pecopteris (Asterotheca) orientalis* that extend their range from Beds 21 and 24 respectively (Fig. 9). Above this level, plant fossils are extremely rare and limited to fragments of *Tomioostrobus* (= *Annalepis*) in Bed 27, which occur above the first occurrence of the bivalve *Pteria variabilis* at this location. This bivalve also occurs above the EPPC boundary in the Tucheng and Mide sections (Figs 8, 9). According to the presence of the *Pteria variabilis*-*Promyalina schamarae* bivalve assemblage in Beds 26–28 (Song T. et al., 2018), the age of plant assemblage in Beds 26–27 from the Chinahe section is considered to be Griesbachian.

### 3.6.2. Tucheng Section

The Tucheng section in Panxian County, western Guizhou Province (Fig. 8) exposes a thick coal (Bed 16) of the Xuanwei Formation, and the overlying Kayitou Formation (Beds 17–23) (Fig. 9; Yu et al., 2015; Broutin et al., 2020). Beds 17–20 are gray-yellow, thin-bedded mudstone except for Bed 19, a gray-yellow sandstone. Fossil plants occur in the middle of Beds 17 and 18, and include *Lepidodendron* sp., *Tomioostrobus* (= *Annalepis*) *zeilleri*, *T. (A.) brevicystis*, *Pecopteris* sp. and *Peltaspermum martini*. The upper part of Bed 21 is gray-green, medium-bedded

siltstone interbedded with thin beds of mudstone. Bed 22 is a gray-brown, medium-bedded siltstone, while Bed 23 changes into gray green siltstone and contains *Sphenopteris* sp., *Peltaspermum mattenii*, *P. lobutalum*, *P. sp.*, *Pecopteris* sp., *Gigantonoclea guizhouensis*, *Gigantonoclea* sp., *Gigantopteris dictyophylloides* and *Gigantopteris* sp. (Fig. 9).

Beds 17–23 at Tucheng contain marine fossils including the bivalves *Unionites fassaensis*, *U. canalensis*, *U. sp.*, *Leviconcha orbicularis*, *L. praeorbicularis*, *Pteria ussurica variabilis* and *P. murchisoni leshanensis* (Fig. 9). Correlation with other sections (Fig. 9), places the termination of the EPPC in the lower middle of Bed 17, below the first appearance of *Tomioostrobus* (= *Annalepis*).

### 3.6.3. Mide Section

The Mide section in Xuanwei City, eastern Yunnan Province (Fig. 8) is composed of thin-bedded, gray green siltstone (Beds 15–17 and 24–26), while Bed 18 is a thin, white volcanic ash (Fig. 9; Chen et al., 2011; Bercovici et al., 2015). Bed 19 is a yellowish green sandstone and Bed 20 a gray-yellow siltstone. Beds 21–23 are pale yellow to gray-brown siltstone. Bed 16 contains *Paracalamites stenocoastatus*, *Gigantonoclea guizhouensis*, *Gigantopteris* sp. Beds 20 and 21 contain *Tomioostrobus* (= *Annalepis*) *zeillerei*, *T. (A) brevicystis*, *Peltaspermum martensii*, *P. sp.*, *Pecopteris* sp. and lycopsid roots of *Stigmaria*. Marine biota is abundant in Beds 18–25 (Fig. 9) and includes the bivalves *Unionites fassaensis*, *U. canalensis*, *U. sp.*, *Leviconcha orbicularia* and *L. praeorbicularis*, the ammonite *Ophiceras* sp. and the ostracod *Langdaia suboblonga* (Forel et al., 2020). The EPPC termination level occurs at the beginning of Bed 19 prior to the appearance of *Tomioostrobus* (= *Annalepis*) (Fig. 9).

### 3.7. Feixianguan Flora (Dienerian or Smithian, Early Triassic)

The lower part of Feixianguan Formation (Fig. 1) is correlative with the Triassic portion of the Kayitou Formation (Tong et al., 2019) and conformably overlies the Xuanwei Formation (Figs. 1, 2). Fossil plants occur at the top of the Feixianguan Formation one metre below the boundary with the overlying Yongningzhen Formation

(Fig. 10). Bivalve data indicate that the age of the fossil plant assemblage in the Feixianguan Formation is Dienerian or early Smithian (Yin et al., 1985; Gou et al., 1996; Tong et al., 2019). In South China, only the Feixianguan Formation in the Pojiao, Lubei sections and the Dongchuan Formation in one section near Lubei Village (Feng et al., 2018) contain plant fossils of this age and all yield the same flora. Due to the similar age and floristic composition of the sections of the Dongchuan and Feixianguan formations, we combine them as one Feixianguan Flora and focus on describing the Feixianguan sections as much less is known about the flora of the Dongchuan Formation. In general, the Pojiao and Lubei sections contain limited plant fossil layers, and each layer yields a few fossil plant fragments. The sedimentary facies of the Feixianguan Formation comprise interacting terrestrial and marine facies according to the lithological succession and marine bivalve fossil yielded in the lower beds below the plant fossil horizons.

### 3.7.1. Pojiao Section

The Pojiao section is located in Pojiao village, Huize County, northeastern Yunnan Province (Fig. 8). It exposes the Feixianguan Formation (Beds 1–9) that comprises cyclic beds of reddish purple and gray black sandstone (Fig. 10), and the overlying Yongningzheng Formation (Beds 10–11) that gradually change from gray green thick-bedded calcareous sandstone (Bed 10), into dark gray limestone (Bed 11). In the Feixianguan Formation, fossil plants occur in at the top of Bed 9 in two layers of thin-bedded siltstone interbedded with gray green thick sandstone. These comprise *Phyllothea* sp., *Neocalamites* sp., *Equisites* sp., *Cladophlebis* sp., *Todites* sp., *Voltzia heterophylla*, *Peltaspermum* sp., *Baiera* sp. and *Taeniopteris* sp. (Fig. 11). The Bed 9 plants are abraded preventing species-level identifications with the exception of *Peltaspermum* and *Voltzia* from which an almost fertile shoot is known. In this flora there are abundant gymnosperm seeds, but these are not listed in the range diagram (Fig. 10) as they most likely represent the seeds of one (or more) of the other gymnosperms in the flora (i.e., *Voltzia*, *Peltaspermum*, *Baiera*, *Taeniopteris*). The bottom and middle parts of the Feixianguan Formation at Pojiao are mostly marine

facies and contain two bivalve assemblages with the lower *Claraia wangi* assemblage typical of the early Induan, and the upper *Eumorphotis multiformis* - *Claraia aurita* - *Claraia stachei* assemblage typical of middle-late Induan of Feixianguan Formation (Gou et al., 1996; Tong et al., 2019).

### 3.7.2. Lubei Section

The Lubei section in Lubei village, Huize County, northeastern Yunnan Province (Xu et al., 2017; Shen J. et al., 2019b) is close to Pojiao (Fig. 8). It exposes the late Permian Xuanwei Formation (Beds 1–3), the early Triassic Feixianguan Formation (Beds 4–8) and later Early Triassic Yongningzhen Formation (Beds 9–13) (Fig. 10). The Feixianguan Formation comprises purple red to gray green, thin to medium-bedded lithic sandstone and siltstone (Xu et al., 2017; Shen J. et al., 2019b). Fossil plants occur in Beds 5–6 and comprise *Phyllothea* sp., *Neocalamites* sp., *Equisites acanthodon*, *Equisites* sp., *Cladophlebis* sp., *Peltaspermum* sp., *Taeniopteris* sp. and *Voltzia* sp. (Fig. 11).

### 3.8. Lingwen Flora (Spathian, Early Triassic)

The Lingwen section in Hainan Province (Figs. 1, 8) was previously documented by Zhou et al. (1979) and Zhang et al. (1992), but the flora has not been investigated subsequently. Only one section contains the Lingwen Flora in South China. The Lingwen Flora is considered to have been deposited during the Olenekian based on plants and palynomorph assemblages that are similar to those from the French Buntsandstein (Gall and Grauvogel-Stamm, 2005). The flora at Lingwen contains elements including *Pleuromeia*? sp., *Todites shensiensis*, *Asterotheca szeiana*, *Ctenozamites cycadea*, *Leuthardtia ovalis*, *Vittaeohyllum* sp., *Albertia*, *Voltzia* and *Pelourdea* (= *Yuccites*) (See full fossil list in supplementary dataset; Fig. 12) that are also common in the lower part of the Badong Flora (see below). The sediments of the Lingwen Formation comprise terrestrial fluvio-lacustrine facies (Zhou et al., 1979; Zhang et al., 1992).

### 3.9. *Badong Flora (Anisian, Middle Triassic)*

Plant fossils in the Badong Formation (Fig. 1) were first reported by Ye et al. (1979) and systematically investigated by Meng et al. (1993, 1995, 1996, 1998). The Badong Formation has a widespread distribution across the Upper and Middle Yangtze area in South China (Fig. 13). It conformably overlies the Jialingjiang Formation (Figs. 1, 14) and comprises five members, but in most areas only three or four are present due to erosion during Ladinian regression. In Hunan Province, the Sangzhi County area yields the longest stratigraphic sections especially around the village of Hongjiaguan (Fig. 13) where an almost continuous section occurs, although it contains few plant fossils. In contrast, the nearby section in Furongqiao Village contains abundant plants but is less continuous. These two sections are correlated with each other and included as the combined Hongjiaguan and Furongqiao section (Fig. 14).

Lithologically the Badong Formation comprises pale gray, yellow to gray green calcareous mudstone to siltstone in Member 1 above a gypsum-karst breccia at the top of Jialingjiang Formation, and purple red, thick-bedded siltstone to sandstone with interbedded blue mudstone to siltstone in Member 2 (Fig. 14). Member 3 comprises gray-yellow calcareous mudstone to siltstone and limestone, and Member 4 purple red, thick-bedded siltstone to sandstone, while Member 5 comprises gray blue to yellow, thin-bedded siltstone and gray black, thin-bedded limestone to calcareous siltstone. In the Hongjiaguan and Furongqiao section, only members 1 and 2 are present (Fig. 14). The boundary between members 4 and 5 contains the first coal in South China after the PTB, and thus represents the end of the “coal gap” (Meng et al., 1995; Retallack et al., 1996). The sedimentary facies of the Badong Formation are coastal or tidal in members 1, 2, 4 and 5 and the abundant marine biota preserved together with in-situ ‘mangrove-like’ plants of *Lepacyclotes* (= *Annalepis*) and *Pleuromeia* (Meng et al., 1995).

Fossil plants in the Badong Formation mostly come from the boundary of members 1 and 2 (Fig. 14), although less common and more poorly preserved fossils also occur in green blue interlayers in members 2 and 4. We found eight plant fossil

locations at Hongjiaguan with four locations combined as one, and four in Furongqiao Village (Fig. 15). The flora comprises *Lepacyclotes* (= *Annalepis*) *brevicystis*, *L. (A). zeilleri*, *L. (A). sangzhiensis*, *L. (A). angusta*, *Pleuromeia sanxiaensis*, *P. marginulata*, *P. hunanensis*, *Equisites gracilis*, *Neocalamites shanxiensis*, *Todites shensiensis*, *Peltaspermum multicostatum*, *P. miracarinatum*, *Yuccites vogesiacus*, *Y. anastomosis*, *Yuccites* sp., *Voltzia heterophylla*, *V. curtifolia*, *V. sp.*, *Willsiostrobus cordiformis*, *Cardiocarpus triquestrus*, and *C. sp.* (Fig. 15).

In Member 1 of the Badong Formation, typical Anisian bivalves of the *Leptochondria* - *Myophoria goldfussi mansuyi* assemblage are preserved in siltstones–mudstones, whilst Member 3 contains the bivalves *Plagiostoma* sp., *Placunopsis* sp., the conodonts *Neospathodus* sp. and *Enantiognathus* sp., and the ammonoid *Progonoceratites* sp. that indicates an Anisian age (Meng et al. 1995).

### 3.10. Carnian and Norian (Daqiodi and Shazhenxi) flora

Carnian and Norian floras are quite common in South China although the boundary between these stages is poorly constrained. The Carnian/Norian floras are known from the Daqiaodi Formation at Yongren on the border between Yunnan and Sichuan Provinces, the Jiuligang Formation at Yuan'an in western Hubei Province, and the Japeila Formation in eastern Xizang Province (Tibet), collectively from over 24 locations in South China; Xujiache Formation at Guangyuan in Sichuan Province, the Dajing Formation in the border area of Sichuan and Yunnan provinces, the Anyuan Formation in Hunan and Jiangxi provinces, the Bagong Formation in southern Fujian Province and the Malugou Formation at Tianqiaoling in Jilin province (Xu et al., 1979; Li et al., 1995; Liu et al., 2009). The age of this flora is determined by marine biostratigraphy (Li et al., 1995). The lower part of the flora comprises the *Abropteris* - *Pterophyllum longifolium* Assemblage that includes *Equisetites arenaceus*, *Abropteris cottonii*, *Mixopteris intercaearis*, *Pterophyllum longifolium*, *P. jaegeri*, *Angiopteris antiqua*, *Sagenopteris glossopteroides*, *Danaeopsis marantacea*, *Ctenozamites chinensis*, *Stenopteris bifurcata* and *Ctenozamites chinensis* and resembles the early Late Triassic Lettenkohle Flora in western Europe (Li et al.,



1995). The upper part of the flora comprises the *Dictyophyllum* - *Drepanozamites* or *Dictyophyllum* - *Cycadocarpidium* Assemblages, including *Dictyophyllum nathorstii*, *Clathropteris elegans*, *Reteophlebis simplex*, *Drepanozamites nilssonii*, *Doratophyllum hsuchiahoense*, *Anomozamites loczyi*, *Podozamites* (*Cycadocarpidium*) *gigantean*, *Cycadocarpidium swabii* and *Hausmannia ussuriensis*, and thus considered to be Norian (Li et al., 1995), comparable to the Nariwa Flora of Japan.

### 3.II. Rhaetian (Yangbaichong) flora

The Rhaetian Flora (Fig. 1) is represented by the plant assemblage from the Yangbaichong Formation at Hengyang in South Hunan province and comprises the *Ptilozamites* - *Anthrophyopsis* Assemblage. The plant assemblage in the Anyuan Formation probably belongs to this flora as well and comprises *Ptilozamites chinensis*, *Anthrophyopsis leeiana*, *Clathropteris meniscioides*, *Todites crenatus*, *Nilssoniopteris oligotricha*, *N. xuiana*, *Pterophyllum ptilum*, *Podozamites distans*, *Cycadocarpidium erdmannii* and *Stalagma samara* (Li et al., 1995). It is comparable to the *Lepidopteris* zone floras from eastern Greenland and Germany (Zhou et al., 1989), and is considered to be of Rhaetian age (Li et al., 1995).

## 4. Permo-Triassic vegetation change in South China

Artinskian (Middle Permian) to Rhaetian (Late Triassic) macro and micro-floral stratigraphic range data have been compiled to determine the complete range of plant taxa present during the End Permian to Middle Triassic before normalization (Figures 18, 19). Then normalized data from the fossil plant ranges in South China from the Late Permian to the early Late Triassic are analyzed to show species richness and origination and extinction taxa number for the entire flora (Fig. 18), and origination, extinction rates of the entire flora together with the rates for individual plant group (Fig. 19). These data show an increase in total species richness from the Artinskian (late Cisuralian) and peak species richness in the Wuchiapingian, followed by a decrease culminating in a diversity lowpoint either side of the PTB (Fig. 18). There is

no evidence for a floral crisis in the Capitanian although this may be because our data is compiled at the stage level, whilst in the marine realm extinction many losses were intra-Capitanian (Bond et al., 2010). The Lower Triassic saw low species richness (typically <20 species), with values only increasing during the Carnian and Norian (Upper Triassic) before declining again in the Rhaetian.

The plant diversity decline started from the lower Changhsingian with only species richness decline and flora alternation without apparent vegetation abundance reduction, characterized by the decline of gigantopterid flora in South China (Yu et al., 2015). The termination of the EPPC is marked by both these phenomena including the notable and abrupt drop of species together with cessation of coal formation, marking the collapse of terrestrial ecosystems (Fig. 22). The low-diversity survivors in the Kayitou Formation represents a holdover subset of the Cathaysian Flora including *Lepidodendron*, *Paracalamites*, *Pecopteris*, *Sphenopteris*, *Fasciapteris*, *Gigantopteris* and *Gigantonoclea*, mixed with the opportunistic lycopod *Tomioistrobus* (= *Annalepis*). This floral assemblage is only present in the basal-most part of the Kayitou formation suggesting only a short survival interval. In this regard, they are closely comparable with the numerous, short-ranging holdover taxa in the marine record which thrived between two extinction pulses in the early Griesbachian (Song et al., 2012). Previous analyses of species richness within Paleozoic floras suggest Pennsylvanian wetlands of Europe (Cleal et al., 2012) had local standing diversity typically in the region of 40–60 species, but with regular species originations and extinctions (Cleal and Thomas, 2004; Cleal et al., 2012). From our analyses, species richness has been calculated using data compiled in stage-level time bins and from the pre-EPPC Xuanwei Flora values and is more comparable to Pennsylvanian regional-scale richness of the Variscan Foreland with standing diversity of >70 species (Cleal et al., 2012). Although not from the Permian, these data suggest a standing diversity of the pre-EPPC Longtan and Xuanwei floras was comparable to Euramerican Carboniferous peat forming communities, but the early Triassic diversity is significantly below this level (Fig. 18) and more comparable to diversity of the Devonian Rhyniophytic and Eophytic evolutionary floras (Cleal and Cascales-Miñana,

2014).

The species origination rate began to exceed the extinction rate in the Early Triassic Feixianguan Formation, representing the earliest stage of the species richness recovery following the EPPC. This interval is characterized by plant populations with low abundances and an absence of coals. The first post-EPPC coals in South China are in the Anisian, and their reappearance coincides with that of terrestrial herbivores (*Lotosaurus*) in Member 2 of the Badong Formation (Meng et al., 1995; Hagen et al., 2018). In the Upper Triassic, more floras are reported (Li et al., 1995) demonstrating the continued diversification in humid conditions. Peak Triassic species richness occurs in the Carnian and Norian when diversity attained a comparable level to that of the Late Permian (Fig. 18).

Overall, late Permian to middle Triassic plant evolution patterns can be resolved into four distinct phases according to the macro plant fossil data, palynology data, biomarker and wildfire proxies (Fig. 22). Phase 1 occurred during the Changhsingian and terminated at the end of the EPPC. Phase 2 consists of the holdover Permian flora found in the Permian–Triassic transitional Kayitou Formation, including the Chinahe, Tucheng and Mide sections (Changhsingian–Griesbachian interval). Phase 3 represents the recovery of species richness during the late Induan in the upper part of the Feixianguan section. Finally, Phase 4 represents substantial recovery after the Olenekian, as seen in floras of the Lingwen Formation at Lingwen and the Badong Formation, including the Hongjiaguan and Furongqiao sections.

#### *4.1. Phase 1: Pre-extinction floras and the EPPC*

The Changhsingian flora at Chahe (Fig. 3) and Chinahe (Fig. 4) has a typical Cathaysian character. The fragmented plant assemblage shows considerable turnover of short-ranging taxa and a final, rapid loss of almost all taxa, including long-ranging taxa, at the end of the phase. Plant taxa ranges vary between the sections. The minor losses during the initial episode of the EPPC can be considered a turnover of short-ranging taxa while the disappearance of long-ranging taxa marks a severe crisis. For example, the long-ranging elements both in the Chahe and Chinahe sections including

*Lobatannularia multifolia*, *Pecopteris orientalis*, *P. arcuata*, *P. gracilentia*, *P. taiyuanensis*, *Rajahia guizhouensis*, *Fascipteris sinensis*, *Compsopteris contracta*, *C. punctinervis*, *Gigantopteris nicotianaefolia*, *Gigantonoclea largrelii*, *Gigantopteris dictyophylloides* and *Neuropteridium* were common in every layer bearing fossil plants, until their disappearance at the end of the EPPC marked a dramatic ecological crisis.

Floral assemblages from the Chahe and Chinahe sections lack conifer macrofossil remains. This phenomenon is quite common in South China with Guadalupian–Cisuralian floras lacking conifers in terrestrial or terrestrial-marine sections. Conifers are only found in the fully marine facies of the Dalong Formation which yields both conifers and the cycadophyte *Taeniopteris* with well-preserved cuticles (Li et al., 2019). This pattern is in marked contrast to contemporaneous floras from Europe and North China where conifers occur in terrestrial and terrestrial-marine facies (Wang et al., 1985, 1996). According to taphonomic features of the fossils and the sedimentology, the conifers in the Dalong Formation are likely to have lived in coastal settings or on islands. Species of conifer in the Dalong Formation all disappear before or during the EPPC and do not reappear in the Triassic. Mesozoic-type conifers *Voltzia* and *Albertia* appear in South China after the EPPC. Due to lack of understanding of the evolutionary relationships within Paleozoic and Mesozoic conifers as whole plants, it is unknown whether stratigraphically younger Triassic conifers are closely related to the Late Permian conifers from South China.

The abrupt abundance reduction of the terminal EPPC is caused by elevated extinction and declining origination rates that are seen in the entire flora and amongst each plant group (Fig. 19). Most of the plants from Cathaysian floral communities disappeared during this event, including Paleozoic lycopods, noeggerathialean progymnosperms and cordaitalean coniferophytes, leaving only a few survivors. Five sections from different sedimentary facies allow the details of the plant evolution pattern to be deciphered: terrestrial facies from the Chahe section in the Xuanwei Formation, terrestrial-marine transitional facies from the Chinahe section in the Xuanwei Formation, and marine facies from the Xinmin and Duanshan A and B

sections in the Dalong Formation.

The EPPC record is that of coal-swamp flora rather than upland taxa (Yu et al., 2015). Xeric upland taxa took over the empty space after the extinction of coal-swamp taxa a trend that began slightly before the terminal crisis, as shown by the gradually increasing proportion of pollen before the EPPC (Yu et al., 2008). Moreover, the palynological record from the Changhsingian paralic Kayitou Formation in Yunnan Province (Ouyang, 1991) is similar to the marine Yinkeng Formation in Meishan section of Zhejiang Province, and other sections in South China (Zhang et al., 2004). There were few fungal/algal spores before the lithological boundary of the Permian and Triassic. The palynological record from before the crisis in terrestrial locations in Xinjiang differs from that in South China, being mainly composed of gymnosperm pollen, thereby showing an earlier transition from Paleophytic to Mesophytic flora in this northern area (Qu et al., 1986) (Fig. 22). The crisis in the Guodikeng Formation in Xinjiang was coupled with an abundance of lycopod spores (Qu et al., 1986; Chu et al., 2015).

Black carbon (BC) content and biomarkers for combustion process such as polynuclear aromatic hydrocarbons (PAHs) are useful tools for indicating wildfires (Shen W.J. et al., 2011, 2012; Xie et al., 2007; Chu et al., 2020). In the paralic Chinahe section, charcoal content peaks in the upper part of Bed 25 to Bed 26 with a similar peak also seen in the coeval beds 23–24 at Meishan (Fig. 20), although PAHs peak later in Bed 26 in Meishan (Xie et al., 2007; Shen W.J. et al., 2011) suggesting there was still fuel for combustion, after the main plant crisis, albeit for a short period of time (Shen W.J. et al., 2011).

#### 4.2. Phase 2: Griesbachian interval extinction and survival

The Griesbachian plant assemblage from the Kayitou Formation is characterized by pioneering or opportunistic taxa comprising Mesozoic-type lycopods *Tomioostrobus* (= *Annalepis*), mixed with holdover taxa including lycopods (*Lepidodendron*), sphenophytes (*Paracalamites*), ferns (*Pecopteris*) and giantopterids (*Gigantopteridium*). This composition is mirrored in palynological data and marked

as a distinct, Permian–Triassic transitional flora (Chen et al., 2011; Yu et al., 2015). The palynological record in the Dalongkou section in Xingjiang (NW China) also comprises a transitional assemblage, with a mix of Permian and Triassic species, but it differs from the South China record in having a higher percentage of gymnosperm pollen (Qu et al., 1986; Ouyang, 1991, 2007). Although holdover elements persist into the Kayitou Formation, they rarely range more than 30 m above the base in all sections, whilst most disappear within 5 m. The palynology record confirms the short duration of survival of the holdover elements, whilst the pioneers persisted for much longer into the Late Triassic (Ouyang, 1991; Grauvogel-Stamm and Ash., 2005; Yu et al., 2008, 2010). The survival elements are restricted to refuges, for instance swamp facies preserved in the paralic Kayitou Formation (Li et al., 1995; Grauvogel-Stamm and Ash., 2005; Yu et al., 2008).

Post EPPC opportunistic plant species abruptly occupied empty niches but disappeared shortly afterwards following the initial stages of ecosystem recovery. In addition to holdover and opportunist taxa, the early Induan flora also includes the surviving seed fern *Peltaspermum* that rapidly recovered after the EPPC in terms of both its species richness and abundance, together with conifers that gradually radiated (Whittaker & Goodman, 1979; Huston and Smith, 1987; Glenn-Lewin et al., 1992; Ren et al., 2001). The success of *Peltaspermum* and conifers marks forest ecosystem's re-establishment and shows spatial and ecological species richness, such as those from the late Early Triassic Feixianguan and Lingwen Floras that contain various conifers (Zhang et al., 1992; Li et al., 1995).

Following the dominance of spores over pollen in the early Griesbachian substage, the percentage of pollen increases in the South China palynological record (Zhang et al., 2004; Yu et al., 2008; Ouyang and Zhu, 2007). Although there is only a single, rare megafossil species of *Peltaspermum* in the Kayitou Formation, palynology indicates the widespread presence of seed plant groups that are absent from the macrofossil record (Fig. 17).

The majority of the plant taxa in Phase 2 are inherited from the Permian suggesting the Kayitou Flora belongs to the survival stage rather than the recovery

stage. Wildfire proxies, such as black carbon, show that wildfires were still prevalent during this interval (Xie et al., 2007; Shen W.J. et al., 2011, 2012; Yin et al., 2012; Fig. 20),

During Phase 2 in the Kayitou Formation, the plant extinction rate is higher than the origination rate, due to the demise of holdover taxa. This is followed by an absence of plants fossils from the middle Kayitou Formation to the middle of the Dongchuan Formation (Feng et al., 2018) (Fig. 1).

#### 4.3. Phase 3: Late Griesbachian–Smithian species richness recovery

Phase 3 marks the start of the post-EPPC recovery and is recorded in the Dienerian-Smithian Feixianguan Formation. The Feixianguan Formation contains 16 genera and 17 species, thus with low species numbers within individual genera. The origination rate in the Feixianguan Formation exceeds the extinction rate for the first time since the EPPC, although extinctions still occurred but at low levels (< 20 species extinctions per time bin). Within individual plant groups (Fig. 19), the origination rate of Mesozoic lycopod, sphenophyte, cycads, ferns and conifers noticeably exceeds their extinction rates, whilst the origination rates of seed plants for example seed ferns, ginkgophytes and some gymnosperms, such as *Pelourdea* (= *Yuccites*), are similar to the extinction rates.

Plant taxa in the Feixianguan Formation consists of small numbers of Mesozoic-type lycopods, abundant sphenophyll branches (including *Neocalamites* and *Equisites*), and includes Mesozoic-type ferns (*Todites* spp., *Anomopteris*, *Dictyophyllum* (= *Thaumatopteris*)), seed ferns (*Peltaspermum* sp.), cycads (*Taeniopteris* sp.), ginkgophyte (*Baiera* sp., *Sphenobaiera* sp.) and some conifers (*Albertia* sp., *Voltzia heterophylla*, *Voltzia* sp.) (Zhou et al., 1979; Figs. 10). Most of the plants, especially *Peltaspermum* and the conifers, are considered to be floral elements adapted to dry and hot climates based on their thick cuticles (Poort and Kerp, 1990; Huang and Lu, 1992; Taylor et al., 2009).

Early Triassic (Late Griesbachian to Smithian) palynological data from South China is absent whilst the Xinjiang record from North China is derived from the

Jiucaiyuan and Shaofanggou formations (Qu et al., 1986). Spores dominate over pollen in both formations although the younger levels of the Shaofanggou Formation have slightly higher pollen content (Qu et al., 1986). The abundance of the Triassic lycopod spore *Lundbladispora* in those two formations denotes the success of lycopods during the Griesbachian and Smithian (Qu et al., 1986). Using biomarker proxies for plant abundance, retene, simonellite and dehydroabietane, which are likely to be derived from herbaceous rather than woody plants because of low C/N ratios (<10), suggests recovery was underway during the Smithian (Saito et al., 2013). Nonetheless, plant fossils are rare and coal formation is still absent during Phase 3.

#### 4.4. Phase 4: Spathian abundance recovery

The Spathian Lingwen flora and the Anisian Badong flora are dominated by Mesozoic-type lycopods *Lepacyclotes* (= *Annalepis*) and *Pleuromeia* alongside sphenopsids (*Equisites* and *Neocalamites*), while gymnosperms (*Taeniopteris*, *Peltaspermum* (*Vittaeophyllum*), *Pelourdea* (= *Yuccites*) and the conifer *Voltzia*) are common (Figs. 14, 15). Diversity within the Lingwen and Badong formations are broadly similar to that of the Early Triassic Feixianguan Formation with 22 genera and 29 species in Lingwen flora and 17 genera and 27 species in Badong flora present. However, plant abundance is much higher in the Badong Formation, as reflected by fossil abundance and the development of peat (Meng et al., 1995). Significantly, Member 2 of the Badong Formation yields the terrestrial tetrapod *Lotosaurus* (Figs. 14, 15), showing there was sufficient vegetation to support large herbivores (Hagen et al., 2018).

According to palynological data in South China, gymnosperm pollen is the major constituent, especially in the Spathian Lingwen Formation (Zang et al. 1992; Meng et al. 1995). In the Xinjiang area, gymnosperm pollen content slightly exceeds that of spores in the Shaofanggou Formation and is increasingly common in the Karamay Formation of the Xinjiang Dalongkou section. This is similar with the Badong Formation of South China in the Hongjiaguan section (Qu et al., 1990; Meng et al., 1995) and indicates progressive vegetation changes during the Spathian. Increased



abundance of the conifer derived biomarker pimarane during the Spathian in South China denotes a vegetation change from the Griesbachian to Smithian lycopods/herbaceous bryophytes to conifer-dominated floras (Saito et al., 2013) and correlates well with gymnosperm pollen dominance of over 90% in Lingwen flora (Zhang et al., 1992) (Fig. 22). In addition, rapid increases of C/N ratios (>10, reaching 28) after the Smithian-Spathian boundary in South China from the Chaohu section, reveals the flourishing of vascular land plants (Saito et al., 2013). Plant macro fossils, palynology and biomarker data all record species richness and abundance recovery happened after the Spathian.

## 5. Discussion

### 5.1 Distinctions between macro- and micro-floral (palynology) data

In paleobotanical studies across the PTB in South China, the study of Xiong and Wang (2011) stands out for documenting a gradual, stepwise loss in plant megafossil species richness in the run up to the EPPC while concurrent palynological records only recorded a minor fluctuation in species richness. Their study was based on an uncritical compilation of data from literature with identifications that were not verified by examination of original materials, and species were not collected in a detailed, bed-by-bed stratigraphic framework as undertaken here for the EPPC interval. In our study, as well as having the extinction level, our megafossil data also shows a gradual, stepwise loss of megafossil species richness (Figs. 4, 5, 7, 9), presumably related to gradual facies and/or environmental changes (MacLeod, 1997; Stevens et al., 2011) in the run up to the extinction level. These environmental or facies changes adversely affected plants in wetland, peat forming clastic settings (e.g., Wang et al., 2011; Yan et al., 2019; Feng et al., 2020), but they do not provide insights into the vegetation from contemporaneous upland, extrabasinal settings (see DiMichele et al., 2020) such as the Kiangsi Oldland in South China (Fig. 1; Wang et al., 2020).

We consider this is a probable consequence of taphonomic megabias in which the microfossil record potentially samples a larger geographical source area including

uplands compared to megafossil assemblages that are extensively restricted to lowland depositional settings (e.g., Looy et al., 2004; Neregato et al., 2016; DiMichele et al., 2020; Cleal et al., 2021). Support for this comes from the characteristically Mesozoic palynomorphs *Wilsonisporites* (unknown affinity), *Neoraistrickia* (putative isoetalian lycopsid; Singh 1971) and *Pteruchipollenites* (corytosperm gymnosperm) found in conglomerates from the basal Xuanwei Formation (Neregato et al., 2016) whilst the plants that produced them are absent from the megaflora. This shows their parent plants persisted in South China outside the coastal wetlands preservation window and survived the EPPC in this region. In addition, xerophyte palynomorphs recorded in the Chahe section (Yu et al., 2008) are distinct from the contemporaneous wetland megaflora and include disaccate striatites (Coniferopsida), *Protohaploxypinus* and *Vittatina* (Peltaspermales, Ginkgopsida; Balme, 1995), *Lueckisporites* (Majonicaceae, Coniferopsida; Clement-Westerhof, 1974), *Striatopodocarpidites* (Glossopteridales, Ginkgopsida; Pant, 1977; Balme, 1995) and *Taeniaesporites* (= *Lunatisporites*: Podocarpaceae, Coniferopsida; Clement-Westerhof, 1974). While first appearing in the late Permian Xuanwei Formation, these palynomorphs became dominant in the Early Triassic Kayitou Formation where they played significant roles in post-EPPC floras and the EPPC recovery (Fig. 17).

In the Changhsingian, spore producing plants including lycopods, sphenophytes and ferns were dominant in the megafossil record, while Paleozoic lycopod spores are absent from the palynology record (Fig. 16, 17). This discrepancy indicates that to fully characterize the flora information from both sources are required. Palynological data likely samples flora from a wider setting than just the lowland depositional environments of the Xuanwei Formation but has limits in reconstructing the affinity diversity and abundance as it is often hard to correlate palynological species with parent plants. In contrast, plant macrofossil data tends to record more localized areas in the Xuanwei Formation in detail, but it does not necessarily represent the vegetation from the entire basin. The combined macro- and micro-floral data indicates that the end Permian Changhsingian lowlands of the Xuanwei Formation were occupied by Paleozoic lycopods, sphenophytes, fern, progymnosperms and giantopterids

and seed ferns while the uplands were dominated by other gymnosperms including conifers, ginkgophytes, cycads and peltaspermalean seed ferns. The proliferation of fungal spores indicates a widespread land ecosystem crisis in South China during the EPPC. After the EPPC, lowland floras were left with only a few Paleozoic holdover taxa and pioneering Triassic lycopods growing in coastal areas, while the uplands saw the persistence of gymnosperm-like peltasperms, cycadophytes, ginkgophytes and conifers: a Permo-Triassic transitional flora. Soon after the early Griesbachian, the survival flora died out in lowland areas, and gymnosperms previously occupying upland habitats gradually occupied the empty niches and formed what became typical Mesozoic gymnosperm-dominated floras (Fig. 17). The palynological record shows this transformation may have started in the late Changhsingian, although it is only seen in the macrofloral record after the Griesbachian (Fig. 16, 17).

Ouyang (1991) noted that about 30–50% of palynology species from the Permian–Triassic transitional flora at the bottom of the Kayitou Formation in Yunnan province were holdovers from Permian or older ages and comprised exclusively of gymnosperm pollen. Of these only 15–17% extended into the later Early Triassic (Fig. 17). We consider these gymnosperm pollen as Methuselah taxa (see Looy et al., 2004; Blomenkemper et al., 2018; DiMichele et al., 2020) with unexpectedly early stratigraphic occurrences that were living outside the preservationally biased wetland settings in ecological niches such as upland fluvial and lacustrine systems less affected by the EPPC extinction mechanisms. Further study is required to evaluate the taphonomic nature of late Permian palynofloras to confidently identify Methuselah taxa, and where possible, match the dispersed spore and pollen accounts to plant groups to characterize in detail for the first time the composition of these cryptic upland floras.

## 5.2 Permian–Triassic extinction on land and in ocean

As to the age of the terminal phase of the EPPC, the Hg/TOC spikes and the carbon isotope trends in China and many other terrestrial sections can be correlated with the marine GSSP at Meishan (Shen J. et al., 2019b; Chu et al., 2020): a peak of

Hg/TOC was recorded in Meishan Bed 24, and in Bed 26 at Chinahe (Fig. 20). The former records the first, severe phase of the marine mass extinction but at Chinahe the main plant mass extinction occurs below this in Bed 25 indicating an earlier terrestrial crisis. The pioneer lycopod genus *Tomioostrobus* (= *Annalepis*) occurs immediately below the Hg/TOC peak and maybe used for correlation due to its stratigraphically short-ranging and geographically widespread distribution in South China (Yu et al., 2010). Further evidence for this earlier crisis comes from radiometric dating at the Chahe section, where the loss of plants occurs in Bed 69. This level is constrained by a zircon age from Bed 68 of  $252.30 \pm 0.07$  Ma. This is close to the age of  $252.104 \pm 0.089$  Ma in Bed 22 and  $251.941 \pm 0.037$  Ma in Bed 25 at Meishan (Shen S.Z. et al., 2011; Burgess et al., 2014). The first phase of the marine extinction at Meishan therefore lagged behind the floral crisis by tens to hundreds of thousands of years (Fig. 20; Yin et al., 2012; Cui et al., 2017; Dal Corso et al., 2022; Wang Y. et al., 2022). This conclusion is supported by the two fungal spore peaks in Bed 66 and 68, and the proliferation of gymnosperm pollen in Bed 70 and 78 of the Chahe section (Yu et al., 2008). In the marine facies of the Meishan Section, the end Permian to early Griesbachian palynological record is more continuous and shows the increasing dominance of gymnosperm pollen from Bed 27 (Yu et al., 2008; Zhang et al., 2004) after the Permian–Triassic Boundary in the early Griesbachian.

Based on moretane/hopane ( $C_{29}\text{-M}/C_{30}\text{-HP}$ ,  $C_{30}\text{-M}/C_{30}\text{-HP}$ ) ratios and the biomarker DBF index ( $\text{DBF}/(\text{DBF}+\text{DBT}+\text{F})$ ), anomalously high terrestrial organic C inputs occurred in the latest Permian (Beds 25–26) at Meishan, before gradually decreasing in the Early Triassic (Beds 27–30) before increasing again in Bed 34 (Xie et al., 2007, 2009; Wang, 2007). According to this timescale, the marine faunal extinction episode at the base of Bed 25 at Meishan (Fig. 20) and the marine productivity decline before Bed 25 (Song et al., 2012; Shen J. et al., 2015) occurs after the terrestrial EPPC, whilst plant abundance declined to its lowest level after Meishan Bed 24.

### 5.3 Plant and environment co-evolution

To evaluate the paleoenvironmental influences of the floral changes evaluated here, a timescale for environmental events has been compiled through the end Permian to Middle Triassic. This is divided into two phases: the Changhsingian to Griesbachian interval set against the timescale of the marine Meishan section from which precise zircon ages have been determined (Fig. 20), and, with lower stratigraphic resolution, the Induan to Anisian interval (Fig. 22).

The EPPC is thought to coincide with a long-term aridification associated with the formation of Pangaea beginning in the Middle Permian (Kidder et al., 2004; Roscher et al., 2011; Benton et al., 2014; Blomenkemper et al., 2018). Rising extinction rates in South China began in the Changhsingian and coincide the start of a trend that saw pollen percentages climb (see supplementary dataset for the macro and micro spore and pollen plant percentage from Wuchiapingian to Ladinian) (Figs. 16, 19). Increased charcoal concentrations in the latest Changhsingian suggest aridity intensified, likely seasonally, as the climax of the EPPC developed (Shen W.J. et al., 2011; Yan et al., 2019; Chu et al., 2020; Cai et al., 2021). The increase of the chemical weathering index (CIA) in South China at the same time (e.g. Xu et al., 2017) could reflect the loss of plant cover. The increase of fungi could also be caused by more prolonged arid episodes (Berdugo et al., 2020).

Increasing drought and climbing temperature could all have weakened the gigantopterid (Cathaysian) flora in South China and lead to the the mass extinction that marked the culmination of the EPPC. Whether this was a culmination of stresses that began in the early Changxingian or if the terminal EPPC was a distinct event, with a separate causation, can be debated. However, prior to the rapid warming of equatorial, ocean surface-waters in the latest EPPC, temperatures were stable and rather cool during the Changxingian (Joachimski et al. 2020) which argues against the notion of progressive temperature rise reaching a lethal threshold at the end of the EPPC. Instead, the effect of rapid warming appears to have been impact a South China flora that was already experiencing diversity decline perhaps due to increasing seasonal aridity. Siberian volcanism is generally apportioned the blame for the rapid warming episode and other consequences of the eruptions may have been acid rain

and depletion of the ozone layer resulting in increased UVB radiation (Benca et al., 2018; Black et al., 2018; Cai et al., 2021; Fig. 21).

Volcanism-induced weathering on land and increasing terrestrial inputs play significant role to the marine ecosystem (e.g., Shen J. et al., 2022; Huang et al., 2022). Modelling of factors such as volcanism, tectonism, marine redox and acidification, cannot explain the extreme hothouse climate in Early Triassic without including the terrestrial biome (Mills et al., 2021, Fig. 21). We inferred the enhancement of climate instability, seasonal aridity and following loss of lowland peat vegetation during EPPC caused the drop of terrestrial biomass storage, probably contributing to the carbon cycle fluctuation, while this requires further study of land biomass and global carbon cycle.

Wildfire proxies probably indicate the disappearance of the Griesbachian interval vegetation after the early Griesbachian (Fig. 20). The initial loss of the holdover flora might result in a temporary increase of soil erosion (Fig. 20). The flora of this interval was dominated by the herbaceous lycopods *Tomiostrabus* (= *Annalepis*) and *Pleuromeia* which, with their shallow rooting systems (Retallack et al., 1975; Yu et al., 2010), were likely insufficient to effectively bind soils (Algeo et al., 2011; Boyce et al., 2016; Fig. 22).

From our data, plant species richness recovery occurred during the Griesbachian to the Smithian stage, while plant abundance indicated by the palynology data, biomarkers, TOC and C/N ratio data this aspect began to recover in the Spathian (Saito et al., 2013). The first post-EPPC herbivorous tetrapods appeared and coal accumulation re-commenced in the Anisian, indicating a return of diverse and productive terrestrial ecosystems. The soil erosion proxy also indicates the re-stabilization of land surface system after Spathian (Algeo et al., 2011). Diverse marine ecosystems were also reestablished at Anisian but full recovery to a pre-extinction level was not until the Late Triassic (Song H.J. et al., 2018).

#### 5.4 Comparison of floristic patterns between low latitude South China and other geographical areas

Both the North and South China plates occupied low–middle latitude positions during the Late Permian and experienced tropical–subtropical climates (Nowak et al., 2020). The Late Permian vegetation from North China was a mixed Cathaysian, Euramerican and Angara flora, whilst a typical Cathaysian flora occupied South China (Wang et al., 1985; Yu et al., 2015; Wu et al., 2021). In North China terrestrial depositional facies have made identification and correlation of the PTB and PTME difficult, with recent investigations using radiometric ages from ash beds to confirm the End Permian Plant Crisis predates the PTME which concludes with the PTB in the uppermost Sunjiagou Formation from the Liujiang Coalfield (Wu et al., 2021; Wang Y. et al., 2022). The terrestrial ecosystem collapse in North China commenced approximately  $270 \pm 150$  kyrs before the marine crisis (Guo et al., 2022), but occurs approximately 310 kry later than the terrestrial crisis in high southern latitudes in Australia (Lu et al. 2022). Prior to the PTME, the plant macrofossil extinction and origination rates in North China are comparable to those of South China and indicate significant floral turnover (Xiong et al., 2021). In both areas plant extinction rates exceeded origination rate before the EPPC, but in North China the severest plant crisis event, which is shown by the biggest value difference between extinction and origination rates, occurred before the PTB boundary and may been earlier than South China (Xiong et al., 2021), although Lu et al. (2022) considered they may be synchronous. After the terrestrial plant crisis and PTME, the earliest Triassic flora in North China comprised similar pioneering Triassic isoetalean and Pleuromeia lycopods and later in the early Triassic conifer dominated floras (Yu et al., 2015; Xiong et al., 2021).

The fossil record from Australia in high latitude Gondwana reveals that the *Glossopteris* flora suffered abrupt extinction due to rapid warming and increased seasonality somewhat before the Permian–Triassic Boundary (Vajda et al., 2020; Frank et al., 2021; Fielding et al., 2022). This ecological disaster reset Paleozoic terrestrial phytogeographic provincialism and marked the end to the former separation of floras into the low-mid latitude Euramerican and Cathaysian floras and the high-latitude Gondwana floras. The peak of plant species richness decline, last coal seam,

and ecosystem collapse indicated by fungal spike in Australia, South and North China all denote the onset and main peak of the land plant crisis occurred tens of thousands of years before the marine crisis (Yu et al., 2008, 2015; Xiong et al., 2021; Fielding et al., 2022). Spikes of fungal spores are common in Australia, South China, and the Karoo Basin where they occur at several levels at this time (Visscher et al., 1996; Steiner et al., 2003; Ouyang and Zhu, 2007; Yu et al., 2008; Fielding et al., 2022). Early Triassic floras from low to high latitudes comprised a uniform lycopod dominated flora (e.g. in Australia and South and North China).

In the Kuznetsk Basin in Russia, increased aridity may have affected the composition of the Angaran flora, but this region saw floral turnover and migration in response to changing climate rather than an extinction event (Davydov et al., 2021). The regional extinction of the humidity-adapted, cordaites-dominated flora happened approximately 820 kyrs earlier than the PTME marine extinction event in South China (Davydov et al., 2021). Following the floral turnover, plants subsequently diversified across the Permian–Triassic transition when mixed fern (*Cladophlebis*, *Kovuntschania*, *Katasiopteris*, *Kchonomakidium*, *Todites*, *Kedroviella* and *Prynadaeopteris*), sphenophyte (*Neokoretrophyllites*, *Schizoneura*, *Paracalamites*) peltasperm (*Lepidopteris*), seed fern (*Tersiella* and *Madygenia*), cycad (*Tomia* and *Glossozamites*), Ginkgoales (*Rhipidopteris* and *Glossophyllum*), conifer (*Quadrocladus*) and Triassic lycopods (*Tomiostrabus*, *Mesenterihyllum*) characterized the flora (Davydov et al., 2021).

Comparison between floras in different latitudes and in various distances from continental interiors shows that climate instability and expansion of seasonal aridity was a significant control on floral composition and distribution through the Permian and Triassic transition. The plant mass extinction level occurred over wide areas with only the Siberian region recording a diverse flora in the aftermath of the crisis and turnover (Davydov et al., 2021). Given the proximity of this region to the flood basalts of the Siberian Traps it is ironic that the flora of the Phase 2 interval was so diverse. It could be argued that factors that are at their most intense adjacent to volcanism, such as acid rain, may not therefore have been an important factor in the



floral mass extinction. Other factors such as a relatively muted temperature rise, in the high northern Siberian latitudes, and a persistent humid climate may all have favoured this region as a refuge.

In tropical areas such as South China, a rapid temperature rise of over 15°C proved fatal, resulting in ocean surface temperatures > 35°C degrees, and possibly > 42°C on land; such levels are likely to have been directly responsible for the extinction losses (Sun et al., 2012). In higher latitudes, the peak temperatures would have been lower whilst still exceeding the tolerance of indigenous plants (Fielding et al., 2022), although perhaps not in the Siberian region (Davydov et al., 2021). Plants living in higher altitudes may also have been more resilient to extreme temperatures due to temperatures typically decreasing adiabatically with height. Consequently, upland floras were able to colonize lowland settings after the EPPC once competition pressures (and temperatures) in these settings were lower following extinction.

## 6. Conclusions

Investigation of plant macrofossil occurrences from the Artinskian to Rhaetian in South China has shown that floral species richness declined after the Wuchiapingian and experienced a distinct species richness and abundance drop in the Changhsingian that we term the End Permian Plant Crisis (EPPC). During the EPPC plant extinction rates overtook origination rates, with this scenario continuing into the early Triassic although the gap narrowed after the EPPC. The culmination of the EPPC was marked by a major extinction with losses of coal-swamp taxa including tree lycopods (*Lepidodendron*), sphenopsids (*Lobatannularia*, *Annularia*), Noeggerathiales progymnosperms (*Tingia*), Marattiales ferns (*Pecopteris*), giantopterids (*Gigantopteris*) and cordaites gymnosperms (*Cordaite*) which flourished during the Late Paleozoic (Phase 1). There seems to have been a hidden upland gymnosperm-dominated flora at this time which is not preserved in the macrofossil record but is evident in palynological data. Other evidence of terrestrial plants, such as wildfire and terrestrial input proxies obtained from marine sections, indicate the climax of the terrestrial EPPC predated the marine PTME extinction.

In the early Triassic Kayitou Flora, surviving end-Permian elements were mixed with Triassic opportunist herbaceous lycopods with low species richness and abundance. We term this the Griesbachian interval flora (Phase 2). Origination rates only began to exceeded extinction rates in the late Induan, and this trend continued into the Olenekian. The recovery of abundant plant biomass happened later than the diversity recovery, and probably commenced during the Spathian as indicated by increasing conifer biomarker concentrations and C/N ratios, and continued into the Anisian. Triassic floras only attained a comparable species richness in South China to the pre-EPPC flora after the Carnian (early Late Triassic). According to the origination and extinction rates of each plant family, the flora overall changed from a Paleozoic Cathaysian peat forming type into Mesozoic seed plant-dominant type which likely reflects an adaption to drier climate.

#### Declaration of Competing Interest

The authors declare they have no known competing financial interests or personal relationships that could have appeared to influence the work reported in this paper.

#### Acknowledgements

We thank Xiao Shi, Wenchao Shu, Meijia Zhang, Xujie Wang, Yuyang Tian for fieldwork assistance, Professor Jean Broutin and Qisheng Huang for the plant fossil identifications, and Christopher J. Cleal for discussion on methods and species richness, and Jiri Bek for discussion on pollen and spore affinities, and Xin Sun, Bethany J. Allen for discussion on paleontology diversity method. The manuscript benefited from reviews by constructive reviews from Christopher Fielding, Mike Benton and two anonymous reviewers. This research was financially supported by the NSFC (grants 92055201), the 111 Project (grant BP0820004) and Natural Environment Research Council (UK) Biosphere Evolution, Transition and Resilience (BETR) program (grant NE/P0137224/1)

References

- Algeo, T.J., Chen, Z.Q., Fraiser, M.L., Twitchett, R.J., 2011. Terrestrial–marine teleconnections in the collapse and rebuilding of Early Triassic marine ecosystems. *Palaeogeogr. Palaeoclimatol. Palaeoecol.* 308(1–2), 1–11 <https://doi.org/10.1016/j.palaeo.2011.01.011>.
- Allen, B.J., Wignall, P.B., Hill, D.J., Saupe, E.E., Dunhill, A.M., 2020. The latitudinal diversity gradient of tetrapods across the Permo-Triassic mass extinction and recovery interval. *Proc. R. Soc. Bull.* 287(1929), 20201125 <https://doi.org/10.1098/rspb.2020.1125>.
- Allison, P.A., Bottjer, D.J., 2010. Taphonomy: Process and bias through time (Second Edition). Springer [https://doi.org/10.1007/978-90-481-8643-3\\_1](https://doi.org/10.1007/978-90-481-8643-3_1).
- Balme, B.A., 1995. Fossil in situ spores and pollen grains: an annotated catalogue. *Rev. Palaeobot. Palynol.* 87, 81–323 [https://doi.org/10.1016/0034-6667\(95\)93235-X](https://doi.org/10.1016/0034-6667(95)93235-X).
- Bateman, R.M., 1991. Palaeoecology, in: Cleal, C.J. (Ed.), *Plant Fossils in Geological Investigation: The Palaeozoic*. Ellis Horwood, London, pp. 34–116.
- Bateman, R.M., & Hilton, J.M., 2009. Palaeobotanical systematics for the phylogenetic age: applying organspecies, form-species and phylogenetic species concepts in a framework of reconstructed fossil and extant whole-plants. *Taxon* 58(4), 1254–1280 <https://doi.org/10.1002/tax.584016>.
- Bek, J., 2017. Paleozoic in situ spores and pollen. *Lycopsida. Palaeontographica Abt. B* 296(1–6), 1–111 <https://doi.org/10.1127/palb/296/2017/1>.
- Benca, J.P., Duijnste, I., Looy, C.V., 2018. UV-B–induced forest sterility: Implications of Ozone shield failure in Earth’s largest extinction. *Sci. Adv.* 4(2), e1700618 <https://doi.org/10.1126/sciadv.1700618>.
- Benton, M.J., Newell, A.J., 2014. Impacts of global warming on Permian–Triassic terrestrial ecosystems. *Gond. Res.* 25(4), 1308–1337 <https://doi.org/10.1016/j.gr.2012.12.010>.
- Bercovici, A., Cui, Y., Forel, M., Yu, J.X., Vajda, V., 2015. Terrestrial paleoenvironment characterization across the Permian–Triassic boundary in

1253 South China. *J. Asian Earth Sci.* 98, 225–246  
 1254 <https://doi.org/10.1016/j.jseaes.2014.11.016>.  
 1255 Black, B.A., Neely, R.R., Lamarque, J., Elkins-Tanton, L.T., Kiehl, J.T., Shields, C.A.,  
 1256 Mills, M.J., Bardeen, C., 2018. Systemic swings in End-Permian climate from  
 1257 Siberian Traps carbon and sulfur outgassing. *Nat. Geosci.* 11(12), 949–954  
 1258 <https://doi.org/10.1038/s41561-018-0261-y>.  
 1259 Blumenkemper, P., Kerp, H., Hamad, A.A., Dimichele, W.A., Bomfleur, B., 2018. A  
 1260 hidden cradle of plant evolution in Permian tropical lowlands. *Science* 362,  
 1261 1414–1416 <https://doi.org/10.1126/science.aau4061>.  
 1262 Bond, D.P.G., Hilton, J.M., Wignall, P.B., Stevens, L.G., Ali, J.R., Sun, Y.D., and Lai,  
 1263 X. L., 2010. The Middle Permian (Capitanian) mass extinction on land and in the  
 1264 oceans. *Earth-Sci. Rev.* 102, 100–116  
 1265 <https://doi.org/10.1016/j.earscirev.2010.07.004>.  
 1266 Boyce, C.K., Dimichele, W.A., 2016. Arborescent lycopsid productivity and lifespan:  
 1267 constraining the possibilities. *Rev. Palaeobot. Palynol.* 227, 97–110  
 1268 <https://doi.org/10.1016/j.revpalbo.2015.10.007>.  
 1269 Broutin, J., Yu, J.X., Shi, X., Shu, W.C., & Xue, Q., 2020. Terrestrial palaeofloral  
 1270 succession across the Permian–Triassic boundary in the north and south china  
 1271 blocks: a brief review. *Paläontologische Zeitschrift* 94(1), 1–12  
 1272 <https://doi.org/10.1007/s12542-020-00511-0>.  
 1273 Berdugo, M., Delgado-Baquerizo, M., Soliveres, S., Hernández-Clemente, R., Zhao,  
 1274 Y.C., Gaitán, J. J., Gross, N., Saiz, H., Maire, V., Lehmann, A., Rilling, M.C.,  
 1275 Solé, R.V., Maestre, F.T., 2020. Global ecosystem thresholds driven by aridity.  
 1276 *Science* 367(6479), 787–790 <https://doi.org/10.1126/science.aay5958>.  
 1277 Burgess, S.D., Bowring, S., Shen, S.Z., 2014. High-precision timeline for earth's most  
 1278 severe extinction. *Proc. Natl. Acad. Sci. USA* 111(9), 3316–3321  
 1279 <https://doi.org/10.1073/pnas.1317692111>.  
 1280 Cai, Y.F., Zhang, H., Cao, C.Q., Zheng, Q.F., Jin, C.F., Shen, S.Z., 2021. Wildfires and  
 1281 deforestation during the Permian–Triassic transition in the southern Junggar  
 1282 Basin, Northwest China. *Earth-Sci. Rev.* 218, 103670

<https://doi.org/10.1016/j.earscirev.2021.103670>.

Chaloner, W.G., 1986. Reassembling the whole fossil plant, and naming it. Pages 67–78 in Spicer R.A., Thomas, B.A. (Eds), Systematic and taxonomic approaches in palaeobotany. Systematics Association Special, Vol 31. Oxford: Oxford University Press.

Chen, J.H., Yu, J.X., Huang, Q.S., Broutin, J., Song, Q.Q., Chen, B., 2011. New research progress on the paleoflora in the earliest Triassic of western Guizhou and eastern Yunnan, South China. Earth Sci. J. China Uni. Geosci. 36(3), 500–510 (In Chinese with English abstract).

Chu, D.L., Grasby, S.E., Song, H.J., Corso, J.D., Wang, Y., Mather, T.A., Wu, Y., Song, H.Y., Shu, W.C., Tong, J.N., Wignall, P.B., 2020. Ecological disturbance in tropical peatlands prior to marine Permian–Triassic mass extinction. Geology 48, 288–292 <https://doi.org/10.1130/G46631.1>.

Chu, D.L., Tong, J.N., Song, H.J., Benton, M.J., Song, H.Y., Yu, J.X., Qiu, X.C., Huang, Y.F., Tian, L., 2015. Lilliput effect in freshwater ostracods during the Permian–Triassic extinction. Palaeogeogr. Palaeoclimatol. Palaeoecol. 435, 38–52 <https://doi.org/10.1016/j.palaeo.2015.06.003>.

Chu, D.L., Yu, J.X., Tong, J.N., Benton, M.J., Song, H.Y., Huang, Y.F., Song, T., Tian, L., 2016. Biostratigraphic correlation and mass extinction during the Permian–Triassic transition in terrestrial-marine siliciclastic settings of South China. Glob. Planet. Change 146, 67–88 <https://doi.org/10.1016/j.gloplacha.2016.09.009>.

Cleal, C.J., Cascales-Miñana, B., 2014. Composition and dynamics of the great Phanerozoic evolutionary floras. Lethia 47, 469–484 <https://doi.org/10.1111/let.12070>.

Cleal, C.J., Pardoe, H.S., Berry, C.M., Cascales-Miñana, B., Davis, B.A.S., Diez, J.B., Filipova-Marinova, M.V., Giesecke, T., Hilton, J.M., Ivanov, D.A., Kustatscher, E., Leroy, S.A.G., McElwain, J.C., Opluštil, S., Popa, M.E., Seyfullah, L.J. Stolle, E., Thomas, B.A., Uhl, D., 2021. Palaeobotanical experiences of plant diversity in deep time. 1: How well can we identify past plant diversity in the fossil record? Palaeogeogr. Palaeoclimatol. Palaeoecol. 576, 110481

<https://doi.org/10.1016/j.palaeo.2021.110481>.

Cleal, C.J., Thomas, B.A., 2004. Late Carboniferous palaeobotany of the upper Bideford Formation, north Devon: a coastal setting for a Coal Measures flora. *Proc. Geol. Assoc.* 115(3), 267–281 [https://doi.org/10.1016/S0016-7878\(04\)80007-5](https://doi.org/10.1016/S0016-7878(04)80007-5).

Cleal, C.J., Uhl, D., Cascales-Miñana, B., Thomas, B.A., Bashforth, A.R., King, S.C., Zodrow, E.L., 2012. Plant biodiversity changes in Carboniferous wetlands. *Earth-Sci. Rev.* 114, 124–155 <https://doi.org/10.1016/j.earscirev.2012.05.004>.

Clement-Westerhof, J.A., 1974. In situ pollen from gymnospermous cones from the Upper Permian of the Italian Alps—A preliminary account. *Rev. Palaeobot. Palynol.* 17(1–2), 63–73 [https://doi.org/10.1016/0034-6667\(74\)90092-X](https://doi.org/10.1016/0034-6667(74)90092-X).

Cui, Y., Bercovici, A., Yu, J.X., Kump, L.R., Freeman, K. H., Su, S.G., Vajda, V., 2017. Carbon cycle perturbation expressed in terrestrial Permian–Triassic boundary sections in South China. *Glob. Planet. Change* 148, 272–285 <https://doi.org/10.1016/j.gloplacha.2015.10.018>.

Dal Corso, J., Song, H.J., Callegaro, S., Chu, D.L., Sun, Y.D., Hilton, J., Grasby, S.E., Joachimski, M.M., Wignall, P.B., 2022. Environmental crises at the Permian–Triassic mass extinction. *Nature Rev. Earth Environ.* 1–18 <https://doi.org/10.1038/s43017-021-00259-4>.

Davies, N.R., Gibling, M.R., 2010. Cambrian to Devonian evolution of alluvial systems: the sedimentological impact of the earliest land plants. *Earth-Sci. Rev.* 98, 171–200 <https://doi.org/10.1016/j.earscirev.2009.11.002>.

Davydov, V.I., Karasev, E.V., Nurgalieva, N.G., Schmitz, M.D., Budnikov, I.V., Biakov, A.S., Kuzina, D.M., Silantiev, V.V., Urazaeva, M.N., Zharinova, V.V., Zorina, S.O., Gareev, B., Vasilenko, D.V., 2021. Climate and biotic evolution during the Permian-Triassic transition in the temperate Northern Hemisphere, Kuznetsk Basin, Siberia, Russia. *Palaeogeogr. Palaeoclimatol. Palaeoecol.* 573, 110432 <https://doi.org/10.1016/j.palaeo.2021.110432>.

DiMichele, W.A., Bashforth, A.R., Falcon-Lang, H.J., Lucas, S.G., 2020. Uplands, lowlands, and climate: Taphonomic megabiases and the apparent rise of

xeromorphic, drought-tolerant flora during the Pennsylvanian–Permian transition.

Palaeogeogr. Palaeoclimatol. Palaeoecol. 559, 109965

<https://doi.org/10.1016/j.palaeo.2020.109965>.

DiMichele, W.A., Kerp, H., Tabor, N.J., Looy, C.V., 2008. The so-called

"Paleophytic–Mesophytic" transition in equatorial Pangea—multiple biomes and

vegetational tracking of climate change through geological time. Palaeogeogr.

Palaeoclimatol. Palaeoecol. 268(3), 152–163

<https://doi.org/10.1016/j.palaeo.2008.06.006>.

Feng, Z., Wei, H.B., Guo, Y., Bomfleur, B., 2018. A conifer-dominated Early Triassic

flora from Southwest China. Sci. Bull. 63, 1462–1463

<https://doi.org/10.1016/j.scib.2018.09.011>.

Feng, Z., Wei, H.B., Guo, Y., He, X.Y., Sui, Q., Zhou, Y., Liu, H.Y., Gou, X.D., Lv, Y.,

2020. From rainforest to herbland: New insights into land plant responses to the

End-Permian Mass Extinction. Earth-Sci. Rev. 204, 103153

<https://doi.org/10.1016/j.earscirev.2020.103153>.

Fielding, C.R., Frank, T.D., Savatic, K., Mays, C., McLoughlin, S., Vajda, V., Nicoll,

R.S., 2022. Environmental change in the late Permian of Queensland, NE

Australia: The warmup to the end-Permian Extinction. Palaeogeogr.

Palaeoclimatol. Palaeoecol. 594, 110936

<https://doi.org/10.1016/j.palaeo.2022.110936>.

Forel, M., Bercovici, A., Yu, J.X., 2020. Ostracods after the End-Permian extinction in

South China: insights into non-microbial survival. Micropaleont. hal–03098322f.

Frank, T.D., Fielding, C.R., Winguth, A.M.E., Savatic, K., Tevyaw, A., Winguth, C.,

McLoughlin, S., Vajda, V., Mays, C., Nicoll, R., Bocking, M., Crowley, J.L.,

2021. Pace, magnitude, and nature of terrestrial climate change through the end-

Permian extinction in southeastern Gondwana. Geology 49(9), 1089–1095

<https://doi.org/10.1130/G48795.1>.

Gall, J.C., Grauvogel-Stamm, L., 2005. The early Middle Triassic 'Grès à Voltzia'

Formation of eastern France: a model of environmental refugium. C. R. Palevol.

4, 637–652 <https://doi.org/10.1016/j.crpv.2005.04.007>.

- Glenn-Lewin, D.C., Peet, R.K., Veblen, T.T. (Eds.), 1992. Plant succession: theory and prediction. Chapman and Hall, London, ss 352.
- Gou, Z.H., Lin, M.B., 1996. The bivalve fauna of Feixianguan Formation in Majiaoba area, Jiangyou, Sichuan. J. Chengdu Inst. Tech. 23(4), 80–84 (In Chinese with English abstract).
- Grauvogel-Stamm, L., Ash, S.R., 2005. Recovery of the Triassic land flora from the End-Permian life crisis. Comptes. Rendus. Palevol. 4(6–7), 593–608  
<https://doi.org/10.1016/j.crpv.2005.07.002>.
- Grice, K., Twitchett, R.J., Alexander, R., Foster, C.B., & Looy, C., 2005. A potential biomarker for the Permian–Triassic ecological crisis. Earth Planet. Sci. Lett. 236(1–2), 315–321 <https://doi.org/10.1016/j.epsl.2005.05.008>.
- Guo, W.W., Tong, J.N., He, Q., Hounslow, M.W., Song, H.J., Dal Corso, J., Wignall, P.B., Ramezani, J., Tian, L., Chu, D.L., 2022. Late Permian–Middle Triassic magnetostratigraphy in North China and its implications for terrestrial-marine correlations. Earth Planet. Sci. Lett. 585, 117519  
<https://doi.org/10.1016/j.epsl.2022.117519>.
- Hagen, C.J., Roberts, E.M., Sullivan, C., Liu, J., Wang, Y., Owusu Agyemang, P.C., Xu, X., 2018. Taphonomy, geological age, and Paleobiogeography of *Lotosaurus Adentus* (Archosauria: Poposaurioidea) from the Middle–Upper Triassic Badong Formation, Hunan, China. Palaios 33(3), 106–124  
<https://doi.org/10.2110/palo.2017.084>.
- He, B.H., Liu, S.F., Wu, P., 2017. LA-ICP-MS U-Pb geochronology and its geological implications of the detrital Zircons from the lower strata of Upper Permian Xuanwei Formation in Zhehai Town, Eastern Yunnan Province. North China Geol. 40(2), 126–133 (In Chinese with English abstract)  
<https://doi.org/10.3969/j.issn.1672-4135.2017.02.006>.
- Hilton, J.M., and Cleal, C.J., 2007. The relationship between Euramerican and Cathaysian tropical floras in the Late Palaeozoic: palaeobiogeographical and palaeogeographical implications. Earth-Sci. Rev. 85(3–4), 85–116  
<https://doi.org/10.1016/j.earscirev.2007.07.003>.



- Hochuli, P.A., Hermann, E., Vigran, J.O., Bucher, H., Weissert, H., 2010. Rapid demise and recovery of plant ecosystems across the End-Permian extinction event. *Glob. Planet. Change* 74(3–4), 144–155  
<https://doi.org/10.1016/j.gloplacha.2010.10.004>.
- Hochuli, P.A., Sanson-Barrera, A., Schneebeil-Hermann, E., Bucher, H., 2016. Severest crisis overlooked—Worst disruption of terrestrial environments postdates the Permian–Triassic Mass Extinction. *Sci. Rep.* 6(1), 28372  
<https://doi.org/10.1038/srep28372>.
- Huang, Q.S., Lu, S.M., 1992. The primary studies on the palaeoecology of the Late Triassic Xujiahe Flora in eastern Sichuan. *Earth Sci. J. China Uni. Geosci.* 17(3), 329–335.
- Huang, Y.F., He, W.H., Liao, W., Wang, Y.B., Yi, Z.X., Yang, H., Li, G.S., 2022. Two pulses of increasing terrestrial input to marine environment during the Permian–Triassic transition. *Palaeogeogr. Palaeoclimatol. Palaeoecol.* 586, 110753  
<https://doi.org/10.1016/j.palaeo.2021.110753>.
- Huston, M., Smith, T., 1987. Plant succession: life history and competition. *Am. Nat.* 130(2), 168–198.
- Jin, Y.X., Shang, Q.H., Hou, J.P., Li, L., Wang, Y.J., Zhu, Z.L., Fei, S.Y., 2000. Stratigraphical lexicon of China: Permian System. Geol. Publ. Beijing (In Chinese).
- Joachimski, M.M., Alekseev, A.S., Grigoryan, A., Gatovsky, Y.A., 2020. Siberian Trap volcanism, global warming and the Permian-Triassic mass extinction: New insights from Armenian Permian-Triassic sections. *Geol. Soc. Am. Bull.* 132(1–2), 427–443 <https://doi.org/10.1130/B36214.1>.
- Kaiho, K., Saito, R., Ito, K., Miyaji, T., Chen, Z.Q., 2016. Effects of soil erosion and anoxic–euxinic ocean in the Permian–Triassic marine crisis. *Heliyon* 2(8), e00137  
<https://doi.org/10.1016/j.heliyon.2016.e00137>.
- Kidder, D.L., Worsley, T.R., 2004. Causes and consequences of extreme Permian–Triassic warming to globally equable climate and relation to the Permian–Triassic extinction and recovery. *Palaeogeogr. Palaeoclimatol. Palaeoecol.* 203(3–4),

207–237 [https://doi.org/10.1016/S0031-0182\(03\)00667-9](https://doi.org/10.1016/S0031-0182(03)00667-9).

- Knoll, A.H., 1984. Patterns of extinction in the fossil record of vascular plants, in: Nitecki, M.H. (Ed.), *Extinctions*. University of Chicago Press, Chicago, pp. 1–68.
- Krassilov, V., Karasev, E., 2009. Paleofloristic evidence of climate change near and beyond the Permian–Triassic boundary. *Palaeogeogr. Palaeoclimatol. Palaeoecol.* 284(3–4), 326–336 <https://doi.org/10.1016/j.palaeo.2009.10.012>.
- Li, H., Yu, J.X., McElwain, J.C., Yiotis, C., Chen, Z.Q., 2019. Reconstruction of atmospheric CO<sub>2</sub> concentration during the late Changhsingian based on fossil conifers from the Dalong Formation in South China. *Palaeogeogr. Palaeoclimatol. Palaeoecol.* 519, 37–48 <https://doi.org/10.1016/j.palaeo.2018.09.006>.
- Li, P.J., 1964. Fossil plant from the Hsuchiaho Series of Kwangyuan, northern Szechuan. *Mem. Inst. Geol. Palaeont. Acad. Sin.* 3, 101–78.
- Li, X.X., Zhou, Z.Y., Cai, C.Y., Sun, G., Ouyang, S., Deng, L.H., 1995. Fossil floras in China through the geological ages (English edition). Guangdong Sci. Tech. Press, Guangzhou, pp. 1–695 <http://ir.nigpas.ac.cn/handle/332004/7973>.
- Li, X.X., 1997. The origin, evolution and distribution of the Cathaysian flora in East Asia. *Acta Palaeontol. Sin.* 36(4), 411–422 (In Chinese and English).
- Li, X.X., Yao, Z.Q., 1980. Permian coal-bearing formations in South China. *J. Stratigr.* 4, 241–255 (In Chinese).
- Liu, D.D., Yang, Z.R., Yang, Y.D., Bao, Y.Y., Liu, B., 2009. Characteristic of the flora in the Zhenzhuchong Formation and the Jurassic–Triassic boundary in the Sichuan Basin. *J. Earth Sci. Environ.* 31(3), 254–259 (In Chinese with English abstract).
- Liu, L.L., Yao, Z.Q., 2013. The conifer-remains from the Permian of South China. *Acta Palaeontol. Sin.* 52(2), 182–201.
- Liu, L.J., Yao, Z.Q., 2007. Plant megafossils from the Permian Changhsingian marine deposits of Fusui, Guangxi, China. *Acta Palaeontol. Sin.* 46(2), 195–212.
- Looy, C.V., Brugman, W.A., Dilcher, D.L., Visscher, H., 1999. The delayed resurgence of equatorial forests after the Permian–Triassic ecologic crisis. *Proc. Natl. Acad. Sci. USA* 96(24), 13857–13862

<https://doi.org/10.1073/pnas.96.24.13857>.

Looy, C., Kerp, H., Duijnste, I., DiMichele, B., 2014. The late Paleozoic ecological-evolutionary laboratory, a land-plant fossil record perspective. *Sedimentary Rec.* 12(4), 4–18 <https://doi.org/10.2110/sedred.2014.4>.

Lu, J., Wang, Y., Yang, M.F., Zhang, P.X., Bond, D.P.G., Shao, L., Hilton, J. 2022. Diachronous end-Permian terrestrial ecosystem collapse caused by catastrophic wildfires. *Palaeoecol. Palaeogeog. Palaeoclimatol.* 594, 110960 <https://doi.org/10.1016/j.palaeo.2022.110960>.

Luo, C.K., Yang, R.D., Gao, L., Wang, L.B., Zhou, D.F. 2021. Systematics and palaeoecology of fossil plants from the Upper Permian Longtan Formation in western Guizhou Province, southwest China. *Hist. Biol.* 1–13 <https://doi.org/10.1080/08912963.2021.1884244>.

MacLeod, N., Rawson, P.F., Forey, P.L., Banner, F.T., Boudagher-Fadel, M.K., Bown, P.R., Burnett, J.A., Chambers, P., Culver, S., Evans, S.E., Jeffery, C., Kaminski, M.A., Lord, A.R., Milner, A.C., Milner, A.R., Morris, N., Owen, E., Rosen, B.R., Smith, A.B., Taylor, P.D., Urquhart, E., & Young, J.R., 1997. The Cretaceous–Tertiary biotic transition. *J. Geol. Soc.* 154, 265–293 <https://doi.org/10.1144/gsjgs.154.2.0265>.

Marshall, C.R., Ward, P.D., 1996. Sudden and gradual molluscan extinctions in the latest Cretaceous of Western European Tethys. *Science* 274, 1360–1363 <https://doi.org/10.1126/science.274.5291.1360>.

McElwain, J.C., & Punyasena, S.W., 2007. Mass extinction events and the plant fossil record. *Trends Ecol. Evol.* 22(10), 548–557 <https://doi.org/10.1016/j.tree.2007.09.003>.

Meng, F.S., 1993. The *Annalepis–Pleuromeia* plant assemblage in South China and the significance of it. *Chinese Sci. Bull.* 38(18), 1686–1688 (In Chinese).

Meng, F.S., 1994. Discovery of *Pleuromeia–Annalepis* flora in South China and its significance. *Chinese Sci. Bull.* 02, 44–48.

Meng, F.S., 1996. Floral palaeoecological environment of the Badong Formation in the Yangtze Gorges area. *Geol. Miner. Resour. South China* 4, 1–13 (In Chinese

- 1493 with English abstract).
- 1494 Meng, F.S., 1998. Studies on *Annalepis* from Middle Triassic along the Yangtze River  
1495 and its bearing on the origin of *Isoetes*. Acta Bot. Sin. 40(8), 768–774.
- 1496 Meng, F.S., Xu, A.W., Zhang, Z.L., Lin, J.M., Yao, H.Z., 1995. Nonmarine biota and  
1497 sedimentary facies of the Badong Formation in the Yangtze and its neighbouring  
1498 areas. China Uni. Geosci. Press, Wuhan, pp. 1–76 (In Chinese with English  
1499 abstract).
- 1500 Meyen, S.V., 1987. Fundamentals of palaeobotany. Chapman and Hall, London.
- 1501 Mills, B.J.W., Tennenbaum, S., Schwartzman, D., 2021. Exploring multiple steady  
1502 states in Earth's long-term carbon cycle. Am. J. Sci. 321(7), 1033–1044  
1503 <https://doi.org/10.2475/07.2021.01>.
- 1504 Neregato, R., D'Apolito, C., Glasspool, I.J., Wang, S.J., Liu, F., Windslow, P., Lu, J.,  
1505 Shao, L.Y., Hilton, J., 2016. Palynological constraints on the provenance and  
1506 stratigraphic range of a Lopingian (Late Permian) inter-extinction floral  
1507 lagerstatte from the Xuanwei Formation, Guizhou Province, China. Int. J. Coal  
1508 Geol. 162, 139–150 <https://doi.org/10.1016/j.coal.2016.06.005>.
- 1509 Nowak, H., Schneebeil-Hermann, E., Kustatscher, E., 2019. No mass extinction for  
1510 land plants at the Permian–Triassic transition. Nat. Commun. 10(1), 1–8  
1511 <https://doi.org/10.1038/s41467-018-07945-w>.
- 1512 Nowak, H., V  rard, C., Kustatscher, E., 2020. Palaeophytogeographical patterns  
1513 across the Permian–Triassic boundary. Front. Earth Sci. 8, 609  
1514 <https://doi.org/10.3389/feart.2020.613350>.
- 1515 Ouyang, S., 1991. Transitional palynofloras from basal lower Triassic of China and  
1516 their ecological implications, with special reference to Paleophyte/Mesophyte  
1517 problems. Palaeoecology of China 1. Nanjing Uni. Press, Nanjing, pp. 168–196  
1518 <http://ir.nigpas.ac.cn/handle/332004/9027>.
- 1519 Ouyang, S., Zhu, H.C., 2007. Query the assumption of "End-Permian Fungal Spike  
1520 Event", with special reference to the Permo-Triassic transitional palynofloras.  
1521 Acta Palaeontol. Sin. 46(4), 394–410.
- 1522 Peng, Y., Shi, G.R., 2009. Life crises on land across the Permian–Triassic boundary in

1523 South China. Glob. Planet. Change 65, 155–165  
 1524 <https://doi.org/10.1016/j.gloplacha.2008.10.016>.

1525 Poort, R.J., Kerp, J.H.F., 1990. Aspects of Permian palaeobotany and palynology. XI.  
 1526 On the recognition of true peltasperms in the Upper Permian of Western and  
 1527 Central Europe and a reclassification of species formerly included in  
 1528 *Peltaspermum* Harris. Rev. Palaeobot. Palynol. 63(3–4), 197–225  
 1529 [https://doi.org/10.1016/0034-6667\(90\)90100-W](https://doi.org/10.1016/0034-6667(90)90100-W).

1530 Qu, L.F., 1990. Palynological assemblages of Middle and Late Triassic in Sangzhi,  
 1531 Hunan, and their stratigraphical significance. J. Strati. Paleotol. 23, 81–95 (In  
 1532 Chinese with English abstract).

1533 Qu, L.F., Wang, Z., 1986. Triassic spores and pollen, in: Zhou, H.Q. (Ed.), Permian  
 1534 and Triassic strata and fossil assemblages in the Dalongkou area of Jimsar,  
 1535 Xinjiang. Geological Publ. Beijing, pp. 113–173 (in Chinese with English  
 1536 summary).

1537 Rees, P.M., 2002. Land-plant diversity and the End-Permian Mass Extinction.  
 1538 Geology 30(9), 827–830 [https://doi.org/10.1130/0091-](https://doi.org/10.1130/0091-7613(2002)030<0827:LPDATE>2.0.CO;2)  
 1539 [7613\(2002\)030<0827:LPDATE>2.0.CO;2](https://doi.org/10.1130/0091-7613(2002)030<0827:LPDATE>2.0.CO;2).

1540 Ren, H., Cai, X.A., Rao, X.Q., Zhang, Q.M., Liu, S.Z., 2001. The theory on  
 1541 succession of plant community. Ecol. Sci. 20(4), 59–67 (In Chinese with English  
 1542 Abstract).

1543 Retallack, G.J., 1975. The life and time of a Triassic lycopod. Alcheringa 1, 3–29  
 1544 <https://doi.org/10.1080/03115517508619477>.

1545 Retallack, G.J., 1995. Permian–Triassic life crisis on land. Science 267(5194), 77–80  
 1546 <https://doi.org/10.1126/science.267.5194.77>.

1547 Retallack, G.J., 2005. Earliest Triassic claystone breccias and soil-erosion crisis. J.  
 1548 Sed. Res. 75, 663–679 <https://doi.org/10.2110/jsr.2005.055>.

1549 Retallack, G.J., Veevers, J.J., Morante, R., 1996. Global coal gap between Permian–  
 1550 Triassic extinction and Middle Triassic recovery of peat-forming plants. Geol.  
 1551 Soc. Am. Bull. 108(2), 195–207 [https://doi.org/10.1130/0016-](https://doi.org/10.1130/0016-7606(1996)108<0195:GCGBPT>2.3.CO;2)  
 1552 [7606\(1996\)108<0195:GCGBPT>2.3.CO;2](https://doi.org/10.1130/0016-7606(1996)108<0195:GCGBPT>2.3.CO;2).

1553 Romano, M., Bernardi, M., Petti, F.M., Rubidge, B., Hancox, J., Benton, M.J., 2020.  
 1554 Early Triassic terrestrial tetrapod fauna: a review. *Earth-Sci. Rev.* 210, 103331  
 1555 <https://doi.org/10.1016/j.earscirev.2020.103331>.  
 1556 Roscher, M., Stordal, F., Svensen, H., 2011. The effect of global warming and global  
 1557 cooling on the distribution of the latest Permian climate zones. *Palaeogeogr.*  
 1558 *Palaeoclimatol. Palaeoecol.* 309, 186–200  
 1559 <https://doi.org/10.1016/j.palaeo.2011.05.042>.  
 1560 Saito, R., Kaiho, K., Oba, M., Takahashi, S., Chen, Z.Q., Tong, J.N., 2013. A  
 1561 terrestrial vegetation turnover in the middle of the Early Triassic. *Glob. Planet.*  
 1562 *Change* 105, 152–159 <https://doi.org/10.1016/j.gloplacha.2012.07.008>.  
 1563 Shen, G.L., 1995. Permian foras, in: Li, X.X. (Ed.), *Fossil Floras of China Through*  
 1564 *the Geological Ages (English Edition)*. Guangdong Science and Technology  
 1565 Press, Guanzhou, pp. 127–223.  
 1566 Shen, J., Algeo, T.J., Zhou, L., Feng, Q.L., Yu, J.X., Ellwood, B., 2012a. Volcanic  
 1567 perturbations of the marine environment in South China preceding the latest  
 1568 Permian mass extinction and their biotic effects. *Geobiol.* 10, 82–103  
 1569 <https://doi.org/10.1111/j.1472-4669.2011.00306.x>.  
 1570 Shen, J., Algeo, T.J., Hu, Q., Zhang, N., Zhou, L., Xia, W., Xie, S.C., Feng, Q.L.,  
 1571 2012b. Negative C-isotope excursions at the Permian–Triassic boundary linked  
 1572 to volcanism. *Geology* 40 (11), 963–966 <https://doi.org/10.1130/G33329.1>.  
 1573 Shen, J., Lei, Y., Algeo, T.J., Feng, Q.L., Servais, T., Yu, J.X., & Zhou, L., 2013.  
 1574 Volcanic effects on microplankton during the Permian–Triassic transition  
 1575 (Shangsi and Xinmin, South China). *Palaios* 28(8), 552–567  
 1576 <https://doi.org/10.2110/palo.2013.p13-014r>.  
 1577 Shen, J., Schoepfer, S.D., Feng, Q., Song, H.Y., 2015. Marine productivity changes  
 1578 during the End-Permian crisis and Early Triassic recovery. *Earth-Sci. Rev.* 149,  
 1579 136–162 <https://doi.org/10.1016/j.earscirev.2014.11.002>.  
 1580 Shen, J., Chen, J., Algeo, T.J., Yuan, S.L., Feng, Q.L., Yu, J.X., Zhou, L., O’Connell,  
 1581 B., Planavsky, N.J., 2019a. Evidence for a prolonged Permian–Triassic  
 1582 Extinction interval from global marine mercury records. *Nat. Commun.* 10, 1563

1583 <https://doi.org/10.1038/s41467-019-09620-0>.

1584 Shen, J., Yu, J.X., Chen, J.B., Algeo, T.J., Xu, G.Z., Feng, Q.L., Shi, X., Planavsky,  
1585 N.J., Shu, W.C., Xie, S.C., 2019b. Mercury evidence of intense volcanic effects  
1586 on land during the Permian-Triassic transition. *Geology* 47(12), 1117-1121  
1587 <https://doi.org/10.1130/G46679.1>.

1588 Shen, J., Chen, J.B., Algeo, T.J., Feng, Q.L., Yu, J.X., Xu, Y.G., Xu, G.Z., Lei Y.,  
1589 Planavsky, N.J., Xie, S.C., 2021. Mercury fluxes record regional volcanism in  
1590 the South China craton prior to the end-Permian mass extinction. *Geology* 49(4),  
1591 452-456 <https://doi.org/10.1130/G48501.1>.

1592 Shen, J., Yin, R.S., Zhang, S., Algeo, T.J., Bottjer, D.J., Yu, J.X., Xu, G.Z., Penman,  
1593 D., Wang, Y.D., Li, L.Q., Shi, X., Planavsky, N.J., Feng, Q.L., Xie, S.C., 2022.  
1594 Intensified continental chemical weathering and carbon-cycle perturbations  
1595 linked to volcanism during the Triassic–Jurassic transition. *Nat. Commun.* 13(1),  
1596 1-10 <https://doi.org/10.1038/s41467-022-27965-x>.

1597 Shen, S.Z., He, X., Shi, G., 1995. Biostratigraphy and correlation of several Permian–  
1598 Triassic boundary sections in southwestern China. *J. Asian Earth Sci.* 12 (1–2),  
1599 19–30 [https://doi.org/10.1016/0743-9547\(95\)00026-7](https://doi.org/10.1016/0743-9547(95)00026-7).

1600 Shen, S.Z., Crowley, J.L., Wang, Y., Boweig, S.A., Erwin, D.H., Sadler, P.M., Cao,  
1601 C.Q., Rothman, D.H., Henderson, C.M., Ramezani, J., Zhang, H., Shen, Y.A.,  
1602 Wang, X.D., Wang, W., Mu, L., Li, W.Z., Tang, Y.G., Liu, X.L., Liu, L.J., Zeng,  
1603 Y., Jiang, Y.F., Jin, Y.G., 2011. Calibrating the End-Permian Mass Extinction.  
1604 *Science* 334, 1367–1372 <https://doi.org/10.1666/13022>.

1605 Shen, S.Z., Zhang, H., Zhang, Y.C., Yuan, D.X., Chen, B., He, W.H., Mu, L., Lin, W.,  
1606 Wang, W.Q., Chen, J., Wu, Q., Cao, C.Q., Wang, Y., Wang, X.D., 2019. Permian  
1607 integrative stratigraphy and timescale of China. *Sci. China Earth Sci.* 62, 154–  
1608 188 <https://doi.org/10.1007/s11430-017-9228-4>.

1609 Shen, W.J., Sun, Y.G., Lin, Y.T., Liu, D.H., Chai, P.X., 2011. Evidence for wildfire in  
1610 the Meishan section and implications for Permian–Triassic events. *Geochim.*  
1611 *Cosmochim. Acta* 75, 1992–2006 <https://doi.org/10.1016/j.gca.2011.01.027>.

1612 Shen, W.J., Zhang, H., Sun, Y.G., Lin, Y.T., Liang, T., Yang, Z.J., Zhou, Y.Z., 2012.

1613 Evidences for the Permian–Triassic wildfire event: review and appraisal. *Adv.*  
 1614 *Earth Sci.* 27 (6), 613–623 [https://doi.org/10.11867/j.issn.1001-](https://doi.org/10.11867/j.issn.1001-8166.2012.06.0613)  
 1615 [8166.2012.06.0613](https://doi.org/10.11867/j.issn.1001-8166.2012.06.0613).  
 1616 Song, H.J., Wignall, P.B., Tong, J.N., Yin, H.F., 2012. Two pulses of extinction during  
 1617 the Permian–Triassic crisis. *Nat. Geosci.* 6(1), 52–56  
 1618 <https://doi.org/10.1038/NGEO1649>.  
 1619 Song, H.J., Wignall, P. B., Dunhill, A.M., 2018. Decoupled taxonomic and ecological  
 1620 recoveries from the Permo-Triassic extinction. *Sci. Adv.* 4(10), eaat5091  
 1621 <https://doi.org/10.1126/sciadv.aat5091>.  
 1622 Song, Q.Q., Feng, J.P., Yu, J.X., Huang, Q.S., 2013. Study on palaeophytoecology of  
 1623 the Dalong Formation (Late Permian) in south Guizhou. *Guizhou Geol.* 30(4),  
 1624 255–261 (In Chinese with English abstract).  
 1625 Song, Q.Q., Yu, J.X., Feng, J.P., Huang, Q.S., 2015. Palaeobotany of the upper  
 1626 Permian Dalong Formation (marine facies) in south Guizhou. *Geol. Sci. Technol.*  
 1627 *Inf.* 34(1), 63–66 (In Chinese with English Abstract).  
 1628 Song, T., 2018. Study on the bivalve faunas in Southwestern China during the  
 1629 Permian–Triassic transitional time. Doctoral Thesis, China Univ. Geosci. Wuhan  
 1630 1–181.  
 1631 Stanley, S.M., 2009. Evidence from ammonoids and conodonts for multiple Early  
 1632 Triassic mass extinctions. *Proc. Natl. Acad. Sci. USA* 106(36), 15264–15267  
 1633 <https://doi.org/10.1073/pnas.0907992106>.  
 1634 Steiner, M.B., Eshet, Y., Rampino, M.R., Schwindt, D.M., 2003). Fungal abundance  
 1635 spike and the Permian–Triassic boundary in the Karoo Supergroup (South  
 1636 Africa). *Palaeoecol. Palaeogeog. Palaeoclimatol.* 194(4), 405–414  
 1637 [https://doi.org/10.1016/S0031-0182\(03\)00230-X](https://doi.org/10.1016/S0031-0182(03)00230-X).  
 1638 Stevens, L.G., Hilton, J.M., Bond, D.P.G., Glasspool, I.J., Jardine, P.E., 2011.  
 1639 Radiation and extinction patterns in Pennsylvanian–Permian floras from North  
 1640 China as indicators of environmental and climate change. *J. Geol. Soc.* 168, 607–  
 1641 619 <https://doi.org/10.1144/0016-76492010-042>.  
 1642 Sun, Y.D., Joachimski, M.M., Wignall, P.B., Yan, C.B., Chen, Y.L., Jiang, H.S., Wang,



- L.N., Lai, X.L., 2012. Lethally hot temperatures during the Early Triassic greenhouse. *Science* 338 (6105), 366–370  
<https://doi.org/10.1126/science.1224126>.
- Taylor, T.N., Taylor, E.L., Krings, M., 2009. *Paleobotany, the biology and evolution of fossil plants*, 2nd ed. Acad. Press, Amsterdam.
- Tong, J.N., Chu, D.L., Liang, L., Shu, W.C., Song, H.J., Song, T., Song, H.Y., Wu, Y.Y., 2019. Triassic integrative stratigraphy and timescale of China. *Sci. China Earth Sci.* 62, 189–222 <https://doi.org/10.1007/s11430-018-9278-0>.
- Vajda, V., McLoughlin, S., Mays, C., Frank, T.D., Fielding, C.R., Tevywa, A., Lehsten, V., Bocking, M., Nicoll, R.S., 2020. End-Permian (252 Mya) deforestation, wildfires and flooding—an ancient biotic crisis with lessons for the present. *Earth Planet. Sci. Lett.* 529, 115875 <https://doi.org/10.1016/j.epsl.2019.115875>.
- Visscher, H., Brinkhuis, H., Dilcher, D.L., Elsik, W.C., Eshet, Y., Looy, C.V., Rampino, M.R., Traverse, A., 1996. The terminal paleozoic fungal event: evidence of terrestrial ecosystem destabilization and collapse. *Proc. Natl. Acad. Sci. USA* 93(5), 2155–2158 <https://doi.org/10.1073/pnas.93.5.2155>.
- Wang, C.J., 2007. Anomalous hopane distributions at the Permian Triassic boundary, Meishan, China—evidence for the End-Permian marine ecosystem collapse. *Org. Geochem.* 38, 52–66 <https://doi.org/10.1016/j.orggeochem.2006.08.014>.
- Wang, H., Shao, L., Hao, L.M., Zhang, P.F., Glasspool, I.J., Wheeley, J.R., Wignall, P.B., Yi, T.S., Zhang, M.Q., Hilton, J.M., 2011. Sedimentology and sequence stratigraphy of the Lopingian (Late Permian) coal measures in southwestern China. *Int. J. Coal Geol.* 85, 168–183 <https://doi.org/10.1016/j.coal.2010.11.003>.
- Wang, J., Pfefferkorn, H.W., Zhang, Z., Zhou, F., 2012. Permian vegetational Pompeii from Inner Mongolia and its implications for landscape palaeoecology and palaeobiogeography of China. *Proc. Natl. Acad. Sci. USA* 109, 4927–4943  
<https://doi.org/10.1073/pnas.1115076109>.
- Wang, Y., Sadler, P.M., Shen, S.Z., Erwin, D.H., Zhang, Y.C., Wang, X.D., Wang, W., Crowley, J.L., Henderson, C.M., 2014. Quantifying the process and abruptness of the end-Permian mass extinction. *Paleobiol.* 40(1), 113–129

<https://doi.org/10.1666/13022>.

Wang, X., Shao, L., Eriksson, K.A., Yan, Z., Wang, J., Li, H., Zhou, R., Lu, J., 2020.

Evolution of a plume-influenced source-to-sink system: An example from the coupled central Emeishan large igneous province and adjacent western Yangtze cratonic basin in the Late Permian, SW China. *Earth-Sci. Rev.* 207, 103224

<https://doi.org/10.1016/j.earscirev.2020.103224>.

Wang, Z.Q., 1985. Palaeovegetation and plate tectonics: palaeophytogeography of North China during Permian and Triassic times. *Palaeogeogr. Palaeoclimatol.*

*Palaeoecol.* 49(1–2), 25–45 [https://doi.org/10.1016/0031-0182\(85\)90003-3](https://doi.org/10.1016/0031-0182(85)90003-3).

Wang, Z.Q., 1996. Recovery of vegetation from the terminal Permian mass extinction in North China. *Rev. Palaeobot. Palynol.* 91, 121–142

[https://doi.org/10.1016/0034-6667\(95\)00069-0](https://doi.org/10.1016/0034-6667(95)00069-0).

Whittaker, R.H., Goodman, D., 1979. Classifying species according to their

demographic strategy. *Am. Nat.* 113, 185–200 <https://doi.org/10.1086/283378>.

Wignall, P.B., 2015. *The Worst of Times: How Life on Earth Survived 80 Million Years of Extinction*. Princeton University Press, pp. 224

<https://doi.org/10.1515/9781400874248>.

Wignall, P.B., Chu, D., Hilton, J.M., Dal Corso, J., Wu, Y., Wang, Y., Atkinson, J.,

Tong, J., 2020. Death in the shallows: The record of Permo-Triassic mass extinction in paralic settings, southwest China. *Glob. Planet. Change* 189,

103176 <https://doi.org/10.1016/j.gloplacha.2020.103176>.

Wu, Q., Ramezani, J., Zhang, H., Wang, J., Zeng, F.G., Zhang, Y.C., Liu, F., Chen, J.,

Cai, Y.F., Hou, Z.S., Liu, C., Yang, W., Henderson, C.M., Shen, S.Z., 2021.

High-precision U-Pb age constraints on the Permian floral turnovers,

paleoclimate change, and tectonics of the North China block. *Geology* 49(6),

677–681 <https://doi.org/10.1130/G48051.1>.

Xie, S.C., Pancost, R.D., Huang, J.H., Wignall, P.B., Yu, J.X., Tang, X., Chen, L.,

Huang, X.Y., Lai, X.L., 2007. Changes in the global carbon cycle occurred as

two episodes during the Permian–Triassic crisis. *Geology* 35(12), 1083–1086

<https://doi.org/10.1130/G24224A.1>.

- 1703 Xie, S.C., Yin, H.F., Cao, C.Q., Wang, C.J., Lai, X.L., 2009. Episodic changes of the  
1704 earth surface system across the Permian–Triassic boundary: molecular  
1705 geobiological records. *Acta Palaeontol. Sin.* 48(3), 496–506 (In Chinese with  
1706 English abstract).
- 1707 Xiong, C.H., Wang, Q., 2011. Permian–Triassic land-plant diversity in South China:  
1708 was there a mass extinction at the Permian/Triassic boundary? *Paleobiol.* 37(1),  
1709 157–167 <https://doi.org/10.1666/09029.1>.
- 1710 Xiong, C.H., Wang, J.S., Huang, P., Cascales-Minana, B., Cleal, C.J., Benton, M.J.,  
1711 Xue, J., 2021. Plant resilience and extinctions through the Permian to Middle  
1712 Triassic on the North China Block: A multilevel diversity analysis of macrofossil  
1713 records. *Earth-Sci. Rev.* 223, 103846  
1714 <https://doi.org/10.1016/j.earscirev.2021.103846>.
- 1715 Xu, G.Z., Feng, Q.L., Deconinck, J.F., Shen, J., Zhao, T.Y., Young, A.L., 2017. High-  
1716 resolution clay mineral and major elemental characterization of a Permian–  
1717 Triassic terrestrial succession in southwestern China: Diagenetic and  
1718 paleoclimatic/paleoenvironmental significance. *Palaeogeogr. Palaeoclimatol.*  
1719 *Palaeoecol.* 481, 77–93 <https://doi.org/10.1016/j.palaeo.2017.05.027>.
- 1720 Xu, R., Zhu, J.R., Chen, Y., Duan, S.Y., Hu, Y.F., Zhu, W.Q., 1979. China Late  
1721 Triassic Baoding Flora. *Sci. Press* 1–130.
- 1722 Yan, Z.M., Shao, L.Y., Glasspool, I.J., Wang, J., Wang, X.T., Wang, H., 2019.  
1723 Frequent and intense fires in the final coals of the Paleozoic indicate elevated  
1724 atmospheric oxygen levels at the onset of the End-Permian Mass Extinction  
1725 Event. *Int. J. Coal Geol.* 207, 75–83 <https://doi.org/10.1016/j.coal.2019.03.016>.
- 1726 Yang, G.X., 1994. *Palaeobotany*. Geological Publishing House, Beijing (In Chinese).
- 1727 Yang, S.P., 1993. *Paleoecology: principles and methods*. Geol. Publ. Beijing (In  
1728 Chinese).
- 1729 Yang, T.L., 2015. The Bivalve Fauna From Deep-water Facies of South China During  
1730 the Permian–Triassic Interval. Doctoral Thesis, China Univ. Geosci. Wuhan, pp.  
1731 25–36 (In Chinese with English abstract).
- 1732 Yang, W., Wan, M.L., Crowley, J.L., Wang, J., Luo, X.R., Tabor, N., Angielczyk, K.D.,

- 1733 Castaldo, R., Geissman, J., Liu, F., Roopnarine, P., Sidor, C.A., 2021.  
 1734 Paleoenvironmental and paleoclimatic evolution and cyclo- and chrono-  
 1735 stratigraphy of Upper Permian–Lower Triassic fluvial-lacustrine deposits in  
 1736 Bogda Mountains, NW China—Implications for diachronous plant evolution  
 1737 across the Permian–Triassic boundary. *Earth-Sci. Rev.* 222, 103741  
 1738 <https://doi.org/10.1016/j.earscirev.2021.103741>.
- 1739 Yang, Y., Sadler, P.M., Shen, S.Z., Erwin, D.H., Zhang, Y.-C., Wang, X.-D., Wang, W.,  
 1740 Crowley, J.L., Henderson, C.M., 2016. Quantifying the process or abruptness of  
 1741 the end-Permian mass extinction. *Palaeobiology* 40, 113–129  
 1742 <https://doi.org/10.1666/13022>.
- 1743 Yang, Z.Y., Zhang, S.X., Yang, J.D., Zhou, H.Q., Cao, H.S., 2000. Stratigraphical  
 1744 lexicon of China: Triassic. Geol. Publ. Beijing (In Chinese).
- 1745 Yao, Z.Q., 1978. On the age of “Gigantopteris Coal Series” and Gigantopteris flora in  
 1746 South China. *Acta Palaeontol. Sin.* 17, 81–89 (In Chinese with English abstract).
- 1747 Yao, Z.Q., Xu, J.T., Zhen, Z.G., Mo, Z.G., 1980. Late Permian biostratigraphy and the  
 1748 Permian–Triassic boundary in Western Guizhou and Eastern Yunnan, in: Nanjing  
 1749 Institute of Geology and Palaeontology (Ed.), *Stratigraphy and palaeontology of*  
 1750 *Late Permian coal-bearing formations in Western Guizhou and Eastern Yunnan*.  
 1751 Sci. Press, Beijing, pp. 1–69 (In Chinese).
- 1752 Ye, M.N., 1979. On some Middle Triassic plants from Hupeh and Szechuan. *Acta*  
 1753 *Palaeontol. Sin.* 18(1), 73–81 (In Chinese with English abstract).
- 1754 Yin, H.F., 1985. Bivalves near the Permian–Triassic boundary in South China. *J.*  
 1755 *Paleontol.* 59(3), 572–600.
- 1756 Yin, H.F., Feng, Q.L., Lai, X.L., Baud, A., Tong, J.N., 2007. The protracted Permo-  
 1757 Triassic crisis and multi-episode extinction around the Permian–Triassic  
 1758 boundary. *Glob. Planet. Change* 55, 1–20  
 1759 <https://doi.org/10.1016/j.gloplacha.2006.06.005>.
- 1760 Yin, H.F., Jiang, H.S., Xia, W.C., Feng, Q.L., Zhang, N., Shen, J., 2014. The End-  
 1761 Permian regression in South China and its implication on mass extinction. *Earth-*  
 1762 *Sci. Rev.* 137, 19–33 <https://doi.org/10.1016/j.earscirev.2013.06.003>.

- 1763 Yin, H.F, Xie, S.C., Luo, G.M., Algeo, T. J., & Zhang, K.X., 2012. Two episodes of  
1764 environmental change at the Permian–Triassic boundary of the GSSP section  
1765 Meishan. *Earth-Sci. Rev.* 115(3), 163–172  
1766 <https://doi.org/10.1016/j.earscirev.2012.08.006>.
- 1767 Yu, J.X., 2008. Floras (macro- and microfloras) and evolutionary dynamics across the  
1768 Permian–Triassic boundary along Guizhou and Yunnan border, South China.  
1769 Doctoral Thesis, China Uni. Geosci. Wuhan & Uni. Pierre et Marie Curie, Paris  
1770 6, 220 pp.
- 1771 Yu, J.X., Broutin, J., Chen, Z.Q., Shi, X., Li, H., Chu, D.L., Huang, Q.S., 2015.  
1772 Vegetation changeover across the Permian–Triassic boundary in Southwest  
1773 China: Extinction, survival, recovery and palaeoclimate: A critical review. *Earth-*  
1774 *Sci. Rev.* 149, 203–224 <https://doi.org/10.1016/j.earscirev.2015.04.005>.
- 1775 Yu, J.X., Broutin, J., Huang, Q.S., Grauvogel-Stamm, L., 2010. *Annalepis*, a  
1776 pioneering lycopsid genus in the recovery of the Triassic land flora in South  
1777 China. *C. R. Palevol.* 9, 479–486 <https://doi.org/10.1016/j.crpv.2010.09.004>.
- 1778 Zhang, K.X., Yu, J.X., Lin, Q.X., Jing, Y.L., Chen, B., 2004. Palynological  
1779 assemblage in section d of Meishan, Changxing, Zhejiang and its significance of  
1780 global correlation. *Earth Sci. J. China Uni. Geosci.* 29 (3), 253–262.
- 1781 Zhang, N., Jiang, H., Zhong, W., Huang, H., Xia, W., 2014. Conodont biostratigraphy  
1782 across the Permian–Triassic boundary at the Xinmin section, Guizhou, South  
1783 China. *J. Earth Sci.* 25(5), 779–786 <https://doi.org/10.1007/s12583-014-0472-0>.
- 1784 Zhang, Z.L., Meng, F.S., Sheng, X.C., 1992. Triassic, in: Wang, X.F., Ma, D.S., Jiang,  
1785 D.H. (Eds.), *Hainan Island geology (1) stratigraphic paleontology*. Geol. Publ.  
1786 Beijing pp. 161–199 (In Chinese).
- 1787 Zheng, R.H., 2011. China pre-Mesozoic structural sequence and lithofacies  
1788 paleogeography atlas. Geol. Publ. Beijing (In Chinese).
- 1789 Zhou, Z.Y., 1989. Late Triassic plants from Shaqiao, Hengyang, Hunan Province.  
1790 *Palaeontol. Cathayana* 4, 131–197 <http://ir.nigpas.ac.cn/handle/332004/5891>.
- 1791 Zhou, Z.Y., Li, B.X., 1979. A preliminary study of the Early Triassic plants from the  
1792 Qionghai District, Hainan Island. *Acta Palaeotol. Sin.* 18(5), 444–466 (In

1793 Chinese with English abstract).

1794 Zuazo, V.H.D., Pleguezuelo, C.R.R., 2009. Soil-erosion and runoff prevention by

1795 plant covers: A review, in: Lichtfouse, E., Navarrete, M., Debaeke, P., Véronique,

1796 S., Alberola, C. (Eds.), Sustainable Agriculture. Springer Dordrecht pp. 65–86

1797 [https://doi.org/10.1007/978-90-481-2666-8\\_48](https://doi.org/10.1007/978-90-481-2666-8_48).

1798

1799

1800 Table and figure captions

1801 Table 1. Example of normalized occurrences for species richness estimates within the

1802 arborescent lycopsids showing the distribution of organ taxa for stems

1803 (*Lepidodendron*), rootstock (*Stigmaria*), sporophylls (*Lepidostrobohyllum*) and

1804 cones (*Lepidostrobus*). In each formation, stems represent the best measure of species

1805 richness as they present the most reliable features to distinguish species, and in each

1806 case show the largest species richness compared to the other organs present. While

1807 more species of rootstock are present in the Xuanwei Formation, we consider this an

1808 unreliable measure of species richness. Species delimitation is less reliable in species

1809 of *Stigmaria* that have few distinguishing features that may vary in different positions

1810 across the rooting system. Furthermore, one of the rootstock accounts from the

1811 Xuanwei Formation has not been identified to the species level (*Stigmaria* sp.) and

1812 most likely represents a poorly preserved or incomplete specimen of one or more of

1813 the other species present. In all cases non-normalised estimates significantly inflate

1814 species richness estimates.

System	Series	Stage/ substages		Lower Yangtze area	Middle Yangtze area	Upper Yangtze area		Eastern Yunnan Western Guizhou area	Hainan area
Triassic	Upper Triassic	Rhaetian		Lalijian Formation	Wanglongtan Formation	Shazhenxi F.	Xujiahe Formation	Baoding F.	Erqiao Formation
		Norian	Jiuligang Formation <sup>(10)</sup>		Xiaotangzi Formation		<b>Dajing F.</b> <sup>(11)</sup>	Huobachong Formation	
					Kuahongdong Formation		<b>Daqiaodi Formation</b> <sup>(10)</sup>	Banan Formation	
		Carnian	Maantang Formation		Bingnan Formation		Falang Formation		
	Middle Triassic	Ladinian	Tongtoujian Formation	<b>Badong Formation Member 4-5</b> <sup>(9)</sup>	Huanglianqiao Formation	Yangliujing Formation			
			Yueshan Formation						
	Anisian	Dongmaanshan Formation	<b>Badong Formation Member 1-3</b> <sup>(9)</sup>	Leikoupo Formation	Guanlin Formation				
	Lower Triassic	Olenekian	Spath. Smith.	Nanlinhu Formation	Jialinjiang Formation	Jialinjiang Formation	Yongningzhen Formation	<b>Lingwen Formation</b> <sup>(8)</sup>	
				Helongshan Formation					
		Induan	Griesb. Dien.	Yinkeng Formation	Daye Formation	<b>Feixianguan Formation</b> <sup>(7)</sup>	Dongchuan Formation		
	PTT								
	Permian	Lopingian	Chang- hsingian		Changxing Formation	Wujiaping F.	<b>Dalong Formation</b> <sup>(5)</sup>		Yelang Formation
Wuchia- pingian			Wujiaping Formation	Heshan F.	<b>Longtan Formation</b> <sup>(3)</sup>		<b>Xuanwei Formation</b> <sup>(3)</sup>	<b>Upper Lower</b>	
Guadalu- pian		Capitanian		<b>Maokou Formation</b> <sup>(2)</sup>	Gufeng Formation			Emeishan Basalt	
		Wordian						Maokou Formation	
		Roadian							
Cisura- lian		Kungurian		Qixia Formation				Qixia Formation	
		Artinskian		<b>Liangshan Formation</b> <sup>(1)</sup>				<b>Liangshan Formation</b>	

**Figure 1.** Correlation of lower Cisuralian to Upper Triassic formations in South China. gray units contain plant fossils, with leaf representing position of separate beds containing plants. Numbers in formations represent: 1. Liangshan section; 2. Maokou section; 3. Longtan and lower Xuanwei section; 4. Chahe and Chinahe sections; 5. Xinmin, Duanshan A and B sections; 6. Chinahe, Mide and Tucheng sections; 7. Lubei, Pojiao and Dongchuan sections; 8. Lingwen section; 9. Hongjiaguan and Furongqiao section; 10. Jiuligang and Daqiaodi sections; 11. Xujahe, Dajing, Anyuan, Bagong sections. PTT = Permo-Triassic transition. Figure modified from Yang et al.



(2000); Jin et al. (2000), Yu et al. (2015), Tong et al. (2019) and Shen et al. (2019).

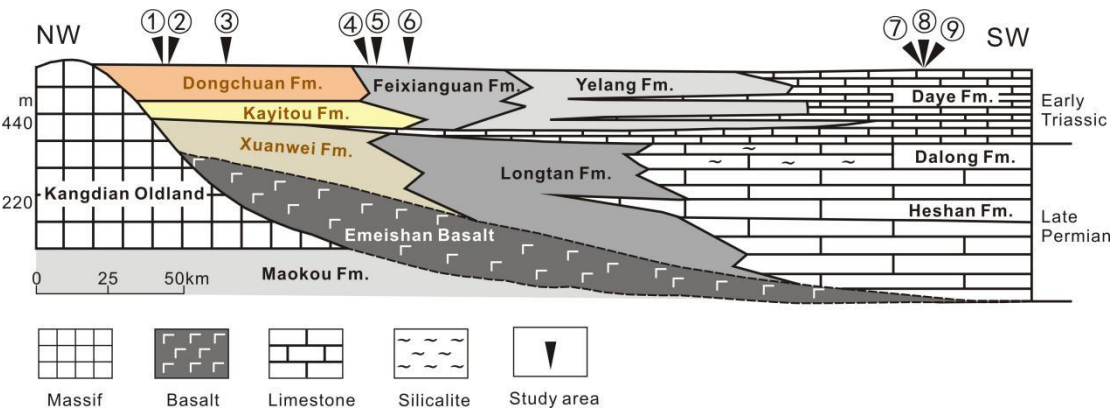


**Figure 2.** Sketch map of the Permian Changhsingian lithofacies in Western Guizhou and Eastern Yunnan, southwestern China. 1. Pojiao section; 2. Lubei section; 3. Chahe section; 4. Chinahe section; 5. Mide section; 6. Tucheng section; 7. Xinmin section; 8. Duanshan A section; 9. Duanshan B section; modified from Yu et al. (2015), Wignall et al. (2020).

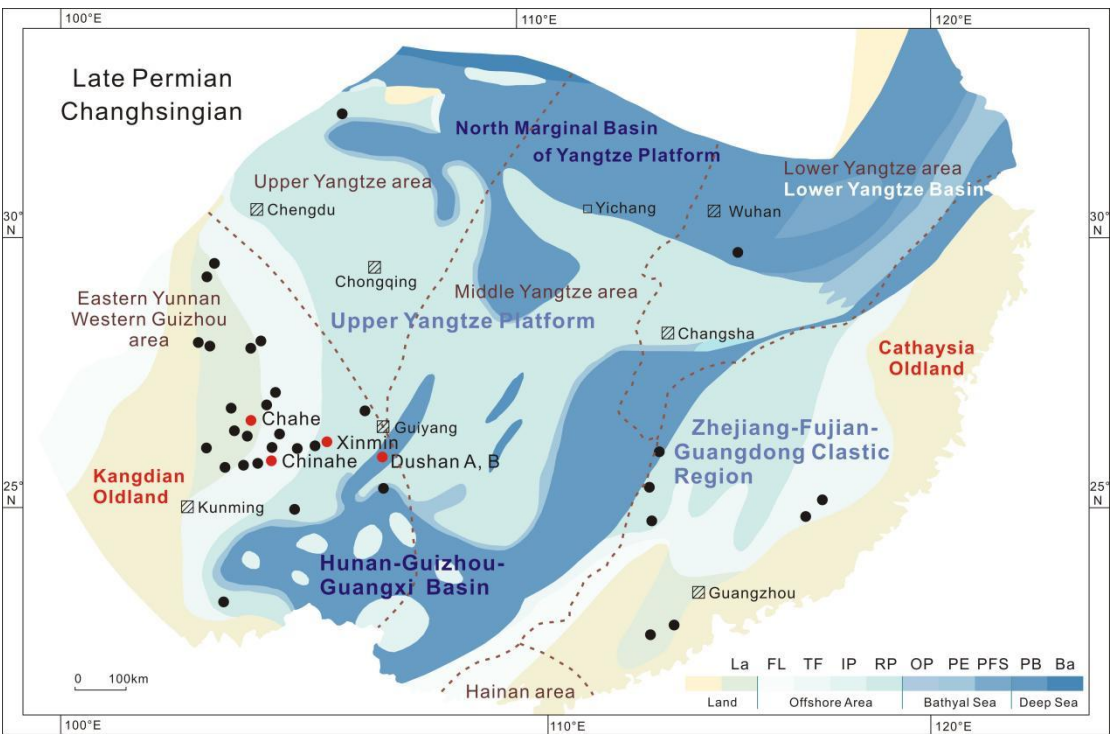
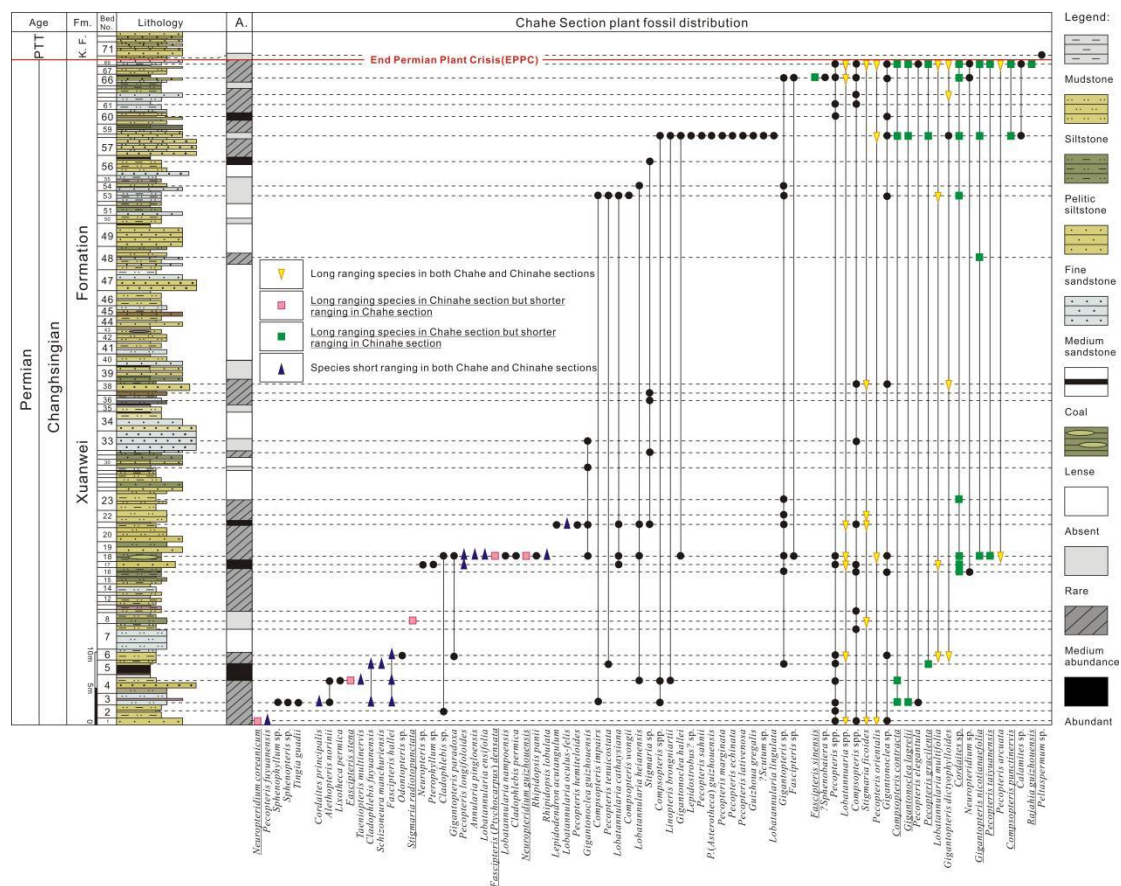


**Figure 3.** Paleogeographic map of South China during the End Permian showing positions of sections studied from the Changhsingian aged Xuanwei and Dalong formations. Red point: studied sections in this paper; Black point: supplementary



1837 sections from literature; La = Lacustrine ; FL = Flood land; TF = Tide flat; IP =  
1838 Isolate platform; RP = Regional platform; OP = Open platform; PE = Platform edge;  
1839 PFS = Carbonate platform fore slope; PB = Platform basin; Ba = Bathyal sea;  
1840 modified from Zheng et al. (2011), Yin et al. (2014) and Yu et al. (2015).  
1841



1842  
1843 **Figure 4.** Plant fossil distributions from the Xuanwei Formation in the Chahe section  
1844 (unnormalized). PTT = Permo-Triassic transition; Grib. = Grisbachian; K. F. =  
1845 Kayitou Formation; A. = Abundance of plant fossil. The color of the lithology column  
1846 shows the real rock color in the field.

1847

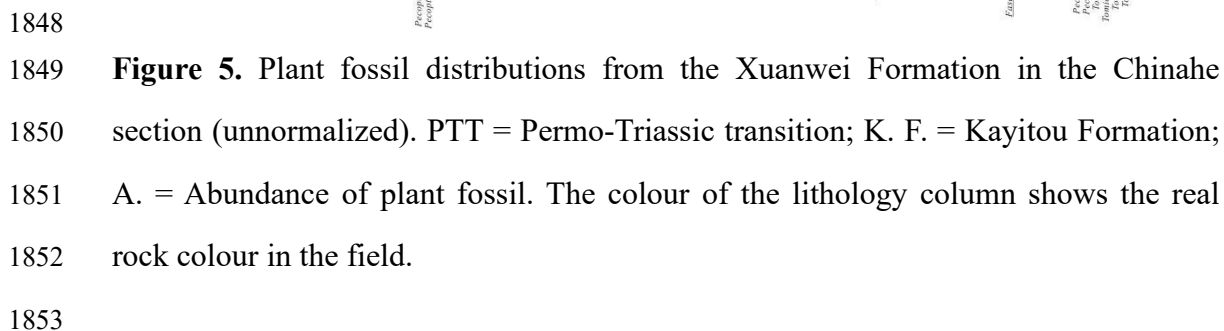


**Figure 5.** Plant fossil distributions from the Xuanwei Formation in the Chinahe section (unnormalized). PTT = Permo-Triassic transition; K. F. = Kayitou Formation; A. = Abundance of plant fossil. The colour of the lithology column shows the real rock colour in the field.

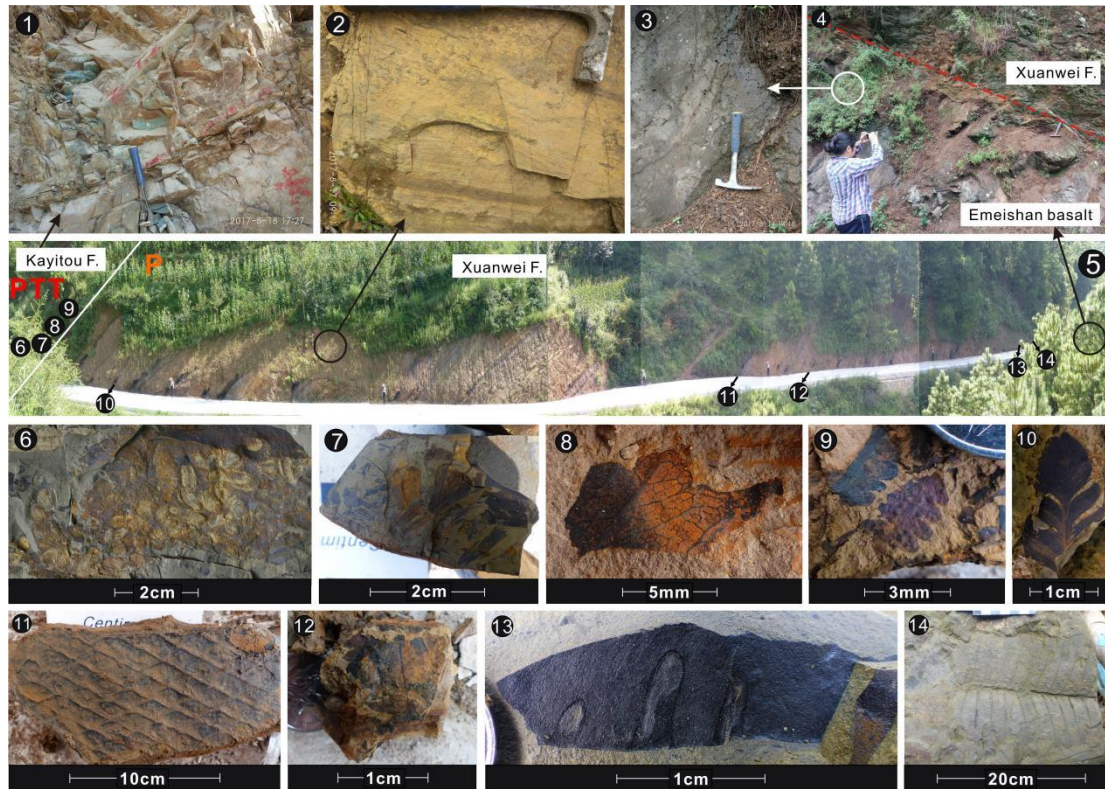


**Figure 6.** Field panorama, sedimentology and representative plant fossils showing preservation condition from the Chinahe section. 1. Strata of the Kayitou Formation; 2. Strata of the upper Xuanwei Formation; 3. Emeishan Basalt with vesicular structure; 4. Boundary between the Emeishan Basalt and the Xuanwei Formation; 5. Panorama of the Chinahe section ranging from the Emeishan Basalt (right) to the Kayitou Formation (left); 6. Conchostraca in the Kayitou Formation; 7. *Tomiostrobus* (= *Annalepis*) layer in the bottom of Kayitou Formation (Bed 26); 8. Abraded *Gigantopteris dictyophylloides* fragments together with *Tomiostrobus* (= *Annalepis*) (Bed 26); 9. Small *Peltaspermum martinsii* together with *Tomiostrobus* (= *Annalepis*) (Bed 26); 10. Broken *Compsopteris* leaf in the upper part of Xuanwei Formation (Bed 22); 11. Layer of *Lepidodendron oculus-felis* in middle of Xuanwei Formation (Bed 10); 12. *Gigantopteris* fragments occurring from the lower to middle of the Xuanwei Formation (Beds 3–10); 13. Well-preserved leaves with insect feeding trace fossils (bed 2); 14. Complete fern branches in the bottom of Xuanwei Formation (Bed 1). PTT = Permo-Triassic transition; P = Permian.



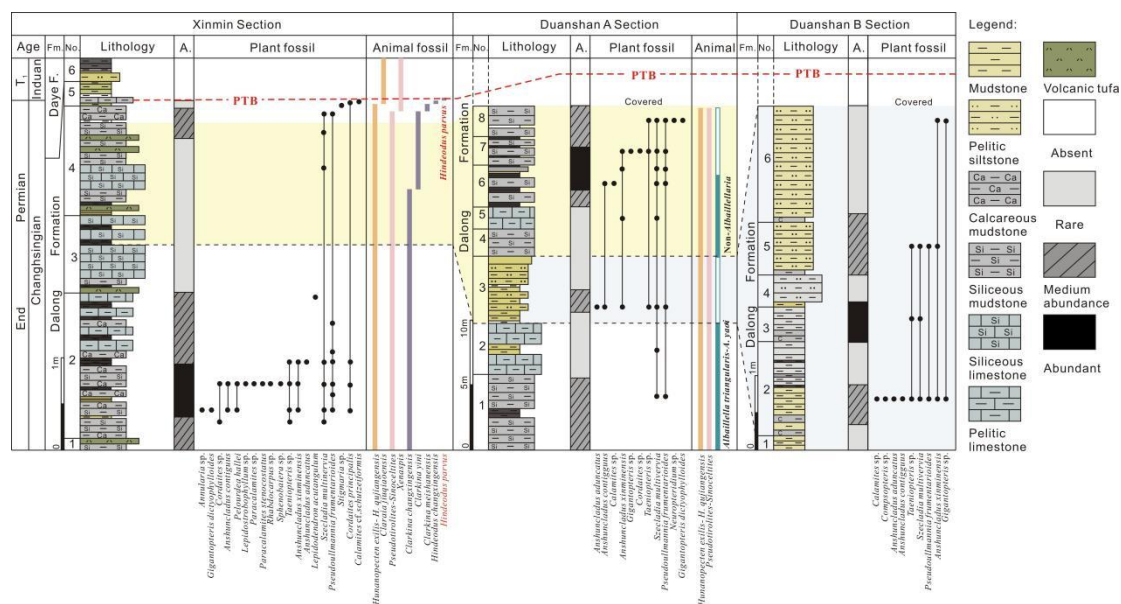


**Figure 7.** Plant and marine animal fossil distributions from the Dalong Formation in the Xinmin, Duanshan A and Duanshan B sections (unnormalized). T<sub>1</sub> = Early Triassic; Fm. = Formation; NO. = Bed number; A. = Abundance of plant fossil; PTB = Permian Triassic boundary. The color of the lithology column shows the real rock color in the field.

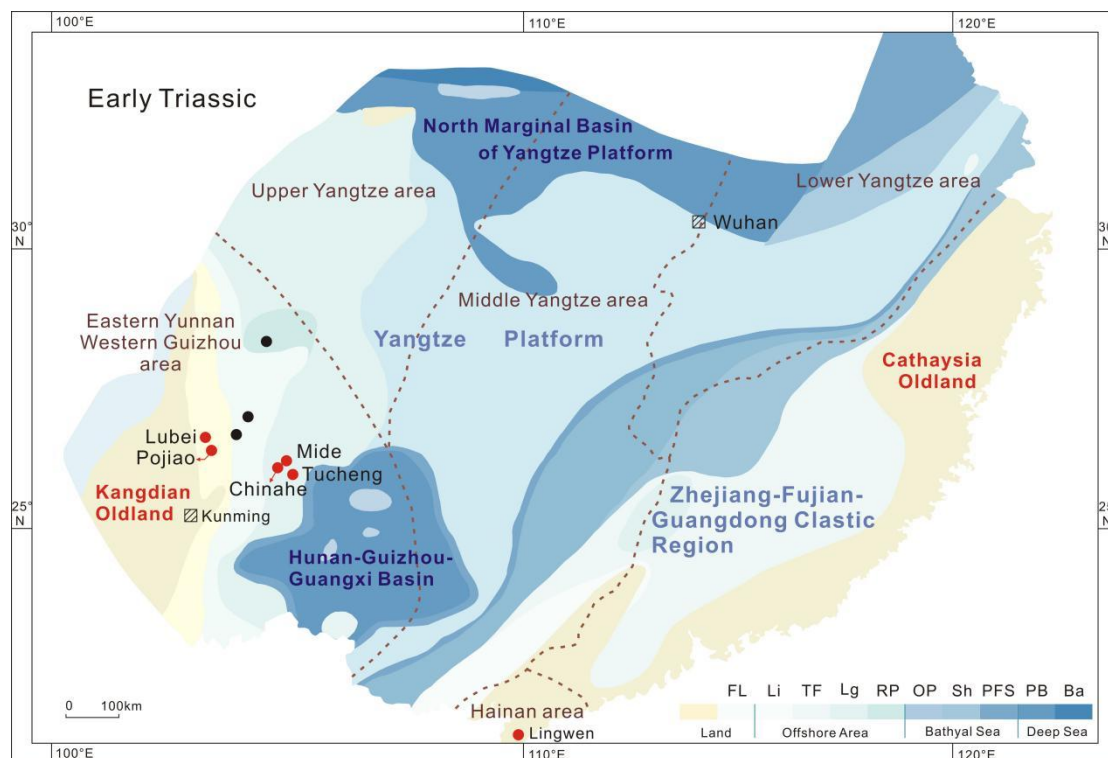


**Figure 8.** Early Triassic paleogeographical map of South China showing locations of

sections containing the Induan Kayitou Formation, Olenekian Feixianguan and Lingwen formations. Red point: studied sections in this paper; Black point: supplementary sections from literature; FL = Flood land; TF = Tide flat; Lg = Lagoon; RP = Regional platform; OP = Open platform; Sh = Shallow sea; PFS = Carbonate platform fore-slope; PB = Platform basin; Ba = Bathyal sea; modified from Zheng et al. (2011) and Yin et al. (2014).

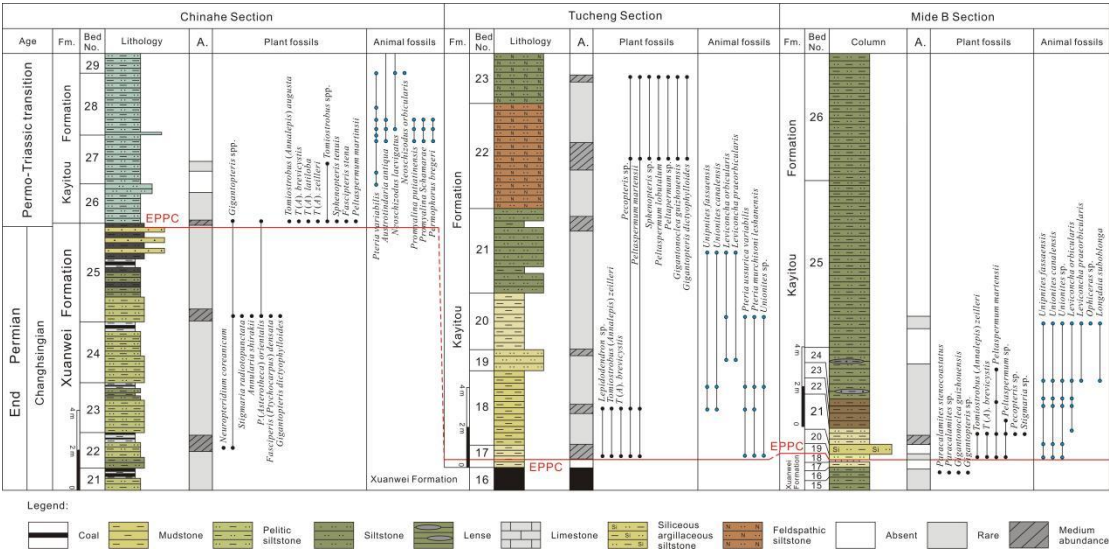


**Figure 9.** Plant and marine animal fossil distributions from the Kayitou Formation in the Chinahe, Tucheng and Mide sections (unnormalized). Fm. = Formation; NO. = Bed number; EPPC = End Permian Plant Crisis; A. = Abundance of plant fossil. The color of the lithology column shows the real rock color in the field.

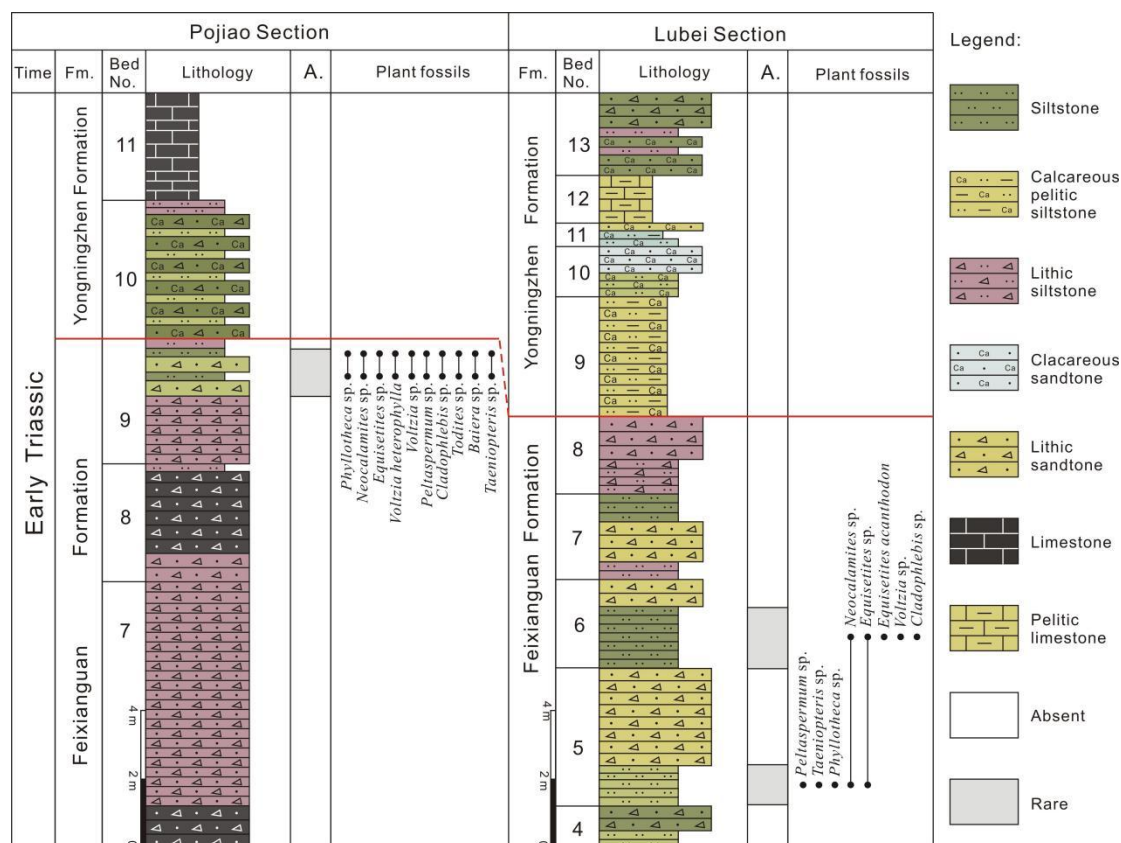


**Figure 10.** Plant fossil distributions from the Feixianguan Formation in the Lubei and Pojiao sections (unnormalized). Fm. = Formation; NO. = Bed number; A. = Abundance of plant fossil. The color of the lithology column shows the real rock color in the field.





**Figure 11.** Representative plant fossils in Kayitou Formation of Chinahe section (1–8) and Feixianguan Formation of Lubei and Pojiao section (9–15). 1. Bivalves; 2. *Tomiostrobus* (= *Annalepis*) spp.; 3. *T. (A.) zeilleri*; 4. *T. (A.) augusta*; 5. *T. (A.) latiloba*; 6. Unkown index; 7. *Fasciapteris stena*; 8. *Peltaspermum martinsii*; 9–12. *Carpolithus* spp.; 13. *Neocalamites* branches, common in both Lubei and Pojiao sections; 14. *Voltzia* sp.; 15. Possible fertile spike?; 16. *Peltaspermum* sp.; 17. Fern; 18. *Todites* sp.

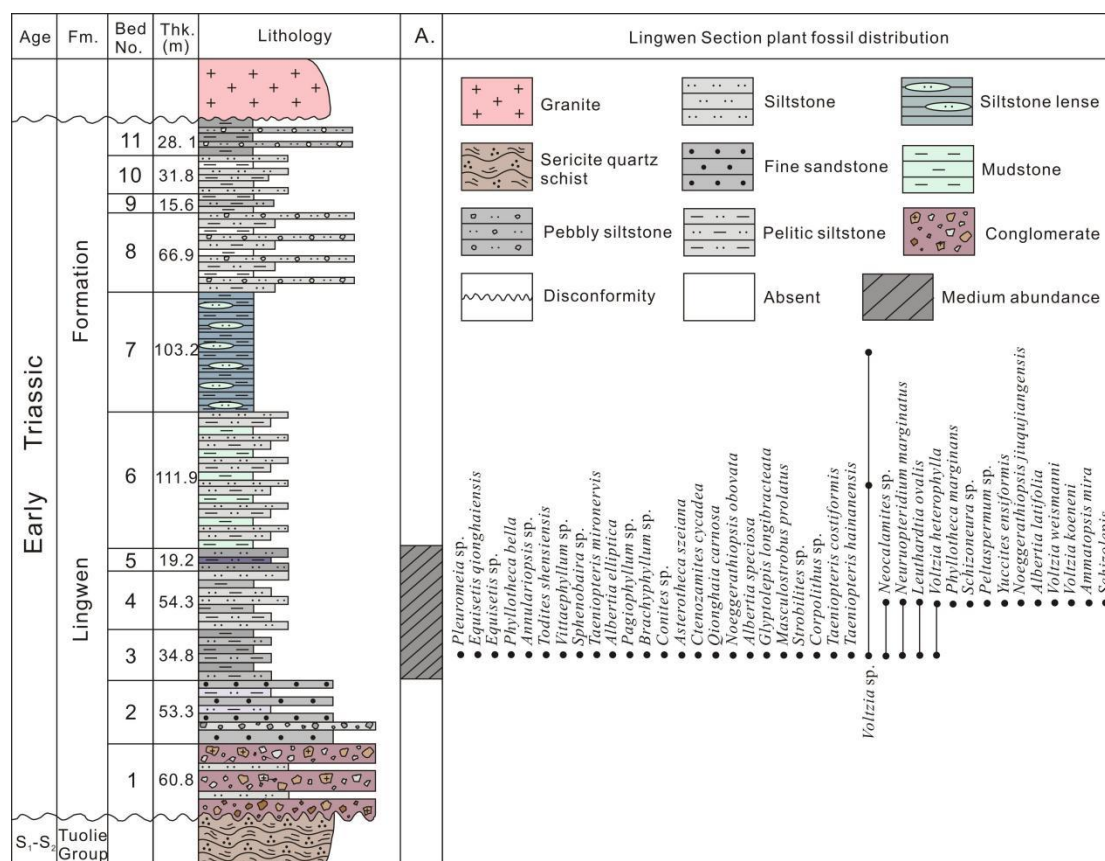


**Figure 12.** Plant fossil distributions from the Lingwen Formation in the Lingwen section (unnormalized). Fm. = Formation; NO. = Bed number; Thk. = Thickness; A. = Abundance of plant fossil. The color of the lithology column shows the real rock color in the field.



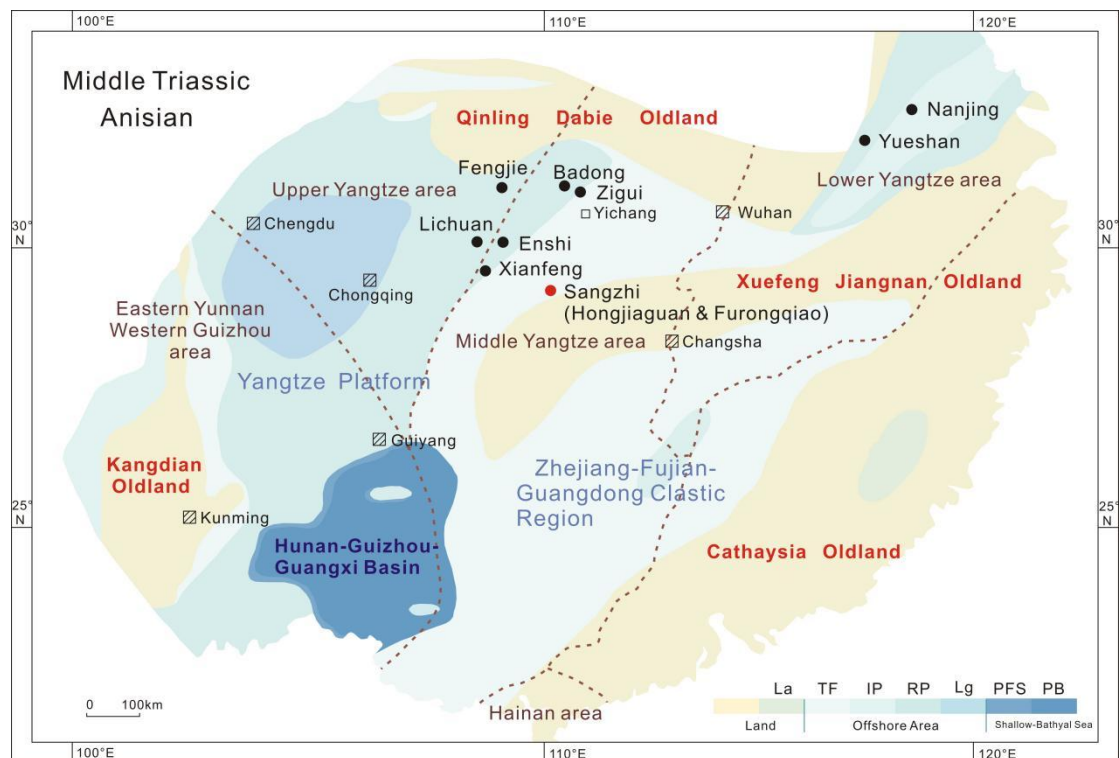


**Figure 13.** Middle Triassic paleogeographic map of South China showing locations for sections of the Badong Formation. Red point: studied sections in this paper; Black point: supplementary sections from literature; La = lacustrine; TF = Tide flat; IP = Isolated platform; RP = Regional platform; Lg = Lagoon; PFS = Carbonate platform fore slope; PB = Platform basin; modified from Zheng et al. (2011).

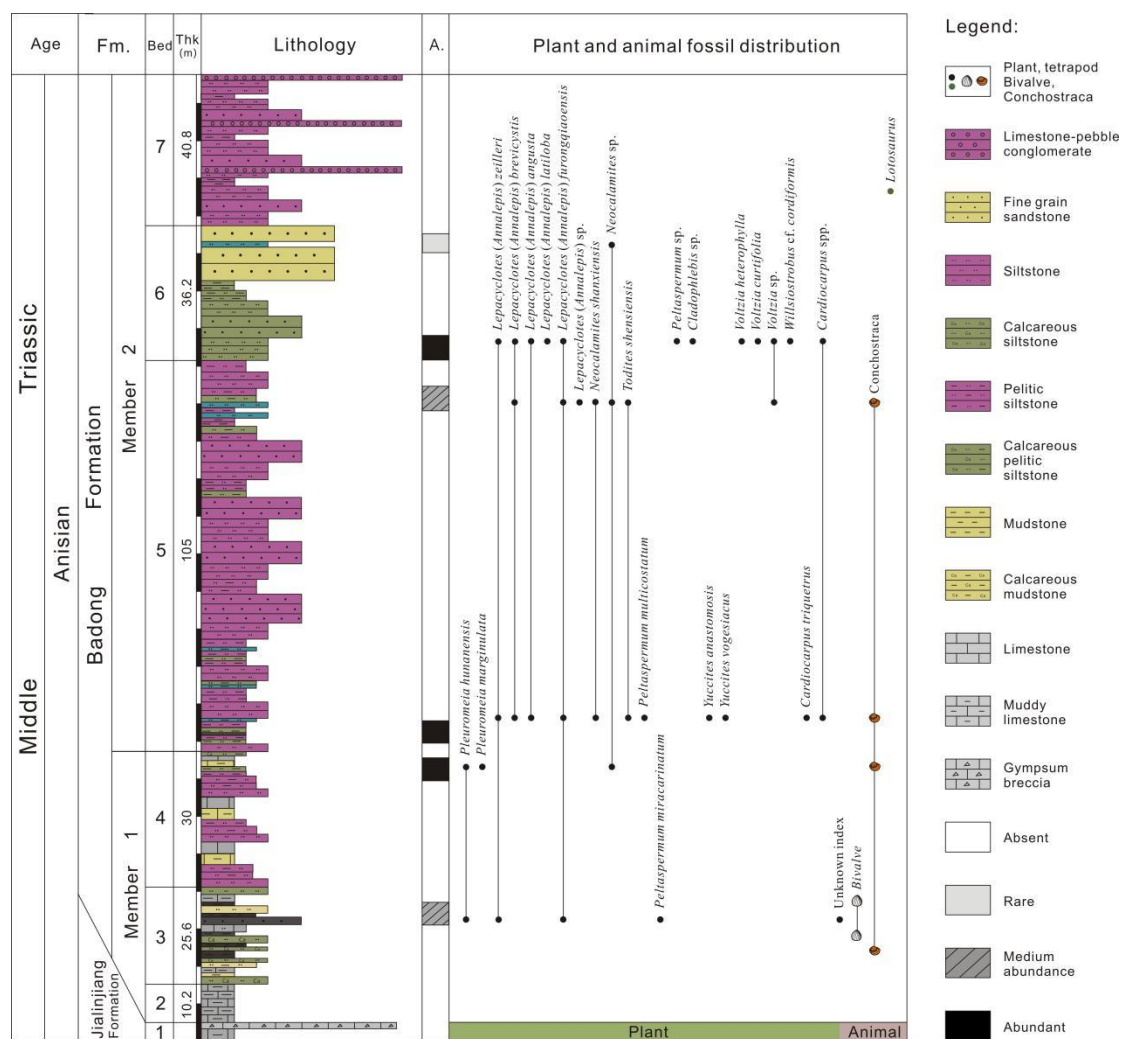


**Figure 14.** Plant fossil distributions from the Badong Formation in the Hongjiaguan and Furongqiao sections (unnormalized). Fm. = Formation; NO. = Bed number; Thk. = Thickness; M. = Mineral; J. = Jialinjiang Formation; A. = Abundance of plant fossil. The color of the lithology column shows the real rock color in the field.

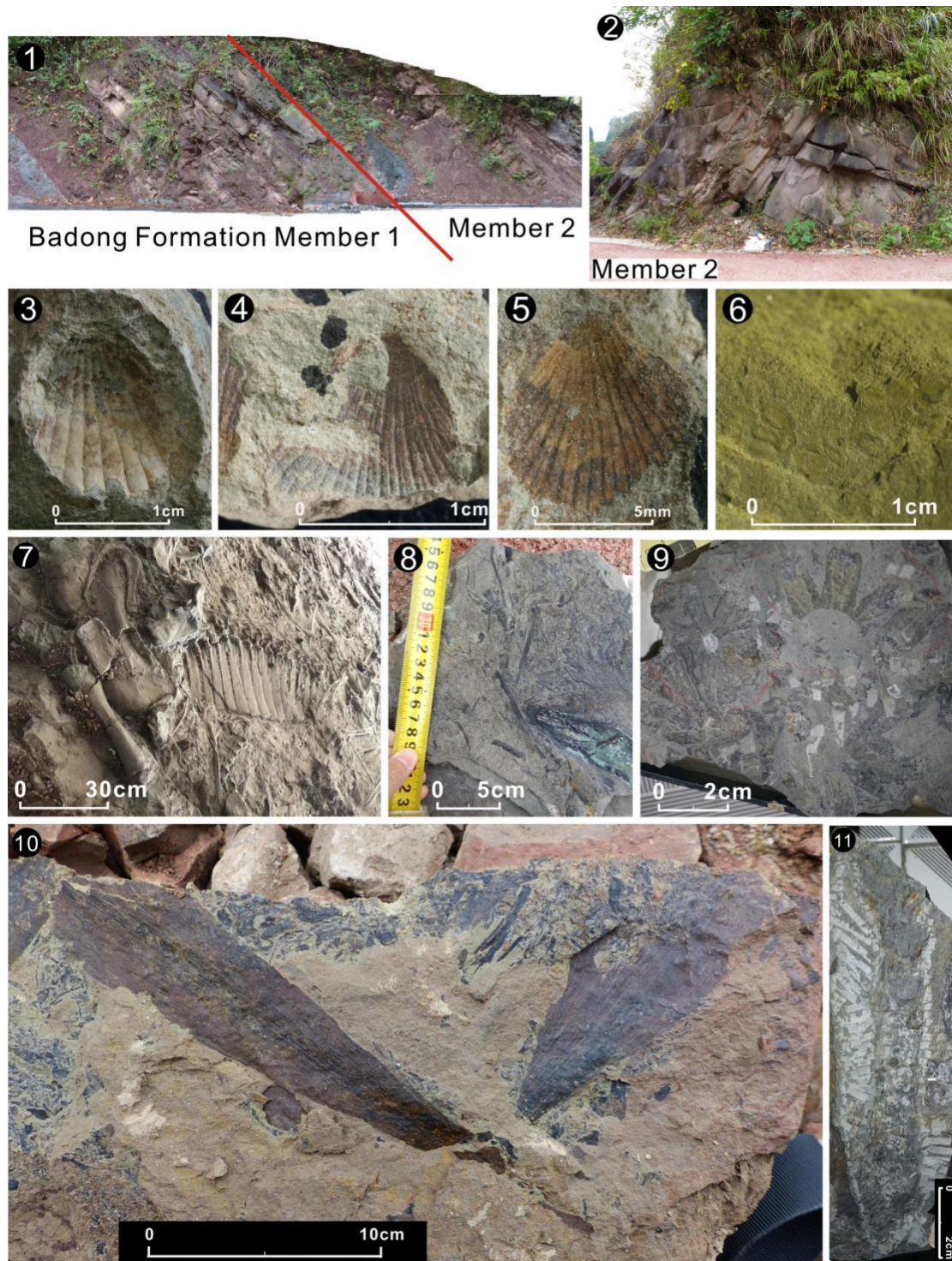


**Figure 15.** Field panorama, sedimentology, representative animal and plant fossils of the Badong Formation from Hongjiaguan and Furongqiao sections. 1. Lithological boundary of Badong Formation Member 1 (left) and Member 2 (right); 2. Thick-bedded sandstone Member 2 (Bed 6 in figure 14); 3. *Myophoria (Costatoria) goldfussi*; 4. *Myophoria (Costatoria) goldfussi mansuyi*; 5. *Leptochondria albertii*; 6. *Euestheria* sp.; 7. *Lotosaurus* in Member 2 in Furongqiao village; 8. Long-distance



transported plant fragments in sandstone from Member 2; 9 *Lepacyclotes* (= *Annalepis*) *sangzhiensis* in the Hongjiaguan section (collected by Fansong Meng); 10. *Yuccites* sp.; 11. Preserved in-situ *Pleuromeia sanxiaensis* in the Dawotang section, Fengjie, Sichuan (collected by Fansong Meng).

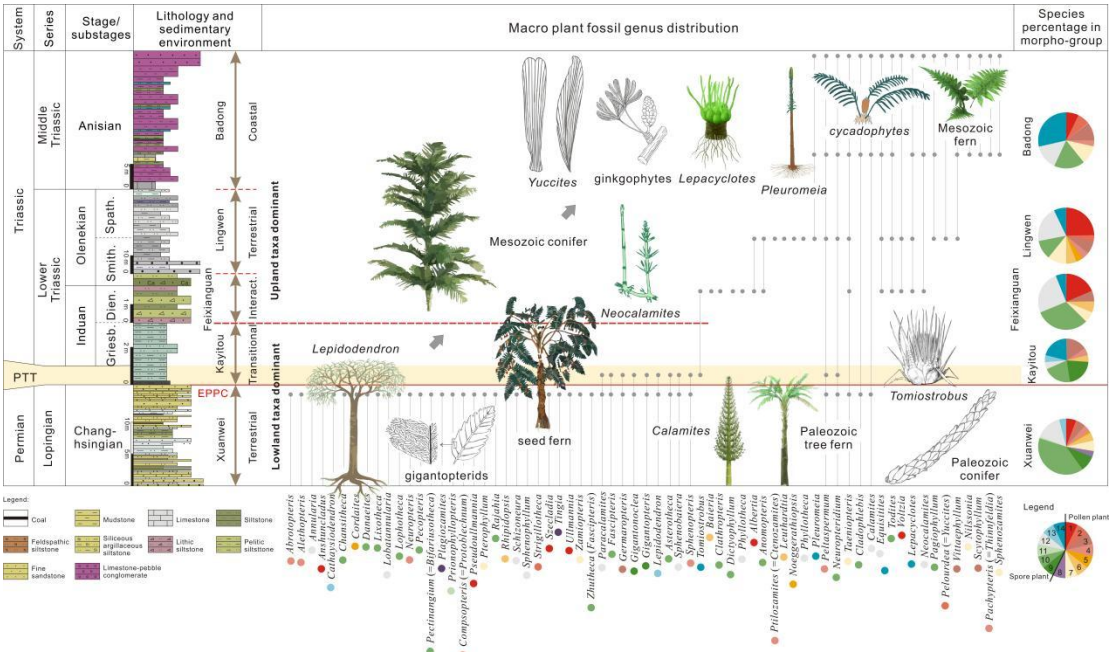


**Figure 16.** Lithology, sedimentary, macro plant fossil distribution range, floral composition from End Permian Changhsingian to Middle Triassic Anisian in South China area. Kayitou Formation conformably overlies on Xuanwei Formation, while Kayitou, Feixianguan, Lingwen and Badong formation does not directly connect with each other and are divided by dash line. Xuanwei Formation: terrestrial facies; Kayitou Formation: terrestrial marine transitional facies; Feixianguan Formation: terrestrial marine interacting facies; Lingwen Formation: terrestrial facies; Badong Formation: coastal facies. Legend of macro plant morpho group: 1. conifer, 2. gymnosperm, 3. peltasperm, 4. seed fern, 5. cordaites, 6. ginkgophyte, 7. cycadophyte, 8. Noeggerathiales, 9. gigantopterid, 10. fern, 11. fern or seed fern, 12. sphenophyte, 13. Paleozoic lycopod, 14. Triassic lycopod. All the plant reconstructions are not to scale. Reconstruction of *Lepidodendron*, *Lepacyclotes*, Paleozoic conifer, Paleozoic tree fern and *Calamite* are drawn by Huisu studio, *Tomiostrabus* reconstruction comes from Naugolnykh (2012), ginkgophytes is modified after Zhou (1990), gigantopterids

comes from Yang (1987), others come from Zhen Xu.

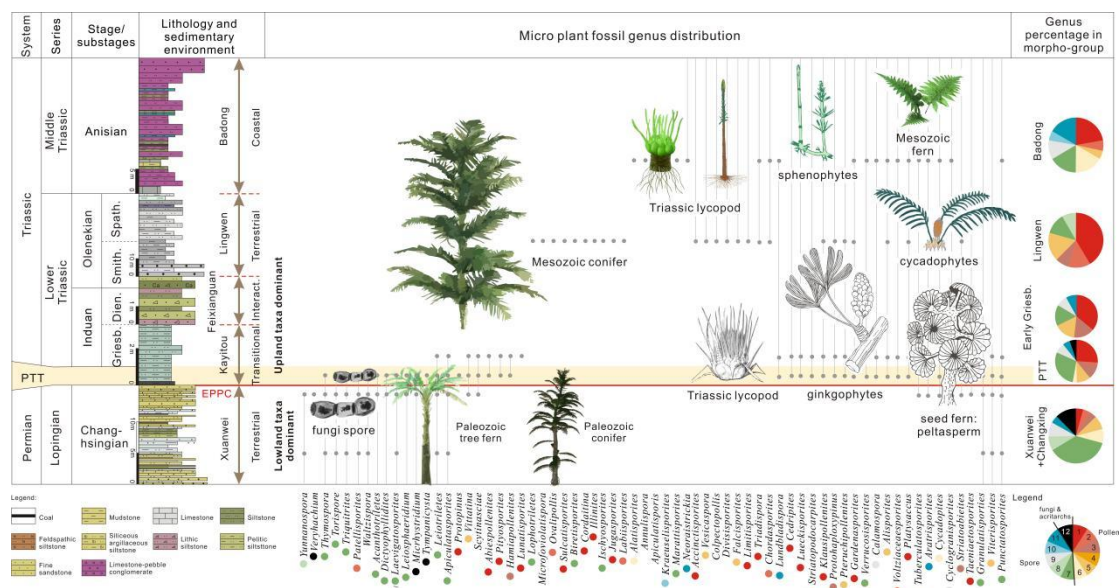


**Figure 17.** Lithology, sedimentary, micro plant fossil distribution range, floral composition from End Permian Changhsingian to Middle Triassic Anisian in South China area. Kayitou Formation conformably overlies on Xuanwei Formation, while Kayitou, Feixianguan, Lingwen and Badong formation does not directly connect with each other and are divided by dash line. Xuanwei Formation: terrestrial facies; Kayitou Formation: terrestrial marine transitional facies; Feixianguan Formation: terrestrial marine interacting facies; Lingwen Formation: terrestrial facies; Badong Formation: coastal facies. Legend of micro plant morpho group: 1. conifer, 2. gymnosperm, 3. peltasperm, 4. cordaites, 5. ginkgophyte, 6. cycadophyte, 7. fern, 8. fern or seed fern, 9. sphenophyte, 10. Paleozoic lycopod, 11. Triassic lycopod, 12. fungi or acritarchs spore. All the plant reconstructions are not to scale. Reconstruction of Middle Triassic lycopod, Paleozoic tree fern are drawn by Huisu studio, Early Triassic lycopod reconstruction comes from Naugolnykh (2012), ginkgophytes is modified after Zhou (1990), peltasperm cone comes from Naugolnykh (2000), Paleozoic conifer comes from Corey A. Ford, others come from Zhen Xu.

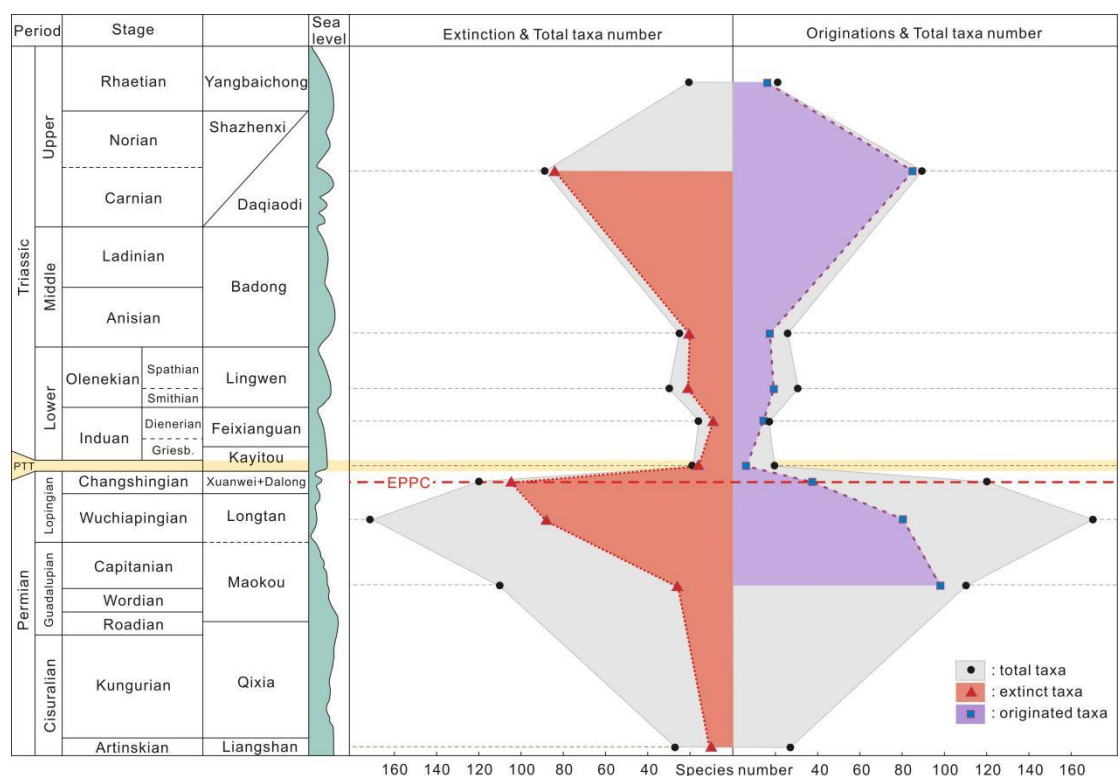


**Figure 18.** Diversity trends for fossil plant species from the Middle Permian Qixia Formation to the Late Triassic Yangbaichong Formation showing originations, extinction and total taxon number. PTT = Permo-Triassic transition; Griesb. = Griesbachian; EPPC = End Permian Plant Crisis.

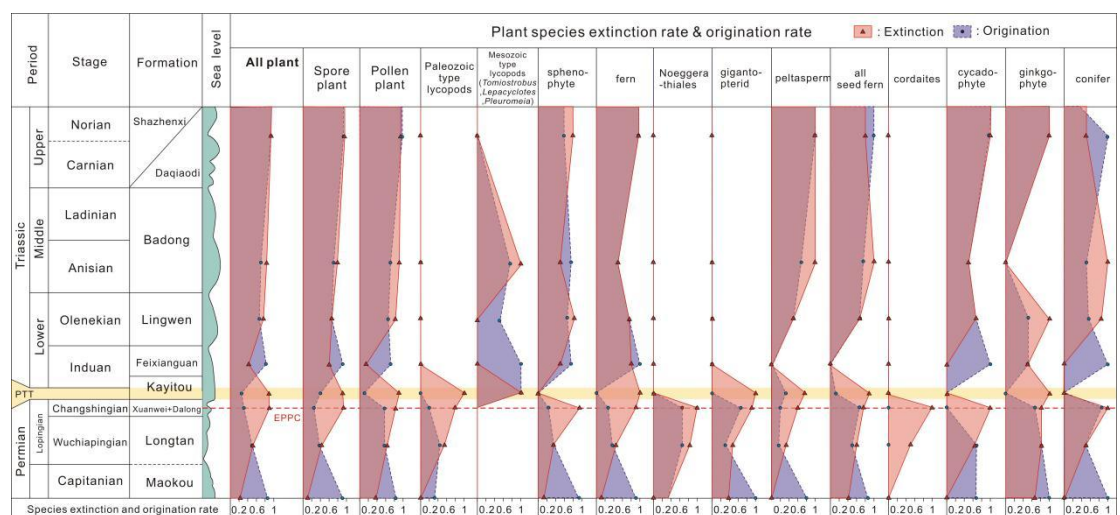


**Figure 19.** Extinction and origination rates from the Middle Permian Maokou Formation to the Late Triassic Dajing Formation showing origination and extinction rates for individual plant groups (PTT = Permo-Triassic transition; EPPC = End Permian Plant Crisis).

Permian Plant Crisis; Red solid line and red area denote extinction rate; purple dashed line and blue–purple area denote origination rates).

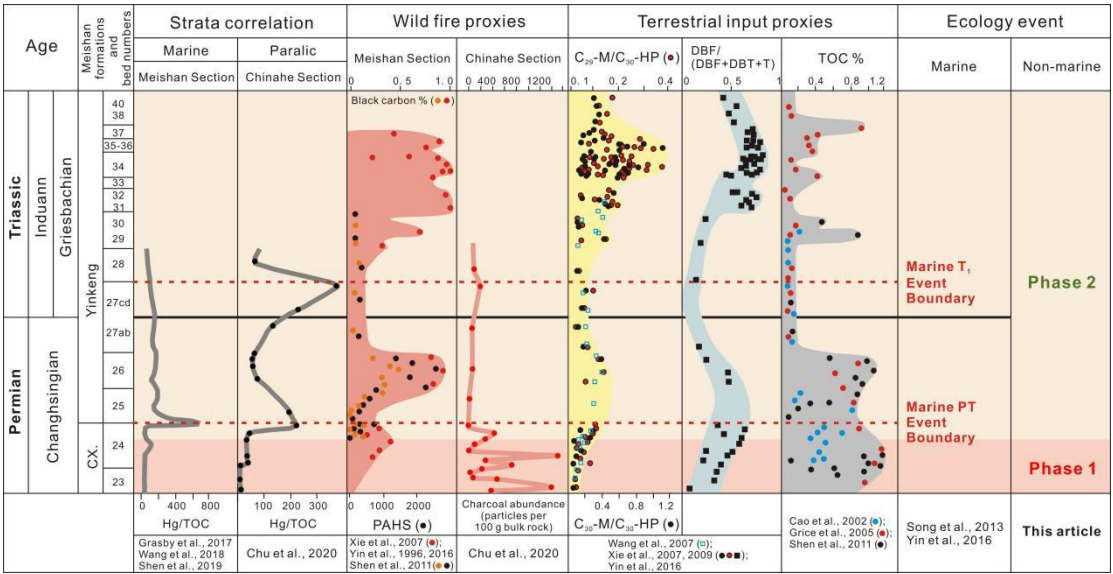


**Figure 20.** High-resolution comparison between terrestrial events and marine feedback from the End-Permian GSSP Meishan section Bed 23 to Early Triassic Bed 40. C. X. = Changhsingian; modified from Yin et al. (2016).

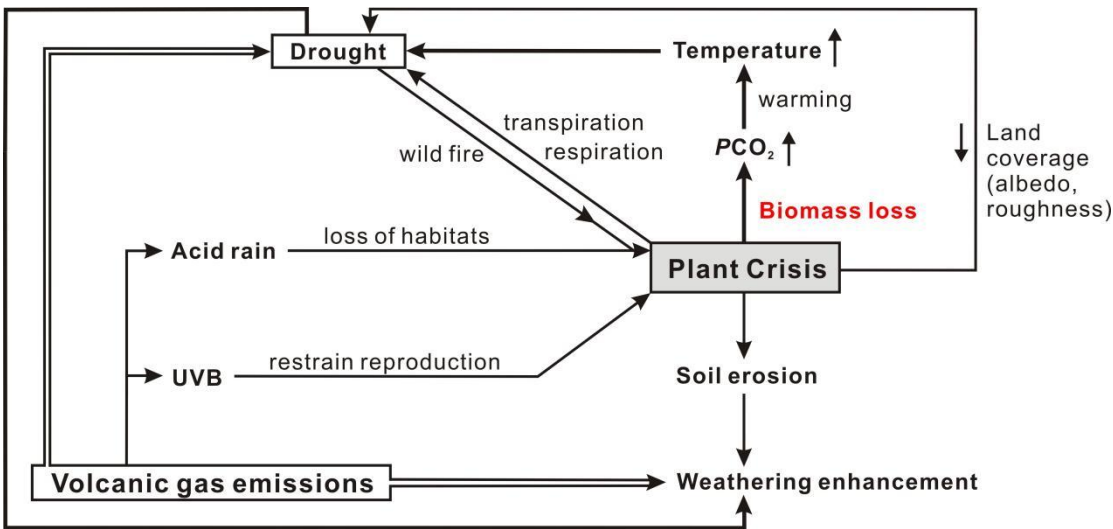


**Figure 21.** Hypotheses for the relationships between environmental changes and plant distribution emphasizing how changes contribute to episodes of plant species richness crisis, and in return causes environmental change.



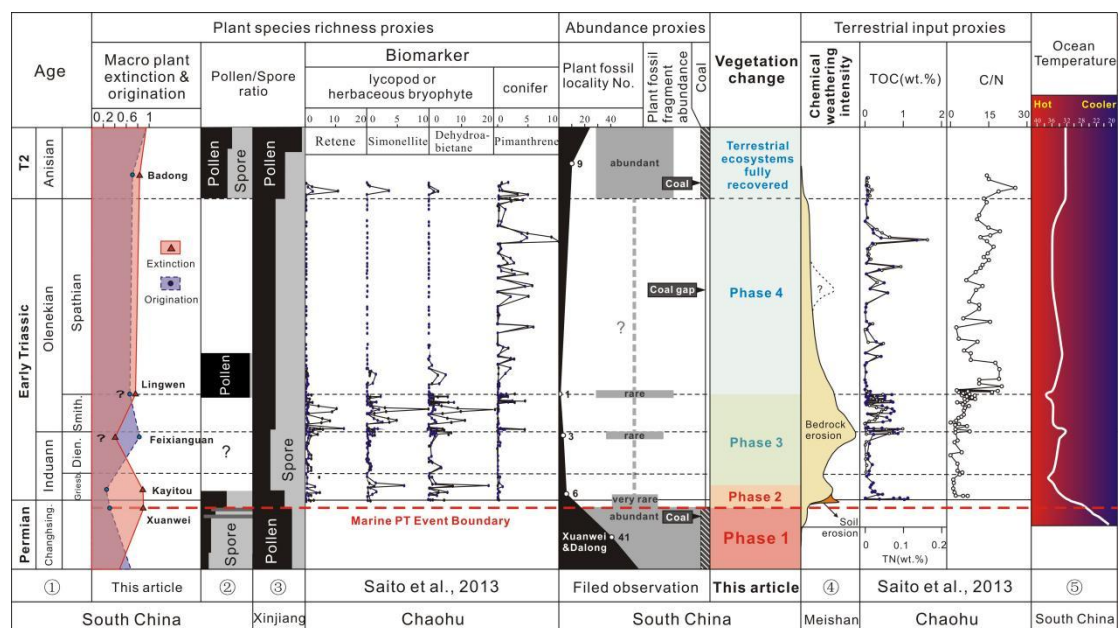


**Figure 22.** Comparison between floral change pattern proxies from macro plant fossils, coal, palynology, biomarker and environment event such as terrestrial input, marine feedback, marine temperature through the End-Permian Changhsingian to Middle Triassic Anisian. Changhsing. = Changhsingian; Griesb. = Griesbachian; Dien. = Dienerian; Smith. = Smithian; T2 = Middle Triassic. (1). Stratal data from Burgess et al. (2014); (2) Palynology data from Changhsingian to Induan of South China from Zhang et al. (2004), Yu et al. (2008), Ouyang et al. (2007), Olenekian Lingwen of South China from Zhang et al. (1992) and Middle Triassic Anisian of South China from Qu et al. (1990) and Meng et al. (1995); (3) Palynology data of Dalongkou section, Xinjiang Province, from Changhsingian to Anisian from Qu et al. (1986); (4) Chemical weathering rate from Algeo et al. (2011); (5) Oceanic temperature from Sun et al. (2012).



2011

Formation	Stem ( <i>Lepidodendron</i> )	Root ( <i>Stigmaria</i> )	Megasporophyll ( <i>Lepidostrobophyllum</i> )	Cone ( <i>Lepidostrobus</i> )	Species richness	
					Non-normalised	Normalised
Xuanwei	<i>L. acutangulum</i> <i>L. lepidophylloides</i> <i>L. oculus-felis</i>	<i>S. ficoides</i> <i>S. rugulosa</i> <i>S. radiatopunctata</i> <i>S. sp.</i>	<i>L. xiphidum</i>		8	3
Longtan	<i>L. lepidophylloides</i> <i>L. polygonale</i> <i>L. xuanweiense</i> <i>L. emeishanense</i> <i>L. oculus-felis</i>	<i>S. ficoides</i> <i>S. rugulosa</i> <i>S. sp.</i>	<i>L. caudatun</i> <i>L. hastum</i> <i>L. junlianense</i> <i>L. mucronatum</i>	<i>L. acutisquanmus</i>	13	5
Maokou	<i>L. asymmetricum</i> <i>L. oculus-felis</i>	<i>S. ficoides</i> <i>S. sp.</i>	<i>L. caudatun</i>		5	2
Qixia	<i>L. asymmetricum</i> <i>L. oculus-felis</i> <i>L. cf. szeianum</i>	<i>S. ficoides</i> <i>S. sp.</i>			5	3

2012

2013    Table 1

2014